Secretary: D H Napper
School of Chemistry
University of Sydney
NSW 2006
Australia

IPCG

INTERNATIONAL POLYMER COLLOIDS GROUP

NOVEMBER 1993

VOLUME 24 NUMBER 2

# NEWSLETTER

## INDEX

PAGE



## CONTRIBUTIONS

# FROM THE EDITOR'S DESK

## MEMBERSHIP

We welcome with pleasure to the IPCG our new members: Drs Junghyun Kim (Korea), Tatyana Aslamasova (Russia), Haruma Kawaguchi (Japan), Rudolf Müller-Mall (Germany), Joaquin Delgado (USA) and James Taylor (USA). We also welcome to alternate membership a longstanding contributor to polymer colloids Dr Gregor Ley (Germany). We look forward to reading your contributions in future Newsletters.

Several of our more recent members have provided their first contributions to this Newsletter: Drs Aslamasova, Lovell and Okubo. Thank you for your interesting reports. Long my you contribute.

Agienus Vrij has informed me that he is taking early retirement from his Chair of Physical Chemistry at Utrecht University but intends to remain active (although with reduced intensity) in the colloids field in the future. I am sure all members will join with me in thanking Agienus for his many seminal contributions to colloid science (especially to steric stabilization) and in wishing him a long and happy retirement

## CONFERENCE

Alice Gast has asked me to bring to your attention the 68th ACS Colloid and Surface Science Symposium to be held at Stanford University, 19–22 June, 1994.

## PREMATURE APOLOGY

Normally I would like to leave at lease a week between the receipt of the last contribution and the preparation of the Newsletter. This was not possible on this occasion in view of the lateness of the submission of some contributions. I apologies in advance for any contributions tha may have to be held over.

## NEXT NEWSLETTER

Contributions for the next Newsletter should reach me at the University of Sydney by **30 April 1994**, even though I will be visiting the Institute of Polymer Science, University of Akron, Akron, OH USA from February through to July 1994.

D H Napper
Editor

# CONFERENCES

| CONFERENCE | LOCATION | DATE/CONTACT |
|---|---|---|
| **1994** | | |
| 8th International Conference on Colloid & Interface Science | Adelaide | 11–19 February |
| 207th ACS National Meeting | San Diego | 13–18 March |
| Copolymerization in Dispersed Media | Lyon | 18–22 June (Pichot) |
| 68th Colloid & Surface Science Symposium | Stanford | 19–22 June (Gast) |
| 35th IUPAC Macromolecules Symposium | Akron | 11–15 July |
| 208th ACS National Meeting | Washington | 21–26 August |
| Polymers at Surfaces and Interfaces (Discussion of Faraday Society) | Bristol | 12–14 September (Ottewill) |
| **1995** | | |
| 20th Australian Polymer Symposium | Adelaide | 5–8 February (Napper) |
| 209th ACS National Meeting | Anaheim | 2–7 April |
| 210th ACM National Meeting | Chicago | 20–25 August |
| Pacific Basin Congress | Honolulu | 17–22 December |

University of Sydney
NSW 2006
Australia

IPCG

INTERNATIONAL POLYMER COLLOIDS GROUP

# MINUTES OF 1993 GENERAL MEETING

Minutes of the General Meeting held at Tilton School on 1 July, 1993.

**ATTENDANCE:** D Bassett (Chair), J Asua, F Candau, M El-Aasser, R Fitch, R Gilbert, A Hamielec, S Jayasurija, J Joosten, I Krieger, Do Ik Lee, P Lovell, D Napper, N Nomura, T Okubo, R Ottewill, R Pelton, C Pichot, I Piirma, R Rowell, P Sperry, D Sundberg, K Tauer, K Takamura, T van der Ven, M Winnick.

## BUSINESS

*Membership*

1. It was agreed that Dr Aslamazova would replace Dr Eliseeva as the Russian Academy of Science representative. Secretary to write to Dr Eliseeva to thank her for her contributions to the Group and extend best wishes for her retirement.

2. Agreed the Dr Rudolf Müller-Mall would replace Dr Hans Kast as BASF representative in Germany. Dr Gregor Ley to be invited to be alternative.

3. The following to be invited to join IPCG:

| | |
|---|---|
| J Kim, Korea | H Kawaguchi, Keio Uni |
| J Delgardo, 3M | M Fryd, Du Pont |
| J Taylor, Eastman | Liesing, Rhone-Polenc |

## GENERAL BUSINESS

*Gordon Conferences.* Gordon Conference organization unsympathetic to request to hold a European conference in alternate years. New President to advise organization that Group wishes to retain its biennial conferences at Tilton with only occasional Gordon Conference meetings in Europe.

## FUTURE MEETINGS

| Year | Topic | Date | Location | Contact |
|---|---|---|---|---|
| 1993 | Polymers at Interfaces | 8–10 Sept. | Bristol | Ron Ottewill |
| 1994 | Copolymerization | 17–21 Apr. | Lyons | Christian Pichot |
| 1994 | National Colloids Conference | 19–22 June | Stanford | Alice Gast |
| 1994 | Faraday Discuss. | 17–21 Sept | Bristol | Ron Ottewill |
| 1995 | Multiphase Material by EP | 4–7 April | Lancaster | Peter Lovell |
| 1995 | Gordon Conference | (?)2–7 July | Tilton | Theo van der Ven |
| 1996 | NATO Workshop | (?)30 June–5 July | Spain | Jose Asua |
| 1997 | Gordon Conference | | Tilton | Don Sundberg |
| 2000 | European Gordon Conference | | | |

# 68th

## ACS Colloid and Surface Science Symposium
## Stanford University, Stanford, California
## June 19-22, 1994


***Chairperson***
**Alice P. Gast**
Assoc. Professor
Chemical Engineering
Stanford University
(415) 725-3145
FAX (415) 725-7294

***Local Organizing Committee***

**Curtis W. Frank**
Professor
Dept. Chem. Eng.
Stanford University
(415) 723-4573

**George M. Homsy**
Professor
Dept. Chem. Eng.
Stanford University
(415) 723-2419

**Robert Pecora**
Professor and Chair
Dept. Chemistry
Stanford University
(415) 723-3507

**Clayton J. Radke**
Professor
Dept. Chem. Eng.
University of California
(510) 642-5204

**Eric S. G. Shaqfeh**
Assistant Professor
Dept. Chem. Eng.
Stanford University
(415) 723-3764

**Lindi Bauman**
Conference Coordinator
Dept. Chem. Eng.
Stanford University
(415) 723-0153
FAX (415) 723-9780


22 September 1993

Dr. Donald H. Napper
Department of Physical Chemistry
University of Sydney
Sydney NSW
Australia 2006

Dear ~~Dr. Napper~~ Don,

Enclosed is the Announcement (Call for Papers) of the 68th ACS Colloid and Surface Science Symposium, to be held June 19-22, 1994, at Stanford University.

Would it be possible to place this announcement, or any portion of it that fits your format, in the next Newsletter of the International Polymer Colloids Group?

Many thanks.

Sincerely yours,

Alice

Alice P. Gast

APG:lb

enclosures

* * * * * CALL FOR PAPERS * * * * *

# 68th COLLOID AND SURFACE SCIENCE SYMPOSIUM

**Stanford University, Stanford, California 94305-5025**
**June 19-22, 1994**

**Supported by a grant from the Henkel Corporation with additional support from the Industrial Affiliates Program of Chemistry and Chemical Engineering, Stanford University.**

CHAIRPERSON Professor Alice P. Gast, Department of Chemical Engineering, Stanford University
(415) 725-3145, FAX (415) 725-7294, E-mail gast@leland.stanford.edu

| Symposia | Organizers | Affiliation | Phone | E-mail |
|---|---|---|---|---|
| **Polymers at Interfaces** | Curtis W. Frank | ChE, Stanford University | (415) 723-4573 | cwf@rio.stanford.edu |
| | Ravi Sharma | Eastman Kodak Company | (716) 477-8261 | ravi.sharma@kodak.COM |
| **Rheology** | Andrea W. Chow | Lockheed | (415) 424-2015 | |
| | Eric S. G. Shaqfeh | ChE, Stanford University | (415) 723-3764 | eric@chemeng.stanford.edu |
| **Dynamics, Aggregation and Flocculation** | Robert Pecora | Chem, Stanford University | (415) 723-0681 | bob@bogart.stanford.edu |
| | Charles F. Zukoski IV | ChE, University of Illinois | (217) 333-7379 | |
| **Physics of Proteins at Interfaces** | Robert Tilton | ChE, Carnegie Mellon Univ | (412) 268-2230 | tilton@andrew.cmu.edu |
| | Abraham Lenhoff | ChE, Univ Delaware | (302) 831-8989 | lenhoff@che.udel.edu |
| **Interfacial Fluid Dynamics** | George M. Homsy | ChE, Stanford University | (415) 723-2419 | bud@chemeng.stanford.edu |
| | Sandra J. Troian | ChE, Princeton University | (609) 258-4574 | stroian@phoenix.princeton.edu |
| **Nucleation Symposium** | Joseph L. Katz | ChE, Johns Hopkins Univ. | (410) 516-8484 | jlk@jhuvms.hcf.jhu.edu |
| **Thin Films and Self-Assembly** | Clayton J. Radke | ChE, UC Berkeley | (510) 642-5204 | radke@cchem.berkeley.edu |
| | David Devore | Henkel Corporation | (215) 628-1586 | |
| **Catalysis Symposium honoring M. Boudart** | Robert J. Madix | ChE, Stanford University | (415) 723-2402 | rjm@rio.stanford.edu |
| | Daniel J. Sajkowski | Amoco Oil Company | (219) 473-3384 | |
| **Electron Microscopy** | Ishi Talmon | The Technion, Haifa | 011/972-4-292007 | ceritit@technion.bitnet |
| | John Minter | Kodak Research Labs | (716) 722-3407 | minter@kodak.com |
| **Microemulsions and Complex Fluids** | John S. Huang | Exxon Res and Engineering | (908) 730-2865 | jshuang@erenj.bitnet |
| | Eric Kaler | ChE, Univ. of Delaware | (302) 831-3553 | kaler@che.udel.edu |
| **General Papers** | Anastasia Morfesis | PPG Industries | (412) 967-2122 | |
| | Dennis Prieve | Carnegie Mellon University | (412) 268-2247 | dp4h+@andrew.cmu.edu |

**Persons wishing to submit papers should contact the appropriate session chair with a title as soon as possible but no later than December 1, 1993.**

Camera-ready abstracts typed on the standard American Chemistry Society (ACS) forms must be received by the Session Chairman prior to January 15, 1994. The ACS forms, which are available from the organizers, provide space for the title (all capital letters), authors, address, and an abstract of approximately 150 words, all to be typed in a rectangle 8 cm high by 19 cm wide with an indentation 1 cm high by 1.5 cm wide in the upper left hand corner reserved for ACS session labeling.

Stanford University, adjacent to Palo Alto, is 25 miles south of San Francisco, easily accessible from the San Francisco and San Jose International Airports. American-plan housing has been reserved for participants in Governor's Corner, an attractive student residence approximately 10 minutes walk from the classrooms and auditorium to be used by the Symposium. All meals are included, with the exception of the Symposium banquet, which will be included in the registration fee. Some rooms have also been booked in hotels near the campus, but most hotels are already commited to World Cup Soccer. We strongly encourage participants to stay in campus housing. Pre-registration materials will be mailed to ACS Division members early next year, with all details on accommodations.

CALL FOR PAPERS

# Polymers at Interfaces

American Chemical Society
68th Colloid and Surface Science Symposium

June 19-22, 1994

Stanford University
Stanford, California

Submissions are solicited for oral presentations devoted to experimental or theoretical molecular-scale investigations of polymer behavior at solid or fluid interfaces. Topics of interest include, but are not limited to:

Langmuir films of homopolymers, block copolymers or polymeric liquid crystals at the air-water interface

Homopolymer and block copolymer adsorption on solid surfaces

Polyelectrolyte layer-by-layer adsorption on solid surfaces

Blend compatibilization by block copolymers

Applications of polymers in adhesion, friction or lubrication

Submissions of titles must be received by **November 29, 1993**. Camera-ready abstracts for accepted papers must be typed on ACS forms and received prior to January 12, 1993. Fax copies of the abstract are unacceptable.

Session Chairs:

Curtis W. Frank
Department of Chemical Engineering
Stanford University
Stanford, California 94305
Tel: (415) 723-4573
Fax: (415) 723-9780

Ravi Sharma
Eastman Kodak Company
Building 83 Research Labs
Rochester, New York 14650
Tel: (716) 477-8261
Fax: (716) 722-3925

## CALL FOR PAPERS

### 68th ACS COLLOID AND SURFACE SCIENCE SYMPOSIUM
### Stanford University, Stanford, California
### June 19-22, 1994

# Session on RHEOLOGY

We are interested in papers concerning the rheology of colloidal and Brownian suspenions in Newtonian or non-Newtonian media including electrorheological fluids. Studies on constitutive modeling, experimental methods, and numerical simulations are welcome.

Deadlines: Submit title to session chair by December 1, 1993
Camera-ready abstracts typed on the standard ACS forms must be received by January 15, 1994

Session Co-chairs:


Andrea W. Chow
Lockheed Palo Alto Res Lab
O/93-50, B/204
3251 Hanover St
Palo Alto, CA 94304
(415) 424-2015
(415) 354-5795 FAX
andrea_chow%qm.rdd.lmsc.lockheed.com

Eric S. G. Shaqfeh
Chemical Engineering Dept
Stanford University
Stanford, CA 94305

(415) 723-3764
(415) 723-9780 FAX
eric@chemeng.stanford.edu

## CALL FOR PAPERS

# Physics of Proteins at Interfaces

## American Chemical Society
## 68th Colloid and Surface Science Symposium

## June 19-22, 1994

## Stanford University
## Stanford, California

Submissions are solicited for oral presentations devoted to experimental or theoretical molecular scale investigations of protein behavior at solid or fluid interfaces. Topics of interest include, but are not limited to:

- conformation of adsorbed proteins
- two-dimensional order
- protein dynamics
- interfacial transport
- intermolecular and surface forces
- molecular recognition by adsorbed or immobilized proteins
- competitive adsorption

Submissions must be received by **December 1, 1993**. Camera-ready abstracts for accepted papers must be typed on ACS forms and received prior to January 15, 1994.

Session Chairs:

Prof. Robert D. Tilton
Department of Chemical Engineering
Carnegie Mellon University
Pittsburgh, PA 15213-3890

tel: (412) 268-8168
fax: (412) 268-7139
tilton@andrew.cmu.edu

Prof. Abraham M. Lenhoff
Department of Chemical Engineering
University of Delaware
Newark, DE 19716

tel: (302) 831-8989
fax: (302) 831-1048
lenhoff@che.udel.edu

# The Johns Hopkins University

**Department of**
**Chemical Engineering**

**Joseph L. Katz**
*Professor*

**116 Maryland Hall**
**Baltimore MD 21218-2689**
Tel: (410) 516-8484
FAX: (410) 516-5510
E-mail: JLK@JHUVMS.HCF.JHU.EDU


August 27, 1993

Dear Colleague:

The *Nucleation Symposium* is a meeting of persons interested in the various aspects of nucleation phenomena. It has been in existence since 1979, meeting biennially as part of a larger meeting. After two symposia at national ACS meetings, sentiment for its association with a smaller and more closely associated meeting caused it to move into the 1983 Colloid and Surface Science symposium (Blacksburg, VA). This move was very successful. Regular "Nucleation" attendees found many of the papers presented at other sessions were of interest to them, and many "Colloid and Surface Science" attendees found the nucleation papers, especially the overview talks of great interest. Therefore, in 1985, the Nucleation Symposium was again held as part of the Colloid and Surface Science Symposium (Potsdam, NY). However, at that meeting, a European "nucleator", Dr. Paul Wagner strongly urged that the next Nucleation Symposium be held in conjunction with the 12th International Conference on Atmospheric Aerosols and Nucleation in Vienna in 1988. Perhaps it was the attraction of Vienna, but sentiment was strongly for this move. This too was a successful conjunction of interests. Since these two meetings attract quite different audiences, but *both* are interested in nucleation, we decided to continue the Nucleation Symposium biennially, but alternating between the Colloid and Surface Science Symposium, and the International Conference on Atmospheric Aerosols and Nucleation. In 1990, it was at the Colloid Symposium at Penn State and in 1992 at the International Conference... at Salt Lake City. In 1994 it will be part of the 68th ACS Colloid and Surface Science Symposium, to be held June 19-22, 1994 at Stanford University, which leads us to the purpose of this letter. (In 1996, it will again rejoin the International Conference on Atmospheric Aerosols and Nucleation meeting, to be held in Helsinki.)

I invite you and any colleagues who are interested in nucleation to consider attending the symposium and, if you are presently active in nucleation, to consider presenting a talk on your research. Talks are welcome on all aspects of Nucleation (though those of strongly atmospheric interest may be more appropriate for the next symposium). We especially welcome talks on nucleation involving two condensed phases, liquid crystals, polymers, glasses, crystals, .... For consideration for presentation, the following *absolute* deadlines apply: I must have received at least a Title by December 1,1993 and a filled out ACS Abstract Form (which we will send to you) by January 14, 1994. However, I would greatly appreciate it if you would do both significantly earlier, i.e., no later than October 30th and January 3rd, respectively. It would also be very helpful if you would include a *tentative* abstract with your initial Title submission (you can change it in when putting it on the ACS Abstract Form if you wish). Please send titles and abstracts to me at the address on the letterhead of this letter. Meeting information can be obtained from Lindi Bauman, Conference Coordinator, Dept. Chem. Eng., Stanford University, Stanford CA 94305. (Tel: 415-723-0153, Fax: 415-723-9780).

Sincerely yours,

Joseph L. Katz

# CALL FOR PAPERS

68th ACS Colloid and Surface Science Symposium
Stanford University
Stanford, CA
June 19-22, 1994

# THIN FILMS AND SELF-ASSEMBLY

Both theoretical and experimental papers are invited on the topics of thin liquid films and self-assembly systems. Suggested areas may include interaction forces, hydrodynamic and equilibrium film stability, wetting phenomena, foams and emulsions, surfactant structuring in micelles, liquid crystals, bilayer membranes, vesicles, etc.

Session Co-Chairmen

**Professor Clayton J. Radke**
Chemical Engineering Department
University of California
Berkeley, CA 94720

FAX (510) 642-4778
radke@cchem.berkeley.edu

**Dr. David Devore**
Henkel Corporation
300 Brookside Ave.
Ambler, PA 19002

FAX (215) 628-1261

## IMPORTANT DATES

| | |
|---|---|
| Tentative title: | December 1, 1993 |
| ACS Abstract: | January 15, 1994 |

## Call for Papers
## Session on Microscopy of Colloidal Systems
## 68th ACS Colloid and Surface Science Symposium
## Stanford University from June 19-22, 1994

We are organizing a session on the microscopy of colloidal systems as part of the 68th ACS Colloid and Surface Science Symposium at Stanford University from June 19-22, 1994. This session will include invited and contributed papers covering new developments in all areas of microscopy of colloidal systems and the application of these techniques to the elucidation of structure / property relations in these systems. The organizers would like contributed papers emphasizing the application to colloidal systems of all types of microscopy including light, electron, and scanned probe microscopy and quantitative image analysis.

This is the first session to be devoted to microscopy as part of a Surface and Colloid Science Symposium, signifying the value the scientific community places upon microscopy.

Further information on the program and accommodations and abstract forms are available from the conference organizers at the addresses listed below. Abstracts must be submitted on official ACS abstract forms and received by the session organizers by January 1, 1994. The program chairperson will not accept abstracts after that date. Because the Soccer World Championships are in the area at the same time, we strongly encourage you to book your airline and hotel reservations early. Some accommodations are available in the university residence halls.


Prof. Yeshayahu Talmon
Department of Chemical Engineering
Technion - Israel Institute of Technology
Haifa, 32000
Israel
Voice: 972 4 292 007
FAX: 972 4 221 581
Email: CERITIT@TECHNION.BITNET

Dr. John R. Minter
Eastman Kodak Company
Analytical Technology Division
Bldg. 49, Kodak Park
Rochester, NY 14652-3712
Voice: (716) 722-3407
FAX: (716) 477-3029
Email: minter@Kodak.COM

CALL FOR PAPERS

# 68th ACS Colloid and Surface Science Symposium

19 - 22 June 1994

Stanford University
Stanford, CA

## MICROEMULSIONS AND COMPLEX FLUIDS

We seek theoretical and experimental papers discussing structure-property relations and thermodynamic features of complex fluids in general, and of microemulsions and micellar solutions in particular. Areas of special interest are:

- Relations between Complex Fluid Structure and Phase Behavior
- Thermodynamics, Statistical Mechanics and Computer Simulations of Micelle Formation
- Thermodynamics of Mixed Micelles, Microemulsions, and Solubilization
- Materials Synthesis in Complex Fluids

Important Dates

| | |
|---|---|
| December 1, 1993 | Title to Organizers |
| January 15, 1994 | Abstract due on ACS form. *This is a firm deadline.* |


Eric W. Kaler
Department of Chemical Engineering
University of Delaware
Newark, DE 19716
(302) 831-3553
FAX (302) 831-4466
kaler@che.udel.edu

John S. Huang
Exxon Research and Engineering
Clinton Township, Route 22
Annandale, NJ 08801
(908) 730-2865
FAX (908) 730-3031
jshuang@erenj.com

# On stability of free-emulsifier acrylate latexes

Aslamazova T.R.

The author has been working on the problem of free-emulsifier latexes (FEL) stability in view of considering electrostatic, structural and molecular components of potential energy of particles interaction.

The first experiments were carried out with active participating prof.V.I.Eliseeva and based on considering the role of hydrophilicity of particles surface in stabilization of free-emulsifier copolymer latexes of butylacrylate (BA)-methylmethacrylate (MMA) latexes ("Newletters", 1989, No.2, p.62) at different relations of their concentration as well as of styrene (St)-BA and St-2-Ethylhexylacrylate (2EHA)-MMA polymerized in the presence of changing monomeric acid concentration ("Newletters", 1990, No.2, p.28).

The results obtained permitted to suggest the definite role of structural forces of particles surface interaction in their stabilization.

In this report I would like to present the results on the theoretical and experimental investigations on estimation of structural factor of stability of free-emulsifier acrylate latexes.

The role of structural factor (structural component of disjoining pressure) in FEL stability has been studied at considering the coagulation of BA-MMA latexes in the nearest potential well (irreversible coagulum).

Polymer hydrophobicity is changed by copolymerization of BA and MMA at their different concentration.

According to the DLVO Theory the potential energy of particles interaction can be written as

$$V = Ve + Vs + Vm = \frac{8\varepsilon r(kT)^2 \gamma^2 \exp(-\varkappa H)}{z^2 e^2} -$$

$$- K r \exp(- H / Hs) - Ar/12H \qquad (1),$$

where Ve,Vs,Vm - electrostatic, structural ,molecular components of potential energy, $\varepsilon$ - dielectric water permeability, k - Boltzman constant, T - absolute temperature, r - radius of particles, $\varkappa$ - opposite Debye radius, H - distance between particles, z - valency of counterion, e - electron charge, Hs - distance between particles when energy of attraction decreases at e times, $\gamma = \text{th}( ze\psi_1 / 4kT)$, $\psi_1$ - Schtern potential of particles, K -coefficient of structural forces, A -Hamaker constant.

Taking into account the values of $\varepsilon$, kT, $\gamma$, $\varkappa$, H, z, e, r and A the electrostatic and molecular components of energy can be calculated.

Structural factor of FEL stabilization is connected with hydrophobic-hydrophilic properties of particles surface and water structure near by it. These properties of surface can

be directly characterized by water contact angle. Its determination is based on measuring the angle for the latex film. The comparison of hydrophobicity-hydrophilicity of films, particles and surface-active oligomers formed at free-emulsifier polymerization is possible due to the identity of their composition.

The account of coefficient K is based on estimation of the probability of particles adhesion. Particles concentration coagulated in the nearest potential well per time unit (coagulum weight) is proportional to particles contacts per time unit and probability of overcoming it:

$$N \sim N_1 W \sim N_1 \exp ( v^{max}/ kT) \qquad (2),$$

where N, $N_1$ - concentration of particles and their contacts, $V^{max}$,W - potential well and probability of its overcoming. As $N_1 \sim C_p$ ($C_p$ - particles concentration), so the equation for coagulum weight can be obtained as

$$m_c \sim r^3 N \sim r^3 C_p^2 \exp (-V^{max}/kT) \qquad (3).$$

Relation of coagulum weights in two experiments: i and 1 can be written as

$$m_{ci}/m_{c1} = (c_{pi}^2 r_i^3 / C_{p1}^2 r_1^3) \exp[-(V_i^{max} - V_1^{max})/kT] \quad (4).$$

With taking a logarithm of eq.4 the equation for changing potential well in experiments i and 1 can be obtained as

$$(V_i^{max} - V_1^{max})/kT = 3\ln(r_i/r_1) + 2\ln(c_{pi}/C_{p1}) - \ln(m_{ci}/m_{c1}) \qquad (5).$$

Taking into account the eq.5 and the second term of eq.1 (structural component of energy) as well as the close values of radius and zeta-potential of BA and MMA latexes (zeta-potential is aqual -30 and - 25 mv consequently) the approximate theoretical equation of dependence of coagulum $m_c/m_o$ ($m_o$ - total monomer weight) upon coefficient K can be obtained:

$$K_i = K_1 + \frac{\ln(m_{ci}/m_{c1}) - 2\ln(C_{pi}/C_{p1})}{r \exp(- H^{max}/H_e)} kT \qquad (6).$$

(It should be mentioned that molecular component of eq.1 is too small in comparison with structural and electrostatic ones so it is not considered at calculating).

Coefficient K is calculated with using experimental data on coagulum weight, radius and concentration of particles given in table for MMA-BA latexes obtained at their different relation as well as taking into account the experiment No.1 for which polymer surface is characterized by $\theta_r = 63^o$ and according literature data $K=6.10^6$ din.

Table. Effect of BA on properties of MMA-BA latexes and contact angles of films $\theta_r$ on their base

| No. | [M]/$H_2O$ | MMA/BA | $r^{a)}$, nm | $\bar{r}$, nm | $C_p$. $10^{-12}$, cm | $b)$ $m_c/m_o$, % | $\theta_r$, ° $c)$ |
|---|---|---|---|---|---|---|---|
| 1 | | 1:0 | 166 | | | 0 | 63,0 |
| 2 | 20:80 | 2:8 | 165 | 155 | 10,7 | 0,5 | 82,0 |
| 3 | | 0:1 | 135 | | | 2,0 | 84,5 |
| 4 | | 1:0 | 185 | | | 1,5 | 72,5 |
| 5 | 30:70 | 1:2 | – | 170 | 14,1 | 5,9 | 89,1 |
| 6 | | 0:1 | 153 | | | 15,9 | 89,0 |

a) Particles radius is measured by using the light-scattering method.
b) $C_p$ is calculated by using average value of particles radius.
c) The angle is measured by using the method of slow descent of polymer film into water.

The dependence of coefficient K calculated according to the eq.6 and experimental data of table upon contact angle is given on fig.

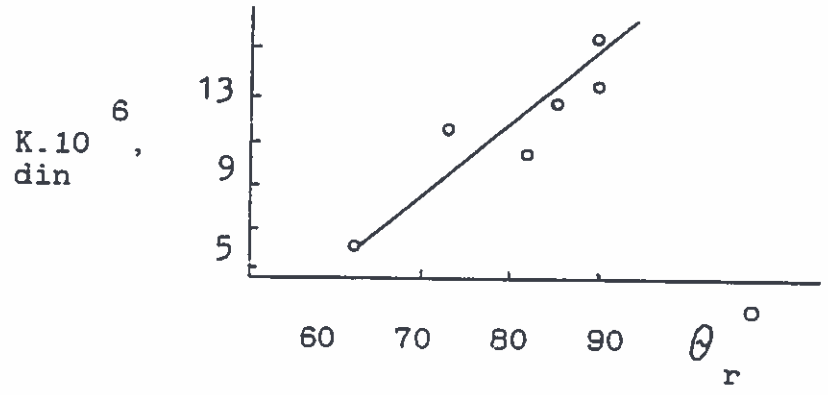


Fig. Dependence of coefficient K upon contact angle for BA-MMA films

The results obtained testifies to the correlation of coagulum concentration, contact angle and coefficient of structural forces of interaction and confirms the hypothesis of the definite role of structural component of energy in particles stabilization. Account of the probability of hydrophobic particles adhesion permits satisfactorily to estimate the free-emulsifier latex stability in the course of polymerization.

INTERNATIONAL POLYMER COLLOIDS GROUP NEWSLETTER

Contribution from the Grupo de Ingeniería Química, Facultad de Ciencias Químicas, Universidad del País Vasco, Apdo. 1072, 20080 San Sebastián, Spain.

Reported by José M. Asua

## HIGH SOLIDS CONTENT EMULSION TERPOLYMERIZATION OF VINYL ACETATE, METHYL METHACRYLATE AND BUTYL ACRYLATE. II.- OPEN LOOP COMPOSITION CONTROL.

(Agustín Urretabizkaia, Gurutze Arzamendi, María J. Unzué and José M. Asua)

A method for the calculation of the optimal monomer addition policies for polymer composition control in emulsion terpolymerization is developed. The method is applied to reactors with and without limited heat removal capacity. A mathematical model that incorpores the main features of the vinyl acetate / methyl methacrylate / butyl acrylate high solids content emulsion terpolymerization system, allows the calculation of the composition of the initial charge of the reactor and the time dependent monomer addition rates required.

## ON-LINE TERPOLYMER COMPOSITION CONTROL IN SEMICONTINUOUS EMULSION POLYMERIZATION

(Agustín Urretabizkaia, José R. Leiza and José M. Asua)

A closed-loop strategy for terpolymer composition control in semicontinuous emulsion polymerization of high solids content systems is presented. This strategy is based on a non-linear adaptive controller that calculates the flow rate of the more reactive monomers to be added into the reactor to produce a terpolymer of a given composition. The non-linear adaptive controller is based on a simplified mathematical model of the process that includes the on-line estimation of an adjustable parameter. The addition of a conventional feedback proportional-integral (PI) controller to the prediction of the non-linear controller was studied by simulation. It is shown that the contribution of the PI controller is negligible. The controller was checked by computer simulation and also experimentally verified during the semicontinuous emulsion terpolymerization of high solids content (55 wt%) of vinyl acetate, methyl methacrylate and butyl acrylate.

# MINIMUM-TIME STRATEGY TO PRODUCE NONUNIFORM EMULSION COPOLYMERS

(José C. de la Cal, Antonio Echevarría, Gregorio Meira and José M. Asua)

A method for calculating the optimal monomer addition policy to produce emulsion copolymers with a given copolymer composition profile is presented. The approach allows the calculation of the time evolution of the monomer feed rates that ensure the formation of the desired copolymer composition profile at a maximum polymerization rate. The method was applied by simulation to obtain widely different copolymer composition profiles during the emulsion copolymerization of butyl acrylate and styrene. The results were compared with those obtained by means of the classical starved process.

# International Polymer Colloid Group Newsletter

Contribution from the Department of Polymerization Reactions, Polymer Institute, Slovak Academy of Sciences, Dubravska cesta 10, 842 36 Bratislava, Slovak Republic.

Reporter: Jaroslav BARTOŇ

## A report about 9th Bratislava Conference on "Modification of Thermoplastic Polymers" June 14-18,1993,the House of Scientists in Stara Lesna, High Tatras (cf.IPCG Newsletter, 24 No.1 May 1993 p.3)

The conference was organized at the occasion of the 30th anniversary of the foundation of the Polymer Institute of the Slovak Academy of Sciences.

The thematic orientation of the conference was the process of modification and characterization of the macromolecular product, covering examination of chemical / microscopic /up to supermolecular structure.

The scientific programme of the conference was divided into: 9 main lectures /45 min/, 22 short lectures /20 min/ and 66 posters presented in a couple of 2-hour sessions.

Two interesting and thought provoking introductory lectures stood slightly apart from the general theme. The role of specialty polymers in chemical and pharmaceutical industry, and new unusual applications of this type of polymers were outlined by D. Bellus. N. A. Plate followed up with a lecture enumerating the possibilities of application of modified hydrogels at immobilization of enzymes, anticoagulants and living cells. A well-founded review of new processes in modification and functionalization of polymers was given by O. Vogl in his lecture: "Molecular Architecture of Polymers." The lectures of A. D. Jenkins, W. Schnabel and F. Tudos were devoted to different aspects of preparation of modified polymers. A.D. Jenkins dealt in detail with the possibilities of preparation of graft, block and star polymers by so called "group-transfer polymerization"of methacrylic acid esters, initiated by enolates. W. Schnabel spoke about light-induced preparation of block and graft copolymers. He gave a full account of partial reactions at preparation of copolymers, and compared such processes with the thermo-induced ones. F. Tudos, in his lecture: "Isodisperse Telechelic Polymerization", determined the kinetic conditions for formation of mono-disperse telomers with active end groups under the conditions of radical initiation. The lecture of P.J.Lemstra: "Polymer Blending Using Reactive Diluents" showed the possibilities of preparation of composites with special structure and optimal properties. The production of new types of materials with interpenetrating networks was clarified in the lecture of M. Ratzsch: "Synthesis of New IPNs and Reactive Coupling of Polymers in the Interface". He also talked about the preparation of blends with partial compatability. J. Verdu, in his lecture : "Effect of Ageing on the Mechanical Properties of Polymeric Materials", concentrated on age-induced changes of mechanical properties of polymers, such as toughness and stiffness, at molecular, macromolecular and morphological scales.

Other aspects of the general theme were dealt with in a number of short lectures and posters. The preparation of the modified polymers itself was the theme of five lectures.

The conference was organized by the Slovak Chemical Society and the Polymer Institute. It was attended by 110 participants from 16 countries, 51 of them from the Slovak Republic.

# DSC and TG Study of Polyacrylamide Prepared by Free - Radical Polymerization in Inverse Microemulsion and in Water Solution.

*(Ivica Janigová, Katarína Csomorová, Martina Stillhammerová, Jaroslav Bartoň)*

## INTRODUCTION

Free - radical polymerization of acrylamide in inverse microemulsion was studied in numerous papers [1-4]. This polymerization has special features in comparison to classical free-radical polymerization of acrylamide in solution. In inverse microemulsion polyacrylamide is in the form of spherical particles. The diameter of these particles lies between 30-70 nm. The average number of polyacrylamide molecules in polyacrylamide particle ranges between 1-10. Owing to small particle size and relatively high molecular mass of polyacrylamide the polyacrylamide chain in polyacrylamide particle is in the collapsed state. Polymer dispersions containing disperse phase in the form of particles in continuous phase can form non-percolating or percolating systems. In non-percolating polymer dispersion particles of the dispersed phase form clusters and aggregates containing more than two particles. Percolating behaviour influences the physical properties of the polymer dispersion such as electrical conductivity[2] and the course of chemical reactions in disperse phase, e.g. kinetics of acrylamide polymerization[5]. Acrylamide monomer in inverse microemulsion acts as co-surfactant and is located in between paraffinic chains of emulsifier at water/oil interface of inverse micelles[1]. It was also shown on the basis of spin probe mobility measurements in environment of polyacrylamide particles and in the polyacrylamide coils in water solution that the environment of polyacrylamide particles in comparison to the environment of polyacrylamide in solution more significantly hinders the rotational rate of spin probe[5]. This might be a result of polyacrylamide formation by polymerization of acrylamide located at the water/oil interface (polymerization of acrylamide in a matrix) and by polymerization of acrylamide in core of water pool of inverse micelle (polymerization of acrylamide in water droplet). If this suggestion were true, then the polyacrylamide after isolation from the polymer particle should have different physical properties in reference to properties of polyacrylamide prepared by polymerization in water solution. On the other hand if the chemical and physical effects observed in acrylamide polymerization in inverse microamulsion and found for polyacrylamide particles in inverse microemulsion were connected with the existence of polyacrylamide in different surrounding (the collapsed state of polyacrylamide chains in polymer particle and in relatively expanded polyacrylamide chain in polyacrylamide coils in a good solvent), then no differencies in physical properties of polyacrylamide separated from the inverse microemulsion and from water solution should be found.

In order to distinguish between these two possibilities DSC and TG study of polyacrylamide prepared by free-radical polymerization in non-percolating and percolating inverse microemulsion toluene/sodium bis(2-ethyl hexyl) sulfosuccinate/water/acrylamide and by free-radical polymerization in water was performed.

## EXPERIMENTAL

Acrylamide (puriss., recrystallized, from Serva Feinbiochimica GmbH and Co., Heidelberg, Germany), sodium bis (2-ethyl hexyl) sulfosuccinate (AOT) (purum, from Fluka Chemie, AG Buchs, Switzerland), toluene (p.a. from Lachema, Prague, Czech Republic) and potassium nitrosodisulfonate (Fremy's salt, FS) (from Aldrich Chemical Co. Inc. Milwaukee, Wisc. USA) were used without further purification. Dibenzoyl peroxide and ammonium peroxodisulfate (purum, from Lachema, Prague, Czech Republic) were recrystallized from ethanol. Distilled water was deprived of oxygen by heating to the boiling point and cooling under a stream of argon.

Details on the preparation of inverse microemulsion containing acrylami-

de and on the free-radical polymerization of acrylamide in inverse microemulsion are describe elsewhere[3,4].

Water/isopropanol solution of polyacrylamide was prepared by free-radical polymerization of acrylamide in water/isopropanol mixture. Some of the characteristics of acrylamide containing inverse microemulsion and of water solution of acrylamide are given in Table 1.

Limiting viscosity number of polyacrylamide of polymer particles of inverse microemulsion and of polyacrylamide prepared by solution polymerization was determined in water at 25°C. Relative viscosity average molecular mass of polyacrylamide was calculated from the equation[6]

$$[\eta] = 6.31 \times 10^{-5} M_v^{0.8} \ (\mathrm{dl\ g^{-1}})$$

$M_v$ was converted to number average relative molecular mass $M_n$ according to procedure outlined in [7].

The glass transition temperature of the samples was evaluated by DSC measurements using Perkin-Elmer DSC-2 in nitrogen atmosphere. Indium and lead were used as the temperature standards.

The DSC measurements were carried out by heating the sample to 500 K at a heating rate 10 K/min then immediately cooled to 320 K at a cooling rate 80 K/min. This process was repeated several times.

Thermal decomposition of samples was determined on a Perkin-Elmer thermobalance TGS-1 with a sample amount 3 mg in air. The heating rate was 10 K/min.

## RESULTS AND DISCUSSION

Results of DSC and TG measurements of polyacrylamide prepared by free-radical polymerization of acrylamide in inverse microemulsion and in water solution are presented in Table 2 (DSC measurements) and Fig. 1 (TG measurements).

Polyacrylamide is a hygroscopic polymer, where the presence of water leads to a shift of a glass transition temperature to lower values. The Tg presented in the Table 2 is the last value obtained after five-times repeated heating of a sample, when the influence of water was annulled. For instance the glass transition temperature of polyacrylamide measured after polymerization in inverse microemulsion and/or after subsequent drying by repeated heating (see experimental part) was 387 K and/or 469 K, respectively. Two possibilities may be offered to explain the influence of water on Tg value. One explanation could be the decrease of free volume after water release; the decrease of free volume results in the increase of Tg. Another explanation is based on the water effects as a plasticizer; the removing of plasticizer also leads to the increase of Tg.

In order to see if AOT surfactant was fully removed from polyacrylamide precipitated from inverse microemulsion, also the dependence of the weight loss of AOT vs. temperature (curve 4, Fig. 1) was also shown. The result confirms that polyacrylamide from inverse microemulsion was not contamined by AOT surfactant.

As can be seen from data of Table 2 and of Fig. 1 no differences in DSC and TG characteristics of various polyacrylamide samples were found. This means that the published[1,4,5] characteristics of acrylamide polymerization in inverse microemulsion are connected with the physical properties of inverse microemulsion environment only and not with the supposed effect of spatial arrangement of acrylamide molecules at the water/oil interphase of inverse micelle on the polyacrylamide formation.

The results presented here together with results found in kinetic studies of acrylamide polymerization in inverse microemulsion and in studies of spin probe mobility in polyacrylamide particles of inverse microemulsion[5] confirm once more the validity of the postulated idea[1] on collapsed state of polyacrylamide chains in polymer particles of inverse microemulsion.

## REFERENCES


1. F. Candau, Y. S. Leong, R. M. Fitch, J. Polym. Sci., Polym. Chem. Ed., 23, 193 (1985)
2. M. T. Carver, E. Hirsch, J. C. Wittmann, R. M. Fitch, F. Candau, J. Phys. Chem., 93, 4867 (1989)
3. J. Bartoň, Makromol. Chem., Rapid Commun., 12, 675 (1991)
4. J. Bartoň, Polymer International, 30, 151 (1993)
5. J. Bartoň, J. Tiňo, Z. Hloušková, M. Stillhammerová, Polymer International, submitted
6. W. M. Thomas;"Acrylamide Polymers", in Encyclopedia of Polymer Science and Technology, Vol. 1, H. F. Mark, N. G. Gaylord, and N.M. Bikales, Eds., Interscience, New York, 1974, p. 177
7. C. H. Bamford, W. G. Barb., A. D. Jenkins, P. K. Onyon; "The Kinetics of Vinyl Polymerization by Radical Mechanism", Butterworths, London 1958, chapter 7
8. D. W. Van Krevelen; "Properties of Polymers", Elsevier, Amsterdam 1976, p. 577


Table 1. Characterization of Toluene / AOT / Water / Acrylamide non-percola- ting (A) and percolating (B) inverse microemulsions, water solution of acrylamide (C) and information on polyacrylamide number average molecular mass[a)]

| Run | % mass | | | | b) | c) |
|---|---|---|---|---|---|---|
| | Toluene | Water | AOT | $AA_m$ | $AA_m$ moldm$^{-3}$ | $M_n x10^{-5}$ gmol$^{-1}$ |
| A | 73.9 | 7.4 | 17.7 | 1.0 | 1.88 | 4.5 |
| B | 71.8 | 7.2 | 17.2 | 3.8 | 7.50 | 16.2 |
| C | - | 88.1 | - | 11.9 | 1.70 | 0.8 |

a) Dibenzoyl peroxide ($1x10^{-2}$ mol dm$^{-3}$ of toluene) for runs A and B and ammonium peroxodisulfate ($1x10^{-4}$ mol dm$^{-3}$ of water) for run C were used. Polymerization temperature 60°C. For further details see Experimental part.
b) Acrylamide concentration in water.
c) Number average molecular mass of polyacrylamide obtained after polymerization of individual runs.

Table 2. Glass transition temperature (Tg) of polyacrylamide prepared in inverse microemulsions (runs A and B) and by solution polymerization in water[a)]

| R u n | Tg (K) [b)] |
|---|---|
| A | 468 |
| B | 469 |
| C | 468 |

a) Average value of 3 measurements. For further details see Table 1. and Experimental part.
b) In ref.[8] for polyacrylamide a value 438 K was presented.

Legend to Fig. 1.
Weight loss of polyacrylamide prepared in inverse microemulsions (runs A and B) and in water (run C) and of AOT surfactant vs. temperature.
Heating rate: 10 K/min, Atmosphere: air

1 - Run A
2 - Run B
3 - Run C
4 - AOT surfactant

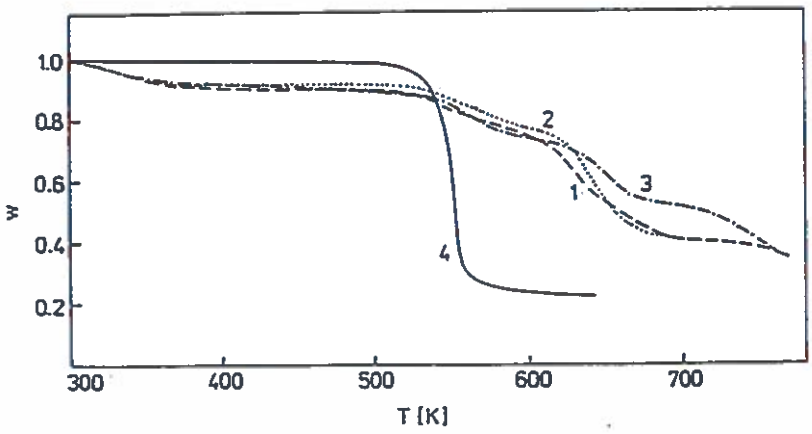

# Effect of Percolation on Free-Radical Polymerization of Acrylamide in Inverse Microemulsion.

*(Jaroslav Barton, Jozef Tino, Zuzana Hlouskova, Martina Stillhammerova)*

ABSTRACT

The kinetics of free-radical polymerization of acrylamide initiated by dibenzoyl peroxide in non-percolating and percolating inverse microemulsion toluene / AOT ( sodium bis(2-ethylhexyl) sulfosuccinate ) / water / acrylamide and properties of polyacrylamide particles formed from these inverse microemulsions were investigated. The acrylamide polymerization rate and polyacrylamide number average molecular mass depend on the acrylamide concentration in dispersed phase of inverse microemulsion. For non-percolating inverse microemulsions these dependencies are described by equation

$$R_p \text{ ( or } M_n \text{ )} \propto [AAm]^{x \text{ (or } y)}$$

where exponents x and y have the value of 1.8 and 1.4, while for percolating inverse microemulsions the respective values of exponents x and y are 1.1 and 0.4, respectively.

Data on polymer particle size and number average molecular mass of polyacrylamide in polymer particles were used for calculation of average number of polymer chains in polymer particles for non-percolating ( $\sim$ 1 chain/particle) and for percolating (>2 chains/particle) inverse microemulsions.

The spin probe potassium nitrosodisulfonate, Fremy's salt correlation time $\tau_c$ expressing the spin probe mobility in water swelled polymer particles and in polyacrylamide water solution pointed at the "collapsed" state of polyacrylamide chains in polymer particles in both kinds of inverse micro - emulsions.

Besides the dependencies of polyacrylamide polymerization rate and of number average molecular mass of polyacrylamide on acrylamide concentration in inverse microemulsion also the dependence of $T_{50G}$ values characterizing the spin probe mobility in polymer particles of inverse microemulsion on polyacrylamide concentration in polymer particle is different for non-percolating and percolating inverse microemulsion, respectively.

# EXTENSIONAL VISCOSITY OF ASSOCIATIVE EMULSION POLYMER SOLUTIONS

Richard D. Jenkins and David R. Bassett
Union Carbide Corporation
UCAR Emulsion Systems
Cary, North Carolina 27511

Alkali - soluble associative polymers thicken a variety of waterborne systems, such as architectural paints and paper coatings. They are made by emulsion polymerizing an acid-containing monomer, an associative "macromonomer" (i.e., a surfactant that has been capped with a polymerizable double bond), and a "non-associative" flexibilizing monomer.

The extensional viscosity of a coating can be important wherever a two dimensional flow field is encountered during its application, such as flow between a roller nip and a substrate, flow under a blade during paper coating, or atomization through a spray nozzle. The improved performance of associative polymers as a class in these applications has been correlated with low extensional viscosity, as compared to materials thickened with conventional polymers. Tension-thinning in extensional viscosity of a associative emulsion polymer solution (shown in the figure below) suggests that the polymer coils in solution are quite flexible. Because the extensional viscosity approaches 3 times the steady shear viscosity for a inelastic non-Newtonian fluid, the extensional data in the figure have been normalized by 3. The extensional viscosity is larger than the steady shear viscosity at high rates of extension due to viscoelasticity.

The figure below also compares the extensional viscosity, the steady shear viscosity, and the complex viscosity. The empirical Cox-Mertz rule extrapolates the relationship between the complex viscosity $|\eta^*(\omega)|$ and simple shear viscosity $\eta(\dot{\gamma})$ to higher frequencies and shear rates. In the limit of zero shear rate, or zero frequency, the complex viscosity tends toward the zero shear limiting viscosity. As is typical for most polymer solutions, the complex viscosity decreases faster at high rates of shear, as compared to the steady shear viscosity. The difference between the steady shear viscosity and the real component of the complex viscosity at large rates of shear can be approximated by a horizontal shift on the plot, which according to non-affine network models measures the degree of non-affine deformation. This non-affine deformation may also explain strain hardening seen in the loss modulus of this solution.

Comparison Of Steady Simple Shear, Complex, and Extensional Viscosities Of Alkaline Aqueous Solutions Of Associative Emulsion Polymers.

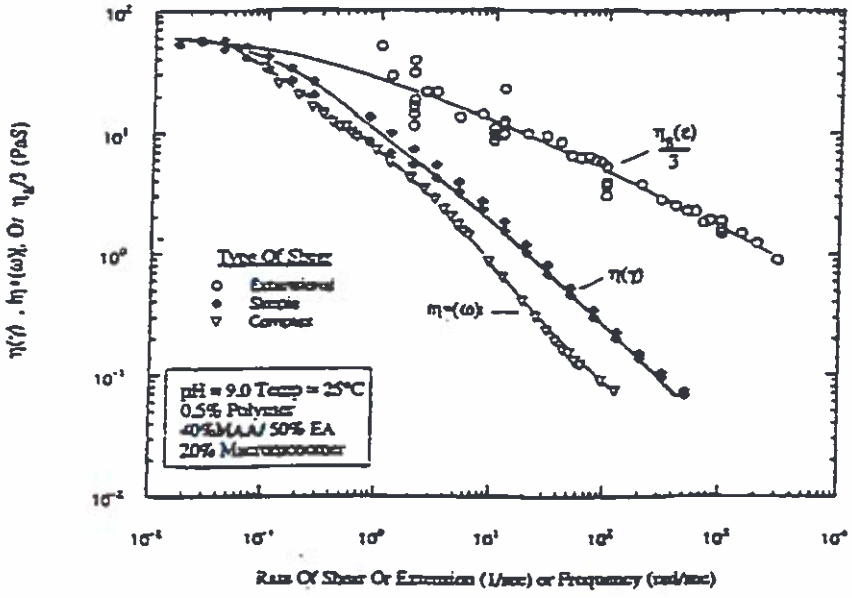

# ZINC DESTABILISATION OF CARBOXYLATE-STABILISED LATICES (CONTINUED)

D. C. Blackley, London School of Polymer Technology,
University of North London, Holloway, London N7 8DB.

This contribution continues the summary of some of the work we have carried out in previous years on the colloidal destabilisation of carboxylate-stabilised latices by sparingly-soluble zinc compounds, in particular, by zinc oxide. The reasons for interest in this topic are given in the first of our three contributions on this subject to the Polymer Colloids Group Newsletter. Reference was made in the first of these contributions to the detailed investigation into the colloidal destabilisation of well-characterised model polystyrene latices by zinc ammine ions which has been carried out by Nithi-Uthai. These polystyrene latices were used as models for natural rubber latex, the intention being to gain deeper understanding of the colloidal destabilisation of ammonia-preserved natural rubber latex. The polystyrene latices were prepared by seeded emulsion polymerisation, and were essentially monodisperse with particle diameters ranging from *ca.* 90 nm to *ca.* 830 nm. In most cases, the latices were stabilised by adsorbed laurate anions, the effective surface potential in alkaline medium being *ca.* -19 mV. The results were interpreted using a value of $4.3\times10^{-21}$ J for the effective Hamaker constant for polystyrene particles in water. The zinc ammine ions used to destabilise the latices colloidally were pre-formed in aqueous solution by dissolving precipitated and washed zinc hydroxide in ammonium hydroxide solution. The kinetics of colloidal destabilisation were followed by measurement of turbidity as a function of time. For this purpose, the latices were diluted sufficiently to reduce the optical density to a value in the range 0.3 - 0.8. The volume fraction of polymer contained in the diluted latices was typically *ca.* $1.5\times10^{-3}$, and the particle concentration typically in the range $10^{10}$ - $10^{11}$ particles $cm^{-3}$. From measurements of the variation of turbidity with time elapsed after the addition of the destabilisative influence, it was possible to calculate values of $k_{11}$, the second-order rate coefficient for the reduction of particle number by binary encounters between primary particles. The coefficient $k_{11}$ was taken as an inverse measure of the colloid stability as initially reduced by the addition of zinc ammine ions, and thus as a direct measure of the extent to which the latex had been initially colloidally destabilised by the zinc ammine ions. The variables investigated included concentration of zinc ammine ions, concentration of ammonia, concentration of ammonium ions, pH, nature and concentration of colloid stabilisers, particle size of latex, concentration of polymer in latex, concentration of other anions, and temperature at which colloidal destabilisation occurred. Some of the conclusions reached from this very extensive investigation were summarised in the second of our three contributions. Other significant conclusions are as follows:

i) The variation of the effective surface potential of the polymer particles with overall concentration of added zinc ions is consistent with the reduction in effective surface potential being attributable to adsorption of zinc-containing ions in accordance with a Langmuir adsorption isotherm. The particular isotherm which represents the data for the latex investigated indicates that the effective surface potential could not be raised above *ca.* -10.7 mV by interaction with zinc-containing ions, this being the value corresponding to adsorption saturation. That the effective surface potential cannot apparently become zero by interaction with zinc-containing ions indicates either that the interaction between the zinc-containing ions and the stabiliser anions is reversible, or that other surface-bound anions contribute to the effective surface potential. It is not clear at present to what extent this observation is applicable to all anionic latices colloidally stabilised by bound carboxylate anions, including, *inter alia*, ammonia-preserved natural rubber latex.

ii) The colloid stability, as quantified by the inverse of the rate coefficient $k_{11}$, increases as the concentration of polymer particles increases. This effect is attributed to increase in the ratio of particle surface to zinc ammine ions with increasing particle concentration, the effect being to decrease the destabilisative effect of the zinc ammine ions.

iii) Measurements using laurate-stabilised latices having particle diameters covering the range 120 - 484 nm indicate that the colloid stability, as quantified by the inverse of the rate coefficient $k_{11}$, decreases as particle size increases.

iv) The destabilisative effect of sodium salts of various anions upon laurate-stabilised latices in the absence of zinc ammine ions decreases in the order

chloride > sulphate > nitrate > acetate

whereas for destabilisation by zinc ammine ions the effect of the added anion is to decrease the rate of destabilisation in the order

formate > acetate > nitrate > sulphate, chloride.

Thus the effect of added anion in the presence of zinc ammine ions is not merely a consequence of effect in the absence of such ions. Specific effects, such as anion adsorption, are clearly indicated.

v) As expected, increasing the temperature decreased colloid stability in the presence of zinc ammine ions. Results for the variation of $k_{11}$ with temperature for a laurate-stabilised latex are shown in Figure 1. The same data are replotted according to the Arrhenius equation in Figure 2. Various explanations for the effect of temperature upon $k_{11}$ have been considered. The conventional explanation in terms of the thermal lability of zinc ammine ions has been rejected as inadequate. The most plausible explanation appears to be that the effect is a consequence of increase in the concentration of ammonium ions as the temperature increases, together with reduction of the inherent colloid stability of the latex by adsorption of zinc-containing ions. It is perhaps relevant that qualitatively very similar results to those for the effect of temperature upon colloidal destabilisation by zinc ammine ions have been obtained for the effect of temperature upon the colloid destabilisation of this latex by ammonium chloride.

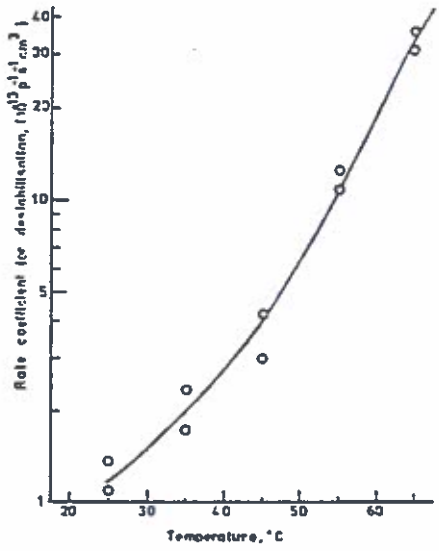


Figure 1

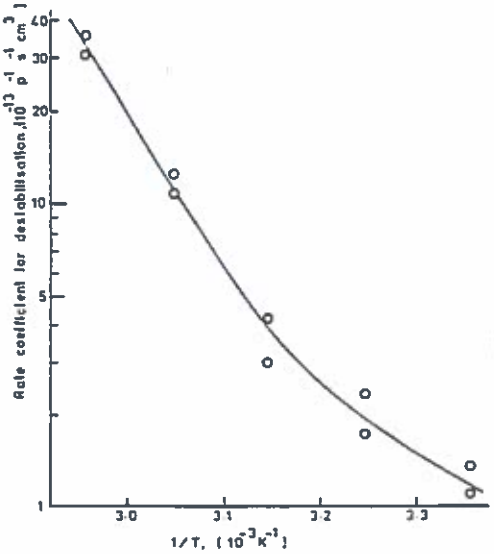


Figure 2

POLYMER COLLOID GROUP NEWSLETTER

Contribution from the Institut Charles Sadron (CRM-EAHP)
6, rue Boussingault, 67083 Strasbourg Cédex, France.

by

Françoise CANDAU

## PHOTOPOLYMERIZATION OF MICELLES-FORMING MONOMERS

(with D. Cochin and R. Zana, 2 papers accepted in Macromolecules)

### Introduction

Several studies have recently been devoted to the polymerization of micelle-forming monomers above their critical micelle concentration (Paleos, C.M. in "Polymerization in Organized Media"; Paleos, C.M. Ed., Gordon and Breach, 1992 and references therein). Research in this field had several objectives. The first was to fix permanently these labile systems in order to get a better description of their structures. The second objective was based on the expectation that covalently stabilized micelles should be more appropriate for technological applications than their unpolymerized counterparts. However, from the various studies performed so far, it is hard to draw definite conclusions regarding the mechanism of micellar polymerization and the characteristics of the polymers thus produced. Indeed the data are often conflicting, rather fragmentary and dealing mainly with only one of the many problems raised by this process, such as the effect of the polymerizable group on the micelle characteristics or the effect of the micellar structure on the kinetics and polymerization mechanism or the structure of the polymerized particles.

### Results and Discussion

We have attempted to gain further insight into these various aspects by a thorough study of the polymerization of cationic micelles formed from akyldimethyl-vinylbenzylammonium chlorides (Cn-STY with n = 8,12,16). The CMC micelle ionization degrees and aggregation numbers of these surfactants prior to polymerization were determined in aqueous solution. These surfactants were then photochemically polymerized in aqueous micellar solution, and the particles present in the system were characterized by various techniques. Light scattering showed that the degrees of polymerization of the polymers formed were much larger than the aggregation number of the micelles before polymerization. This result excludes a topochemical polymerization of the reactive monomers used and implies extensive exchange of material between micelles as polymerization proceeds. The microstructure of the aqueous solutions of poly(Cn-STY) was investigated by viscometry and fluorescence

probing. The structure is essentially controlled by the length of the alkyl chain of the surfactant. Intramolecular hydrophobic microdomains were found to be present in solutions of poly(C16-STY) which adopt a compact conformation similar to that of a polysoap. Microdomains do not form in solutions of poly(C8-STY) and poly(C12-STY) which adopt extended conformations, of the polyelectrolyte type.

The kinetics of the photoinitiated polymerization of the aqueous micellar solutions of Cn-STY has been investigated. The rate of polymerization of C8-STY and C16-STY and the molecular weight $\overline{M}_w$ of the polymers thus prepared have been found to scale with the monomer concentration C and initiator concentration [I] according to $R_p \alpha [I]^{\alpha} C^{\beta}$ and $\overline{M}_w \alpha [I]^{\gamma}$ where the exponents $\alpha$, $\beta$ and $\gamma$ have values close to those characteristic of radically initiated emulsion polymerization. Based on the site of solubilization of the oil-soluble initiator, α,α-dimethyoxy-α-phenylacetophenone (mostly in C16-STY micelles, but close to equally, present in micelles and in the intermicellar solution for C8-STY), we have proposed a detailed mechanism for the micellar polymerization which distinguishes between surfactants having high and low CMC values and strongly emphasizes the importance of the value of the micelle lifetime on the course of the polymerization. Systems with long-lived micelles have small CMC (case of C16-STY) and the polymerization takes essentially place in the nucleated micelles, which grow at the expense of the unnucleated ones. These micelles become progressively more stable as polymerization proceeds because of the increased hydrophobicity of the polymer formed with respect to the monomeric surfactant. Systems with short-lived micelles have a high CMC and the micelles breakdown before a sufficiently long polymer is formed. Polymerization then proceeds both in the aqueous phase and in micelles. The proposed mechanism completely excludes a topochemical polymerization of the micelles.

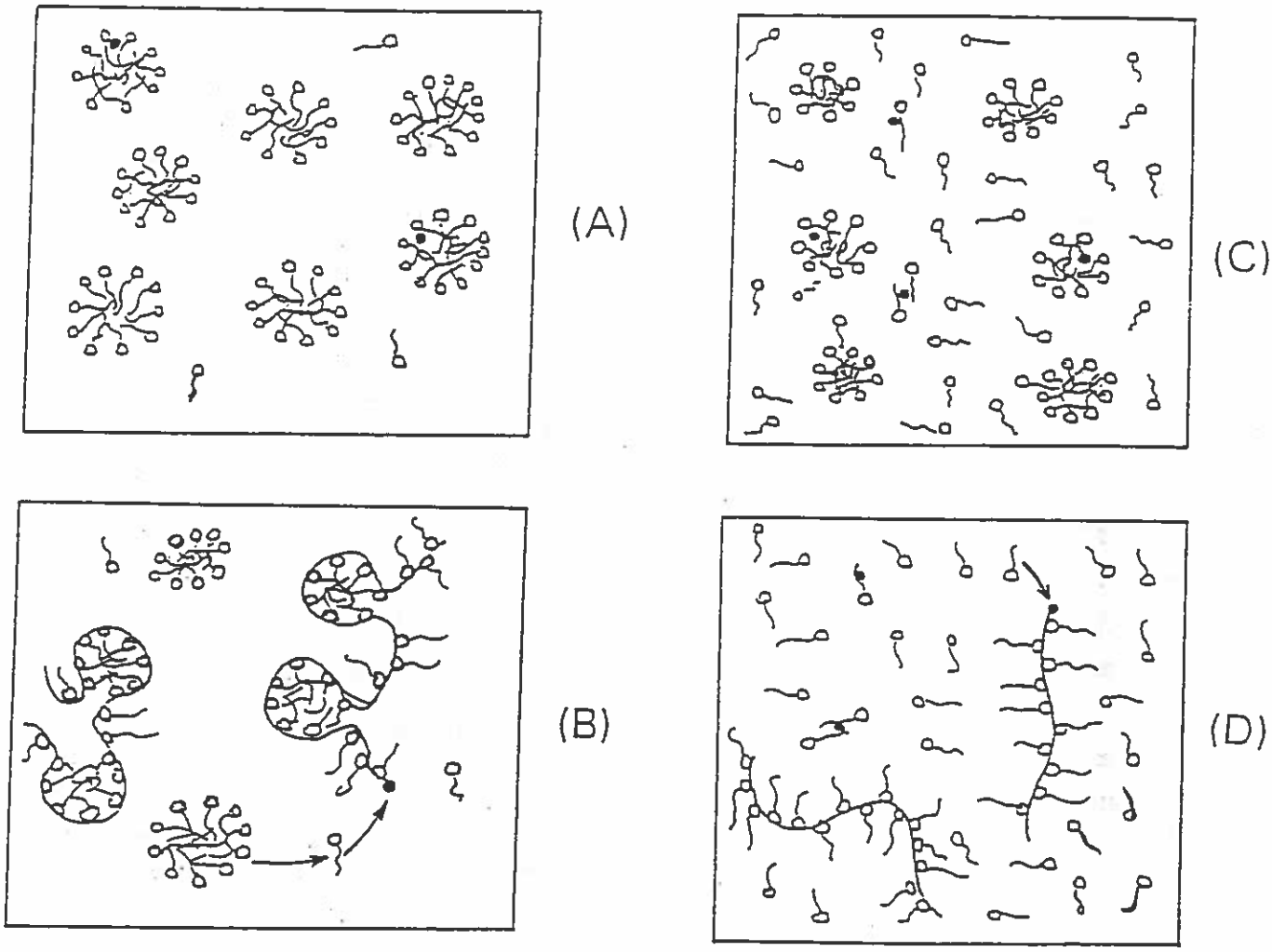


**Figure 1 :** Schematic representation of the polymerization of a micelle-forming-surfactant. **(A) and (B) :** Case of a surfactant with a low CMC (C16-STY). **(A) :** Before polymerization ; (•) stands for the initiator. **(B) :** Same solution in the course of polymerization. **(C) and (D) :** Case of a surfactant with a high CMC (C8-STY). **(C) :** Solution before polymerization at C = 2 CMC. **(D) :** Same solution after time t. The arrows show monomer diffusion from unnucleated micelles towards the active particle.

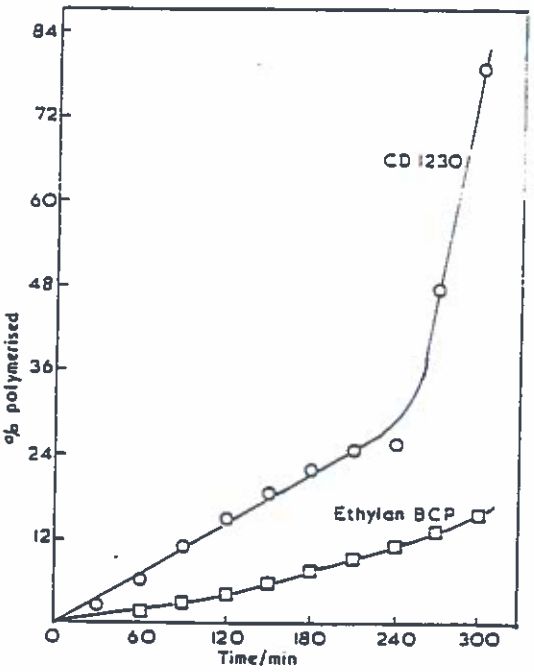


Dr A. S. Dunn,
Chemistry Department

UMIST

PO Box 88
Manchester M60 1QD
United Kingdom

Tel 061-236 3311
Telex 666094
Fax 061-228 7040

Emulsion polymerisation of styrene with non-ionic emulsifiers.

## Is the Rate of Emulsifier Adsorption a Factor?

In my contributions to the 1991 Atlanta and Fukui Symposia (cf. Polym. Int. 30 (1993) 547) I suggested that, on the basis of observations by Klimenko et al. (Coll.J.USSR 37 (1975) 873) on the rates of adsorption of two non-ionic emulsifiers on silica gel at 25 °C that the more slowly adsorbed, higher molecular weight, more hydrophilic emulsifier should produce a latex with larger particles size (and consequently a lower Interval II polymerisation rate). Mr R.D.Nuttall attempted a project to test this prediction. Though the reproducibility he achieved left much to be desired and, with the less hydrophilic emulsifier used, the beginning of Interval II was not reached with styrene at 60 °C after 5 h, the Interval I rates are in the inverse relation to that predicted but do appear to be proportional to the number of micelles present.

Because of the notorious hydroperoxidation problem of 'Triton' X-100 which makes it difficult to reproduce rates using this emulsifier, it seemed advisable to avoid using it. The emulsifiers used were kindly supplied by Harcross Chemicals of Eccles through Dr D.R.Karsa.

| Triton X-100 | 'Ethylan' BCP | E-23 | CD 1230 |
|---|---|---|---|
| $C_9H_{19}C_6H_4(OCH_2CH_2)_{10}OH$ | $C_9H_{19}C_6H_4(OC_2H_4)_{9.5}OH$ | $C_{12}H_{25}(OCH_2CH_2)_{23}OH$ | $C_{12}H_{25}(OCH_2CH_2)_{30}OH$ |
| Diffusion rate x3 | - | x1 | - |
| $a_S$ 0,6 $nm^2$ | - | 0.8 $nm^2$ | - |
| Aggregation no. 276 | | 70 | - |
| Mol.wt. 661 | 638 | 1200 | 1506 |
| Interval I rate - | 0.04 % $min^{-1}$ | - | 0.12 % $min^{-1}$ |
| Interval II rate - | 0.95 % $min^{-1}$ | - | ? |

The critical micelle concentrations of the emulsifiers are similar so, for equimolar concentrations there will be about 4 times as many micelles in the CD 1230 solution as in the Ethylan BCP solution which is similar to the ratio of the Interval I rates. Increasing the initiator concentration by a factor of 10 in the hope of speeding up the Ethylan BCP polymerisation increased the Interval I rate by a factor of about 2.4 which is what would be expected on the basis of Smith-Ewart Theory ($10^{2/5} = 2.5$). It may be that stirring speed is critical in this system which could account for the difficulty in reproducing results.

Recipe: Water:monomer ratio (by volume) = 2.5. Emulsifier $5.7 \times 10^{-2}$ mol $dm^{-3}$. NaOH $6 \times 10^{-2}$ mol $dm^{-3}$, $K_2S_2O_8$ $7.85 \times 10^{-3}$ mol $dm^{-3}$.

**Contribution to the International Polymer Colloids Group Newsletter**

E.S. Daniels, V.L. Dimonie, M.S. El-Aasser, A. Klein,
O.L. Shaffer, C.A. Silebi, E.D. Sudol, and J.W. Vanderhoff

*Emulsion Polymers Institute*
*Lehigh University, Mountaintop Campus, Iacocca Hall*
*Bethlehem, Pennsylvania 18015-4732 USA*

The titles of our current research projects are given in the Contents of our *Graduate Research Progress Reports*, No. 40, July 1993, which can be found at the end of this report. Summaries of progress in several research areas are presented here.

## 1. The Development of Core-Shell Latex Particles as Toughening Agents for Epoxies

Julie Y. Qian and Raymond A. Pearson *(Co-Advisor)*

The properties of structured core/shell latex particles such as size, morphology, composition and crosslink density of the core can be controlled separately during particle preparation by emulsion polymerization techniques. Therefore, the use of structured core/shell latex particles as toughening agents provides a model system which allows the independent examination of the role of particle size, particle-matrix interaction, and the cohesive strength of particles on the toughening of epoxies. The purpose of this work is to investigate the effects of the interfacial architecture between the core/shell particles and epoxy matrix on the toughening efficiency of the core/shell particles.

Uniform P(B-S) [poly(butadiene-co-styrene)] core/PMMA [poly(methyl methacrylate)] shell particles were prepared by seeded emulsion polymerization using a semi-continuous process. The interfacial architectures between the rubber particles and epoxy were systematically controlled by varying the shell composition of the core/shell particles. This included PMMA, P(MMA-AN) with various MMA/AN ratios, P(MMA-GMA), and P(MMA-AN-DVB) [AN = acrylonitrile, GMA = glycidyl methacrylate, DVB = divinylbenzene]. These core/shell latex particles were freeze-dried and then dispersed into an epoxy matrix. The dispersability of the particles in the epoxy matrix was examined by SEM examination of the fractured surfaces of the modified epoxies. The mechanical behavior of the modified epoxies, including the fracture toughness, yield stress, and Young's modulus, was evaluated using a single edge notch 3-point bending (SEN-3PB) test and an ASTM D363 tension test.

Figure 1 shows transmission electron micrographs of P(B-S) core/PMMA shell latex particles with various shell compositions including PMMA, P(MMA-AN), P(MMA-GMA), and P(MMA-AN-DVB) prepared by a semi-continuous process under monomer 'starved' conditions. The P(B-S) cores were stained with $OsO_4$ and appear dark while the shell materials were negatively stained with PTA and appear light. In all cases, a uniform core-shell morphology was observed. The effect of the DVB crosslinking agent on the morphology of the resulting core/shell particles is shown to be significant by comparing the TEM micrograph in Figure 1D with the others in Figure 1. In the case of the core/shell particles with a crosslinked shell, a more uniform and complete coverage of the shell material on the core particles was observed.

Table 1 shows the effect of the shell composition on the mechanical behavior of the rubber-modified epoxies. Incorporating GMA and AN into the PMMA shell increased the $K_{1C}$ value of the modified epoxies from 1.66 to 2.45 and 2.55 MPa-$m^{1/2}$, respectively. Crosslinking the shell by adding DVB to the P(MMA-AN) shell suppressed the toughening efficiency of the core/shell particles from 2.55 to 2.18 MPa-$m^{1/2}$. Table 2 shows the effect of the AN/MMA ratio

in the shell on the fracture toughness of the rubber-modified epoxies. The fracture toughness of the modified epoxies increased significantly to 2.67 and 2.55 MPa-$m^{1/2}$ with AN contents of 5% and 10% in the PMMA shell, respectively, and decreased to 2.26 for an AN content of 25%.

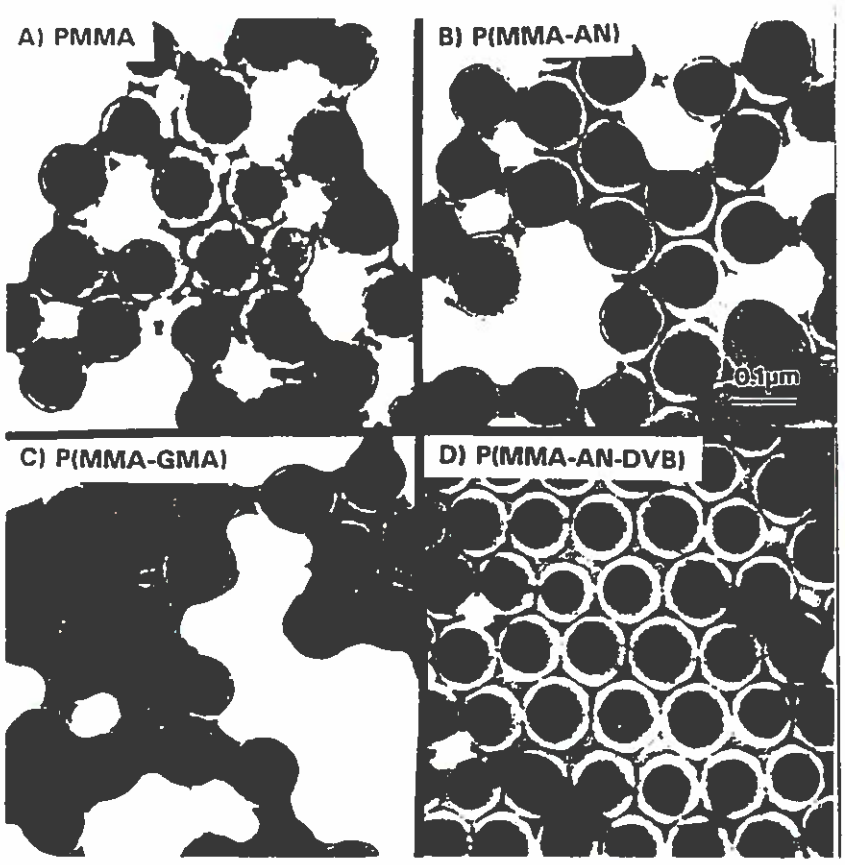


**Figure 1.** *Transmission electron micrographs of the P(B-S) core/PMMA shell latex particles with various shell compositions*

**TABLE 1.** Effect of Shell Composition on the Mechanical Behavior of Rubber-Modified Epoxies

| Shell Composition | $K_{1C}$ (MPa-$m^{1/2}$) | E (GPa) | $\sigma_y$ (MPa) |
|---|---|---|---|
| PMMA | 1.66 ± 0.15 | 2.8 | 64.0 |
| P(MMA-AN) | 2.55 ± 0.02 | 2.4 | 60.6 |
| P(MMA-GMA) | 2.45 ± 0.07 | --- | --- |
| P(MMA-AN-DVB) | 2.18 ± 0.07 | 2.7 | 66.8 |

**TABLE 2.** Effect of the AN/MMA Ratio in the Shell Material on the Mechanical Behavior of Rubber-Toughened Epoxies

| AN/MMA | $K_{IC}$(MPa-$m^{1/2}$) | E(GPa) | $\sigma_y$(MPa) |
|---|---|---|---|
| 0/100 | 1.66 ± 0.15 | 2.8 | 64.0 |
| 5/95 | 2.67 ± 0.09 | 2.5 | 61.2 |
| 10/90 | 2.55 ± 0.02 | 2.4 | 60.6 |
| 25/75 | 2.26 ± 0.05 | 2.8 | 66.1 |

The effect of shell composition on the degree of dispersability of the particles in the epoxy matrix was found to be significant as shown in Figure 2. In the case of core/shell particles having only a PMMA shell, a high level of segregation of the particles was found in the matrix, as illustrated in Figure 2A, where a large number of particles were found in one area, whereas in other areas of the matrix no particles were observed. In the case of the particles having a shell comprised of AN and GMA copolymer, a relatively uniform dispersion was obtained, although the particles still tended to segregate. The effect of the AN content in the PMMA shell on the degree of the dispersability of the particles in the epoxy matrix is clearly illustrated in Figure 3. Increasing the AN content in the PMMA shell improved the degree dispersability of the particles in the epoxy. A uniform dispersion of the particles in the epoxy matrix was achieved with an AN content in the PMMA shell of 25%.

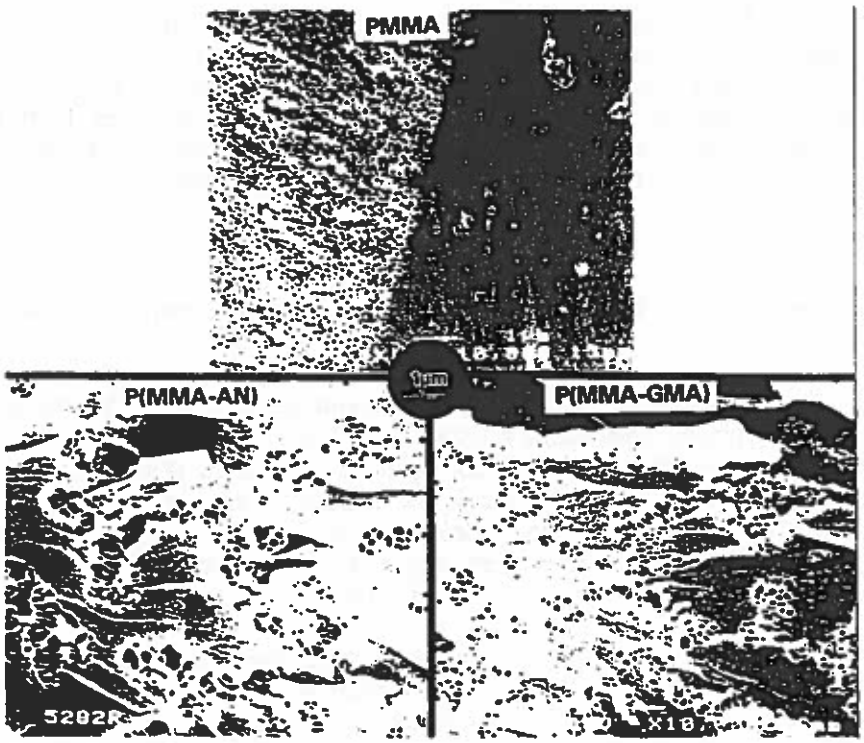


**Figure 2.** *Scanning electron micrographs of the fracture surfaces of the epoxies modified with particles having various shell compositions.*

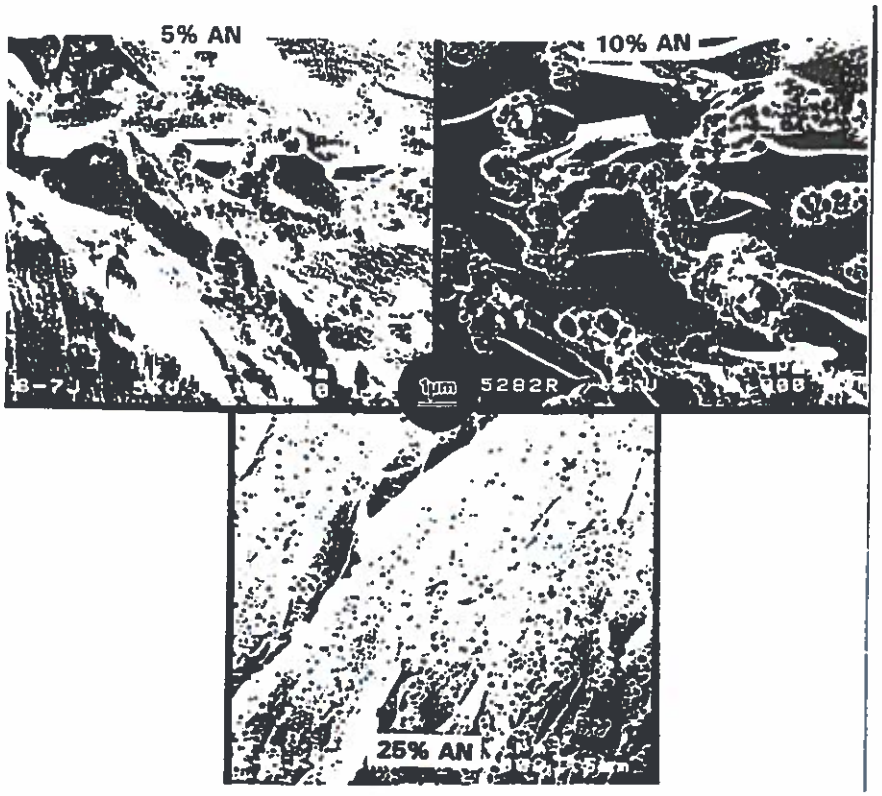


**Figure 3.** *Scanning electron micrographs of the fracture surfaces of the epoxies modified with particles having various AN/MMA ratios in the shell.*

Uniform P(B-S) core/PMMA shell latex particles with various shell compositions were successfully prepared by emulsion polymerization. Incorporation of AN and GMA functional groups into the PMMA shell dramatically improved the dispersability of the particles in the epoxy matrix, and resulted in an improved fracture toughness of the rubber-modified epoxies. Both the dispersion of the particles in the epoxy matrix and the interfacial architecture between the particles and epoxy have significant effects on the final fracture toughness of the rubber-toughened epoxies.

## 2. Copolymerization of Macromonomers as Compatibilizing Agents in Composite Latex Particles (Prapasri Rajatapiti)

Blending a particular pair of polymers together seems to be one of the most efficient ways to achieve properties not attainable from the individual components. Unfortunately, most polymer pairs are immiscible and thus form separate phases when mixed, leading to poor mechanical behaviors. One approach to promote interfacial adhesion is by adding "compatibilizing agents" to immiscible polymer blends. These comprise block or graft copolymers possessing either segments with chemical structures or solubility parameters similar to those of the polymers being blended, or functional groups capable of interacting with each other.

In this project, this concept is being applied to formulate composite latex particles of two incompatible polymers, poly(n-butyl acrylate) (PBA) and poly(methyl methacrylate) (PMMA), having a controlled core/shell type morphology. Compatibilizing agents were prepared *in-situ* during the PBA seed synthesis via miniemulsion polymerization of n-BA in the presence of different PMMA macromonomers. Composite latexes of PBA/PMMA were then prepared by conventional seeded batch emulsion polymerization using the PBA seed latexes prepared in the presence of the PMMA macromonomers.

The PMMA macromonomers used in this project are linear PMMA of different molecular weights, having one terminal vinyl double bond per chain as illustrated at right (n = 5 - 100). Better control over compatibilizing agent structure is allowed since the number of grafts per chain and the length of these branches in the graft copolymers or networks can be regulated by the feed ratio of macromonomer and comonomer, and the molar mass of macromonomer, respectively. Based on the hydrophilicity of the monomers, it is anticipated that the more hydrophilic PMMA chains will partition to the surface of the PBA particles. These PMMA chains on the surface of the core particles will modify the interfacial tension between the first polymer phase (PBA) and the second polymer phase (PMMA) during the second stage polymerization, leading to the improved coverage of the core particles by the shell polymer.

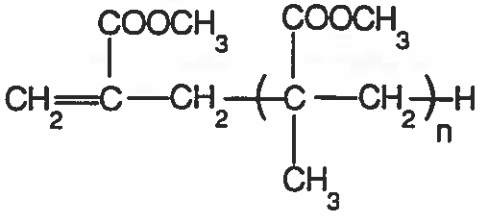

The resulting changes in the average sizes and size distributions of the seed particles, determined by transmission electron microscopy (TEM) and capillary hydrodynamic fractionation (CHDF), revealed that the surfaces of the particles were modified due to the presence of the macromonomers. High performance liquid chromatography (HPLC) indicated different compositions of the PBA as different macromonomers were incorporated. The absence of macromonomer peaks in the HPLC results and the shift in the tan delta peaks in the dynamic mechanical spectra (DMS) of films made from the seed latexes confirmed complete incorporation of the macromonomers in the seed particles. The storage moduli, obtained from the latter experiments, are consistent with a reinforcing of the PBA polymer by the PMMA polymer. The larger particle size averages and the narrower size distributions (CHDF) together with the inferior film formation abilities of the composite latexes compared to the seed latexes led to the conclusion that the second-stage PMMA was successfully incorporated onto the PBA seed particles.

Future work includes investigating the reactivity ratios between n-BA and the PMMA macromonomers via FTIR and GPC, examining the effect of the compatibilizing agents on the morphology of the resulting composite particles by TEM, and analyzing the degree of compatibility between the two phases by means of contact angle measurements and dynamic mechanical spectroscopy (DMS).

### 3. Particle Growth During Miniemulsion Polymerization

Chris M. Miller

Miniemulsions which consist of relatively stable submicron (50 - 500 nm) oil droplets suspended in an aqueous phase, are prepared by an emulsification process using a combination of an ionic surfactant and a co-surfactant, such as a long chain alkane or fatty alcohol. These emulsions exhibit high stability and unique polymerization kinetic behavior when made with monomer as the oil phase.

Due to their small size, nucleation in miniemulsion droplets may compete effectively with other nucleation mechanisms during polymerization. However, it has been determined that not all droplets capture radicals to become growing polymer particles. This, of course, leads to the questions: what determines which droplets capture radicals; and, what is the role in the polymerization of the monomer droplets which are not nucleated (i.e., what is the *fate* of the uninitiated monomer droplets)? One of the objectives of this research is to understand the mechanism of droplet disappearance during the course of a miniemulsion polymerization.

A model system was chosen for determination of miniemulsion polymerization kinetics and particle growth. The recipe selected consists of 80 parts water, 20.2 parts styrene, 10mM sodium lauryl sulfate (SLS), and 30mM cetyl alcohol (co-surfactant, based on the aqueous phase). The miniemulsions were homogenized using a Microfluidizer 110 (Microfluidics Corp.) and polymerized in the Mettler RC1 reaction calorimeter at 70°C by addition of varying amounts of potassium persulfate (KPS) initiator.

Figure 4 shows the rate of polymerization and conversion versus time curves for a miniemulsion polymerized with 0.33mM KPS. Early in the polymerization the rate rises rapidly and reaches a maximum at around 40% conversion. Following this maximum, an 'instability' in the rate of polymerization curve occurs at around 50% conversion. Finally, a stong gel effect is observed. Samples removed during the polymerization and examined by electron microscopy reveal many details of the reaction. Figure 5 shows the evolving particle volume distributions for the unswollen particles at four different conversions. These results reveal that most of the polymer particles are formed relatively early in the polymerization (by 20% conversion). However, some nucleation occurs up to conversions even beyond the maximum in the rate of polymerization, indicating that monomer droplets do not disappear until relatively late in the polymerization. This behavior is reflected in broad particle size distributions which are skewed toward smaller particles. The amount of skewing is highly dependant upon the initiator concentration, with lower initiator concentrations giving longer nucleation periods and consequently more skewed distributions. The instability noted in the rate curves seems to be due to a limited aggregation of polymer particles, perhaps caused by the unavailability of sufficient surfactant to stabilize the increasing surface of the polymer particles. At the instability, the number of particles decreases, and the standard deviation of the particle size distribution increases slightly.

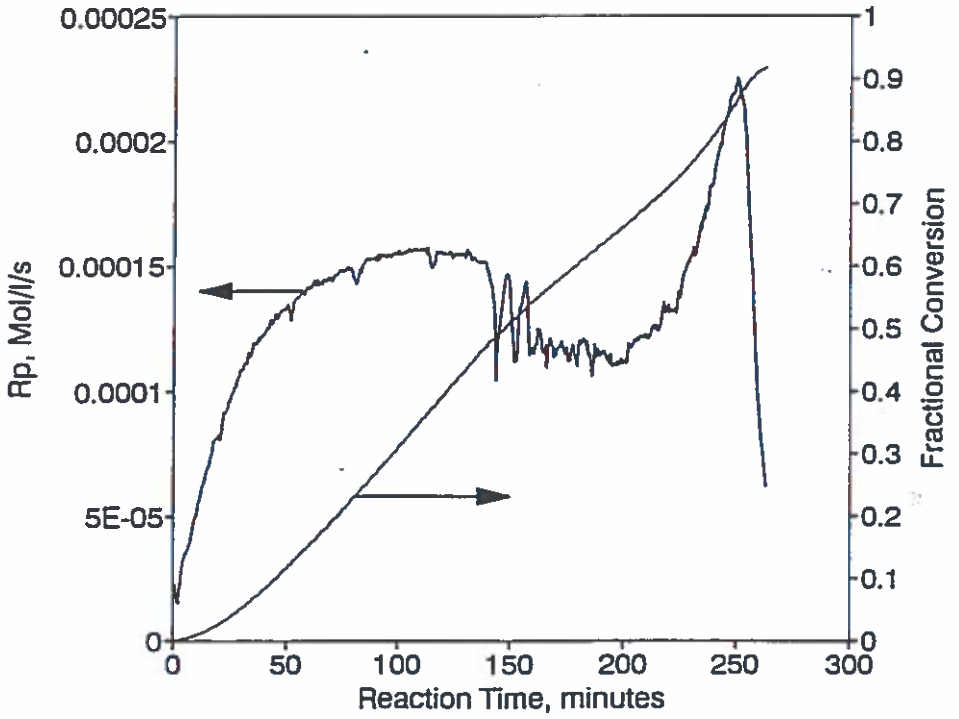


**Figure 4.** *Fractional conversion and rate of polymerization curves for a styrene miniemulsion polymerization initiated with 0.33mM KPS in the Mettler RC1 reaction calorimeter; $T_r$ = 70°C.*

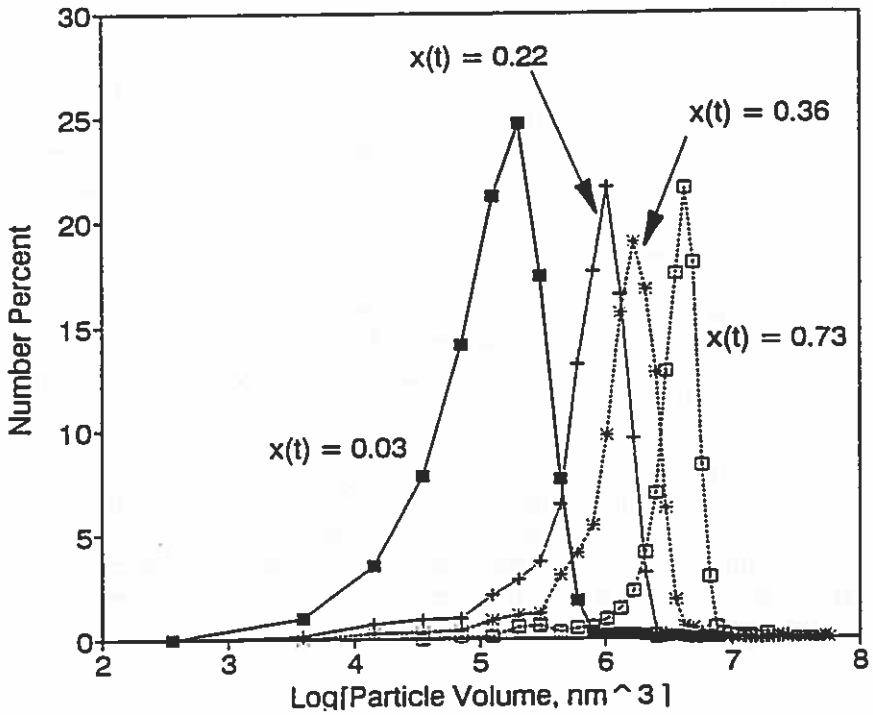


**Figure 5.** *Particle volume distributions at four different conversions for a styrene miniemulsion polymerization in the Mettler RC1 reaction calorimeter. Kinetics for this run are shown in Figure 4.*

These results favor a mechanism whereby miniemulsion droplets are less efficiently entered by radicals than polymer particles, and become increasingly less likely to be entered as the polymerization proceeds (decreasing size and number). In addition, the results indicate that most of the monomer is transferred to the growing polymer particles by molecular diffusion as opposed to collision, and there is no true Interval II in these polymerizations since new particles are generated even beyond the maximum in the rate of polymerization.

In order to determine whether any collisions were occuring between polymer particles and monomer droplets, an experiment was designed to determine the amount of cetyl alcohol in the polymer particles at the end of the polymerization. Samples of the final latexes were centrifuged at 30,000 rpm for 2 hours to isolate the polymer particles from the aqueous phase. After centrifugation, the supernatent was removed, and the polymer was dried at room temperature and weighed. The polymer was then heated to 85°C to remove the cetyl alcohol in the particles, the sample was again weighed, and the percent of the cetyl alcohol in the particles was calculated by a mass balance. It was determined that 80% of the cetyl alcohol is in the polymer particles at the end of the reaction, and that this amount is independant of the initiator concentration employed. Since cetyl alcohol is highly water insoluble, and the amount in the polymer particles at the end of the reaction is independant of the initiator concentration and is much larger than the fraction of droplets believed to be nucleated (ca. 20%), it is likely that collision is occurring between uninitiated monomer droplets and polymer particles. However, such collisions would be occurring late in the reaction after most of the monomer has already been transferred to the polymer particles, and therefore would not significantly affect the polymerization kinetics. In other words, the collisions are occuring between polymer particles and monomer droplets comprised almost entirely of cetyl alcohol.

## 4. Analytical Separation of Colloidal Particles Using Capillary Electrophoresis

Armistice B. Hlatshwayo

There are many techniques which can be used for particle size analysis. However, many are only reliable when used for colloids having narrow particle size distributions (PSD). As such, it becomes necessary to fractionate a sample with a broad distribution before any attempt is made to analyze for the PSD. Furthermore, the ability to separate different particle populations and analyze for the PSD in a single step necessitates that a reliable separation technique must be an integral part of any procedure used to determine the PSD. In particular, capillary electrophoresis (CE) offers some advantages over traditional hydrodynamic techniques in its higher resolution. It has been demonstrated experimentally that the electrophoretic migration of latex particles depends on particle size, as was first suggested by Henry [Henry, D.C., *Proc. Royal Soc., London,* **A133**, 106 (1931)]. Figure 6 shows the separation of negatively charged polystyrene (PS) latex particles as a function of particle size for various sodium lauryl sulfate (SLS) concentrations using a 25 μm ID fused silica capillary and an applied electric field strength of 250 V/cm. The separation depends on the electrophoretic mobilities $\langle \mu_{ep} \rangle$ of the particles and the SLS concentration. The latter determines the electroosmotic mobility $\langle \mu_{eo} \rangle$, which is positive for fused silica capillaries and decreases monotonically with increasing SLS concentration. The ease of resolving different particle populations improves as the differential migration of the particles increases. However, the resolution may be degraded by axial dispersion, which can result from several factors including sample loading and concentration, heterogeneity of the capillary wall, and Joule heating. Furthermore, if the velocity profile of the eluant is not flat, size exclusion effects can enhance the axial dispersion.

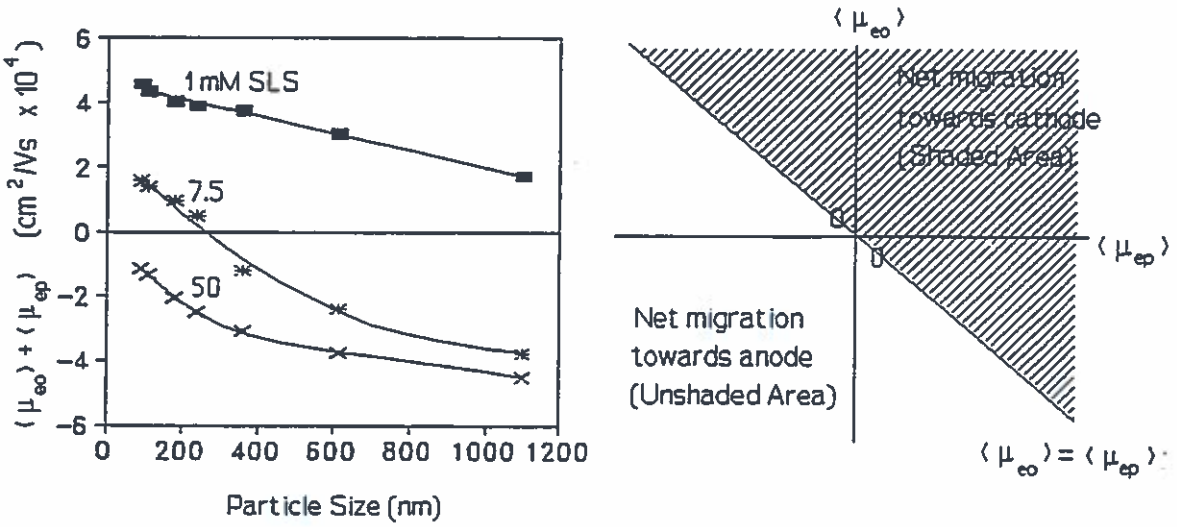


**Figure 6.** *Variation of* $\langle \mu_{eo} \rangle + \langle \mu_{ep} \rangle$ *for monodisperse latex particles, which depends on the magnitudes and signs of* $\langle \mu_{eo} \rangle$ *and* $\langle \mu_{ep} \rangle$.

The characteristic $\langle \mu_{ep} \rangle$ of latex particles does not only depend on size, but also on the intrinsic surface charge density resulting from initiator fragments, the affinity of the ionic species in the supporting electrolyte to adsorb at the particle surface, and the electrodynamic conditions inside the electrical double layer. These factors have to be taken into consideration for electrophoresis experiments to be useful when used for particle size analysis. As a bonus, since the fractograms from CE experiments are monitored using a UV/VIS detector, the turbidimetric data provides information about the particle size, which can be estimated using the Mie theory. However, such an approach requires the PSD to be narrow and its form known, which can be easily obtained using CE.

## 5. Rheology of Associative Polymer Solutions

Li Zhuo

Hydrophobically modified ethoxylated urethanes (HEUR) have found their primary use as rheology modifiers in aqueous latex paints. This type of associative polymer offers a number of performance advantages over conventional cellulose thickeners and other associative thickeners.

An experimental study on the rheological behavior of solutions of hydrophobically modified ethoxylated urethane associative polymers and mixtures of these associative polymers with conventional surfactants was conducted. The associative polymers under study have the structure:

$$C_{16}H_{33}\text{-O-}\{\text{IPDI-O-}(CH_2CH_2O)_{181}\}_n\text{-IPDI-O-}C_{16}H_{33}$$

where, IPDI is isophorone diisocyanate. Three molecular weights are being studied (nominally 34,000, 67,000, and 100,000). The rheological measurements were carried out using a Bohlin VOR Rheometer and a Rheometrics RDA II Rheometer.

A typical viscosity profile of an associative polymer solution consists of three flow regions: 1) Newtonian at low shear rates, 2) shear thickening at moderate shear rates, and 3) shear thinning at high shear rates. It was found that the low shear viscosities of solutions of the three different molecular weight associative polymers fit onto a single curve when graphed against the hexadecyl end-group concentration regardless of the molecular weight of the polymer. This is not surprising since the nonionic HEUR associative polymers rely heavily upon hydrophobic association to build low shear viscosity and derive little thickening power from their relatively low molecular weight flexible backbones. The shear thickening phenomenon was observed in associative polymer solutions over a well defined terminal hydrophobe concentration range for all three molecular weight polymers. On the other hand, the extent of shear thickening (expressed as the ratio of the viscosity maximum at the thickening peak to the low shear viscosity at the Newtonian plateau) is a function of both the end-group concentration and the polymer molecular weight.

Our study suggests that the three region flow profile is a result of the formation of a dynamic association structure in the solution. The type of flow that the solution undergoes at any shear rate is determined by the time scale of deformation (inverse shear rate) with respect to the solution relaxation time. When the time scale of deformation is just larger than or equal to the relaxation time of the solution, an additional energy dissipation contributes to the shear thickening phenomenon due to the elongation of polymer chains or the extension of the quasi-network along the flow direction. However, when the time scale of deformation becomes smaller than the solution relaxation time, the shear stress load on the association junctions quickly surpasses the association energy of the junctions. In this case, the rate of network disruption exceeds the rate of structure reforming and shear thinning is observed. It was found that the shear thickening flow behavior is most favored when the product of the solution relaxation time and shear rate is close to one. The experimental results also showed that the shear stress at the onset of shear thinning is directly proportional to the terminal hydrophobe concentration. It might be anticipated that the association network is broken down into clusters or a layered flow structure under the flow field based on the observation of similar flow relaxation time profiles for associative polymer solutions of different concentrations.

Our experiments indicated that the hydrophobic association between polymer terminal hydrophobes and surfactant hydrophobic tails is the principal interaction which occurs between associative polymer and surfactants. The isophorone diisocyanate linkage in the polyurethane backbone chain is not hydrophobic enough to serve as an active hydrophobe for participation in

a hydrophobic association. On a plot of the low shear viscosity ratio of polymer/surfactant solution to polymer solution against the molar ratio of surfactant to polymer hydrophobe, associative polymer solutions with different concentrations fall onto a single curve upon the addition of nonionic surfactants (Triton X-100 and Brij 35). Therefore, it is apparent that the effect of surfactant concentration on the viscosity of associative polymer solutions is governed by the molar ratio of surfactant to thickener hydrophobes.

It was found that the structure and hydrophilic-hydrophobic balance of the nonionic surfactants (Brij and Triton X series) determine the hydrophobic attractive interaction between hydrophobes of polymer and surfactants, and hence, the viscosity of associative polymer/surfactant solutions. The low shear viscosity of the mixed solution was higher with the nonionic surfactant including long alkyl (and/or short polyoxyethylene) chains than with the one having short alkyl (and/or long polyoxyethylene) chains. This study showed that upon the addition of surfactant, the viscosity of associative polymer solutions increase to a maximum value and then start decreasing with further addition of surfactant. This result is explained by the participation of the surfactant molecules (with their hydrophobic tails) in the physical crosslink junctions formed originally by polymer terminal hydrophobes. The surfactant participation process leads to a change in the association network structure (the density of crosslink junction, the size of the junction, and the functionality of the junction), and hence a change in the rheological behavior of the polymer/surfactant solutions. Anionic surfactants (sodium alkyl sulfates) were found to behave somewhat differently due to the charged head groups.

## Recent Publications


"Interaction of Water-Soluble Polymers with Dilute Lamellar Surfactants", Hessel, J.F., Gursky, R.P., and El-Aasser, M.S., in Colloid-Polymer Interactions: Particulate, Amphiphilic, and Biological Surfaces, Durbin, P.L. and Tong, P., Eds., *ACS Symposium Series* 532, 241 (1993).

"Emulsion Polymerization of Vinyl Acetate Using a Polymerizable Surfactant. III. Mathematical Model", Urquiola, M.B., Sudol, E.D., Dimonie, V.L., and El-Aasser, M.S., *J. Polym. Sci.: Part A: Polym. Chem.*, 31, 1403 (1993).

"Control of Particle Size in Dispersion Polymerization of Methyl Methacrylate", Shen, S., Sudol, E.D., and El-Aasser, M.S., *J. Polym. Sci.: Part A: Polym. Chem.*, 31, 1393 (1993).

"Development of Morphology in Latex Particles: The Interplay Between Thermodynamic and Kinetic Parameters", Chen, Y.C., Dimonie, V.L., Shaffer, O.L., and El-Aasser, M.S., *Polymer International*, 30, 185 (1993).

"New Approach for the Estimation of Kinetic Parameters in Emulsion Polymerization Systems. II. Homopolymerization Under Conditions where n > 0.5", Barandiaran, M.J., Adams, M.E., de la Cal, J.C., Sudol, E.D., and Asua, J.M., *J. Appl. Polym. Sci.*, 45, 2187 (1992).

"Emulsion Polymerization of Vinyl Acetate Using a Polymerizable Surfactant. I. Kinetic Studies", Urquiola, M.B., Dimonie, V.L., Sudol, E.D., and El-Aasser, M.S., *J. Polym. Sci.: Part A: Polym. Chem.*, 30, 2619 (1992).

"Emulsion Polymerization of Vinyl Acetate Using a Polymerizable Surfactant. II. Polymerization Mechanism", Urquiola, M.B., Dimonie, V.L., Sudol, E.D., and El-Aasser, M.S., *J. Polym. Sci.: Part A: Polym. Chem.*, 30, 2631 (1992).

"Adsorption of Model Associative Thickeners on Monodisperse Polystyrene Latex", Jenkins, R.D., Durali, M., Silebi, C.A., and El-Aasser, M.S., *J. Colloid and Interface Sci.*, **154**, 502 (1992).

"Batch and Semicontinuous Emulsion Copolymerization of Vinylidene Chloride and Butyl Methacrylate. I. Kinetics in VDC-BMA Emulsion Polymerization and Surface and Colloidal Properties if VDC-BMA Latexes", Lee, K.C., El-Aasser, M.S., and Vanderhoff, J.W., *J. Appl. Polym. Sci.*, **45**, 2207 (1992).

"Batch and Semicontinuous Emulsion Copolymerization of Vinylidene Chloride and Butyl Methacrylate. II. Physical and Mechanical Properties of Copolymer Latex Films", Lee, K.C., El-Aasser, M.S., and Vanderhoff, J.W., *J. Appl. Polym. Sci.*, **45**, 2221 (1992).

"Theoretical Aspects of Developing Latex Particle Morphology", Chen, Y.C., Dimonie, V.L., and El-Aasser, M.S., *Pure and Appl. Chem.*, **64**, 1691 (1992).

## Recent Ph.D. Dissertations

"An Investigation into the Structure and Breakup of Aggregated Latex Particles" by Mehdi Durali

"Phase Behavior and Properties of Lamellar Surfactants" by John Frederick Hessel

"Structured Latex Particles for the Toughening of Polycarbonate" by Iris Segall.

"Particle Size Sensor Design and Application" by Jaidev Venkatesan.

"Preparation, Stability Studies, and Phase-Transfer Reactions of Polyether-Modified Latexes" by Wei-Chih Chen.

## Recent M.S. Reports

"Characterization of Latex Particle Surfaces: The Effect of Polyoxyethylene Chains" by Rong Hu.

"Molecular Interactions of Water-Soluble Polymer Blends and Their Effect on Drag Reduction in Dilute Aqueous Solution" by Donald P. Eichelberger.

# EMULSION POLYMERS INSTITUTE
Lehigh University

Graduate Research Progress Reports
No. 40 July 1993

## CONTENTS

Alice P. Gast Department of Chemical Engineering
Stanford University
Stanford CA 94305

**Abstracts:**

Glen A. McConnell, Alice P. Gast, and John S. Huang (1)
(1) Exxon Research and Engineering Corporation, Annandale NJ 08801

"Structure in Concentrated Polymeric Micelles"

Polystyrene/Polyisoprene (PS/PI) diblock copolymers suspended in decane form spherical micelles composed of a dense polystyrene core and a diffuse corona of polyisoprene. The thermodynamics of self-assembly are strongly regulated by the degree of polymerization of the polystyrene (insoluble) block. By varying the degree of polymerization of the polystyrene block relative to the polyisoprene block we generate micelles with coronal structures ranging from star-like to brush-like tethered chains. The alteration of tethered chain structure mediates interactions between micelles producing repulsions that vary in their length scale with respect to the core dimension. We probe the internal micellar properties and liquid-state micellar behavior through small angle scattering. At moderate concentrations, these micelles order in close-packed cubic structures in a manner similar to charged colloidal suspensions. We present a semi-quantitative phase diagram based on small angle X-ray diffraction experiments. In addition to the micellar phase behavior, we demonstrate that the application of a shear stress is adequate to induce microstructural transitions. One consequence of this imposed shear is the preferential crystallographic alignment of the micellar crystals yielding 2-dimensional diffraction patterns.

Stephen J. Nilsen, Alice P. Gast, and David J. Pine (1)
(1) Exxon Research and Engineering Corporation, Annandale NJ 08801

"Structure and Dynamics in Colloidal Dispersions"

Dispersions containing mixtures of polymers, particles, and solvent are ubiquitous precursors in materials processing and are often crucial to the manufacture of ceramics, cement,

inks, and coatings. These complex fluids typically exhibit a rich variety of structural and dynamical behavior arising from the interplay between microscopic forces such as those originating from dispersion, electrostatic, and hydrodynamic interactions. To gain insight into this synergy, we study a model system of an aqueous solution of highly charged, polystyrene particles. The screened Coulombic interaction in this system is well modeled by the Yukawa potential and is easily controlled via solution ionic strength to vary between its hard-sphere and plasma-like limits. The particle dynamics in these turbid suspensions is monitored using traditional dynamic light scattering techniques interpreted in the framework of diffusing wave spectroscopy. We study low volume fraction samples ($\phi \approx 0.04$) and monitor changes in particle dynamics with decreasing ionic strength. Comparison of our results to statistical mechanical predictions of the interparticle structure allows us to attribute the changes in dynamics to enhanced, long-ranged, liquid-like correlations.

Pamela B. Gaspers, Channing R. Robertson, and Alice P. Gast

"Enzymes on Insoluble Substrate Surfaces: Reaction and Diffusion"

Many biotechnological applications depend on the function of proteins near or on an interface. Much previous work has been aimed at the macroscopic events in protein adsorption such as isotherms and kinetics, but molecular scale studies on conformation, orientation, and lateral mobility have been limited. An interesting question arises when reactive proteins or enzymes are adsorbed onto surfaces that contain the enzyme's substrate. We have previously shown that proteins move on polymer surfaces and now we want to examine the interplay between reaction and diffusion. The goal of this project is to study proteins on surfaces at the molecular scale by probing the lateral diffusion of enzymes of the adsorbed protein. To further probe the mobility of enzymes at interfaces, we study a reactive protein on a surface that contains the enzyme's substrate. We use a model system of collagenase on an insoluble substrate surface. We make the substrate surface via a two step chemical process. First, we silanize a glass slide with 3-aminopropyltriethoxysilane and then we crosslink the carboxylic end of the peptide to the amine group using 1-ethyl-3(3dimethylaminopropyl) carbodiimide. Collagenase cleaves the synthetic peptide covalently attached to the surface.

We study the surface mobility of both an active and inactive collagenase enzyme. We measure lateral diffusion by a combined technique of total internal reflection fluorescence (TIRF) and fluorescence recovery after pattern photobleaching (FRAPP). Our diffusion experiments give us a time scale of diffusion at $10^{-4}$ s. We are working toward designing a multisurface system to allow us to measure the reaction rate of the protein on the surface.

By measuring both lateral diffusion and reaction rate, we can characterize the reactivity and mobility of the enzyme adsorbed on a surface.

Eric K. Lin and Alice P. Gast

"Morphology of Semicrystalline Diblock Copolymers in Dilute Solution"

In contrast with the spherical micelles formed by amorphous diblock copolymers in solution, diblock copolymers with a crystallizable block, such as poly(styrene)-poly(ethylene oxide) (PS/PEO), form lamellar aggregates having little curvature. The difference between these morphologies motivates our interest in understanding the strong effects crystalline order has on the self-assembly of diblock copolymers in solution. The objective of this work is to predict and understand different morphologies of semicrystalline diblock copolymers given the relative polymer block sizes, the concentration of the copolymers in solution, the solvent characteristics, and other system parameters. Additionally, the close packing of the amorphous block of the copolymer imposed by the crystallizable block results in the formation of a good experimental model for the study of polymer chains in highly stretched configurations or "polymer brushes."

As a first model of the morphology of these copolymer aggregates in dilute solution, we extended the calculations of Whitmore and Noolandi (1) describing the equilibrium structure of a semicrystalline diblock copolymer melt to include a solvent. The characteristics of the equilibrium system such as the thickness of the crystalline region, the local volume fraction of the amorphous block, and the number of folds per crystalline chain can be calculated from the minimization of the total free energy with respect to the crystalline thickness. The resulting calculations exhibited the expected trends and matched the predictions of the parabolic profile limit in its range of validity. Our calculations of the crystalline thickness also compare favorably with the thicknesses determined from small angle neutron and x-ray scattering of dilute solutions of lamellar aggregates. Future work on these systems will include further experiments to test these computational results, the development of new theoretical models to describe more complicated morphologies, and experiments using these copolymers as model systems of "polymer brushes."

(1) Whitmore, M. D. and J. Noolandi, *Macromolecules* 1988, *21*, 1482.

# The Pulsed-Laser Polymerization of Styrene in Microemulsions

Bart G. Manders, Alex M. van Herk, Anton L. German

*Eindhoven University of Technology, P.O. Box 513, 5600 MB Eindhoven, The Netherlands*

The optical transparency of microemulsions, due to the small sizes of the droplets in such an emulsion, permits the use of photoinitiation. This has led to the application of the pulsed-laser polymerization (PLP) method[1,2] in experiments with these microemulsions. Holdcroft and Guillet[3] reported for the first time on PLP in a microemulsion in 1989, but the calculation of their monomer concentration was not straightforward because of the addition of solvent and cosurfactant.

In this investigation a microemulsion of styrene and Aerosol OT (AOT) in water has been used at 60 °C with droplet sizes ranging from 5.7 to 30.8 nm. No solvents or cosurfactants were added. The droplet size was large enough[4] to ensure bulk phase physical properties. An oil-soluble photoinitiator (2,2-dimethoxy-2-phenylacetophenone) was used.

Three differences can be recognized in PLP experiments in microemulsion compared to experiments in bulk. Up to four peaks can easily be discerned in the resulting molecular weight distributions as a result of the laser pulses, whereas in bulk the maximum is two. Also, there is no low-molecular-weight tailing, which is present in the bulk experiments. Finally, a high-molecular-weight peak appears in the microemulsion molecular weight distributions that is absent in bulk. These phenomena can be explained by the compartmentalization of the radicals in microemulsion droplets.

Obviously, there is little tendency to terminate radicals in between laser pulses in a microemulsion. If individually compartmentalized radicals are not prone to termination, the main chain termination event will be transfer to monomer, followed by exit of a low-molecular-weight radical and reentry into another growing particle[5].

Results are summarized in Table 1. In order to obtain a $k_p$ value, the inflection points at the low-molecular-weight side of the PLP molecular weight distributions were used, also in the case of the microemulsions. Only in the case of the smallest droplet sizes a clear deviation of $k_p$ from bulk values of $k_p$= 354 L·mol$^{-1}$·s$^{-1}$ can be seen. Here it seems that the degree of polymerization $k_p \cdot C_m \cdot t_0$, which is approximately 440, can only be reached after almost complete conversion of the monomer present in the original droplet. This could lead to lower (apparent) $k_p$ values because the monomer concentration would drop significantly below the average concentration as seen over the droplets. However, because the experiments with larger microemulsion droplet sizes do not show such a strong devi-

ation, together with the fact that diffusion is slower for these larger droplets, one could argue that the diffusion rate of monomer on the time scale of a propagational step is more than sufficient for the small microemulsion droplets, so one can assume that the monomer distribution is in thermodynamic equilibrium. Nevertheless, some effects on the equilibrium concentration of the monomer can be expected (Morton equation[6]) for these small droplets, possibly influencing the $k_p$ measurement.

On the other hand, an explanation of the deviations in the obtained $k_p$ value for the smallest droplets could be found in the very small volume the radicals are confined to in the microemulsion[7,8] (e.g. one radical in a 10 nm diameter droplet leads to a "bulk" radical concentration of $3 \cdot 10^{-3}$ mol·L$^{-1}$). With computer simulations in bulk a shift could be seen for the degree of polymerization $k_p \cdot C_m \cdot t_0$ from inflection point to peak maximum for such very high radical concentrations.

Some interesting additional information showed up in the determination of $k_p$ through PLP in microemulsions. From these experiments rate constants of transfer to monomer could be determined. The high-molecular-weight peaks, appearing in the microemulsion molecular weight distributions, are a result of termination by chain transfer to monomer. From a molecular weight distribution of an experiment with one radical per microemulsion droplet a value of $k_{tr}$ of $6.05 \cdot 10^{-2}$ L·mol$^{-1}$·s$^{-1}$ has been determined, according to the procedure of Lichti et al[9]. The slope from which $k_{tr}$ was calculated is constant over a molecular weight ranging from $1 \cdot 10^6$ to $4 \cdot 10^6$. With a higher initiator concentration, leading to more than one initiator molecule in a microemulsion droplet, the data can be treated similarly, leading to a $k_{tr}$ value of $3.3 \cdot 10^{-2}$ L·mol$^{-1}$·s$^{-1}$, with a slope constant from molecular weight $1 \cdot 10^6$ to molecular weight $9 \cdot 10^6$.

Pulsed-laser experiments performed in microemulsions give extra information as compared to bulk PLP experiments, due to the compartmentalization of the radicals. These experiments appear to be a promising way of determining the rate constant of transfer to monomer. For the smallest droplet sizes (6 nm) a large deviation can be seen for the apparent $k_p$. The reason for this deviation could be the change of monomer concentration in the droplets. Also the small volume the radicals are confined to could be of importance. Further research is necessary in order to explain this.

Table 1. Pulsed-Laser Polymerizations of styrene in microemulsions (ME) prepared with 20 g of water and 1 g of AOT and in bulk (BU) with 2,2,-dimethoxy-2-phenylacetophenone as photoinitiator at 60 °C

| Experiment[a] | $m_{sty}$[b] g | d[c] nm | [DMPA][d] mol·L$^{-1}$ | $N_i$[e] | $N_m$[f] | f[g] Hz | t[h] min | Φ[i] in % | $k_p$[j] L·mol$^{-1}$·s$^{-1}$ |
|---|---|---|---|---|---|---|---|---|---|
| ME (1) | 2,20 | 13,2 | $1{,}4\cdot10^{-2}$ | 10 | 5924 | 5 | 1 | 1,2 | 328 |
| ME (2) | 2,20 | 13,2 | $1{,}4\cdot10^{-2}$ | 10 | 5924 | 10 | 1 | 2,6 | 338 |
| ME (3) | 0,95 | 5,7 | $1{,}7\cdot10^{-1}$ | 8 | 488 | 5 | 5 | 1,0 | 260 |
| ME (4) | 0,95 | 5,7 | $1{,}7\cdot10^{-1}$ | 8 | 488 | 5 | 5 | 1,0 | 265 |
| ME (5) | 3,01 | 18,2 | $5{,}3\cdot10^{-3}$ | 10 | 15886 | 5 | 5 | 6,5 | 340 |
| ME (6) | 4,73 | 30,8 | $4{,}7\cdot10^{-2}$ | 433 | 76995 | 5 | 5 | 3,7 | 351 |
| BU (1) | | | $1{,}2\cdot10^{-3}$ | | | 5 | 5 | 0,1 | 360 |
| BU (2) | | | $5{,}3\cdot10^{-3}$ | | | 5 | 5 | 0,1 | 351 |
| BU (3) | | | $1{,}4\cdot10^{-2}$ | | | 10 | 1 | 0,1 | 352 |

a) Kind and (number) of experiment.
b) Mass of styrene added to 20 g of water and 1 g of AOT to form the microemulsion.
c) Diameter of microemulsion droplets.
d) Concentration of DMPA.
e) $N_i$ = number of initiator molecules per microemulsion droplet.
f) $N_m$ = number of monomer molecules per microemulsion droplet.
g) f = frequency of laser pulse repetition.
h) t = cumulative polymerization time.
i) Fractional monomer conversion.
j) Propagation rate coefficient $k_p$ as determined from the inflection points of the molecular weight distributions after correction for conversion[10].

*References:*


1. O.F. Olaj, I. Bitai, F. Hinkelmann, *Makromol. Chem.* **188**, 1689 (1987)

2. O.F. Olaj, I. Bitai, *Angew. Makromol. Chem.* **155**, 177 (1987)

3. S. Holdcroft, J.E. Guillet, *J. Polym. Sci., Part A: Polym. Chem.* **28**, 1823 (1990)

4. R. Schomäcker, *Nachr. Chem. Tech. Lab.* **40**, 1344 (1992)

5. I. Lacik, B.S. Casey, D.F. Sangster, R.G. Gilbert, D.H. Napper, *Macromolecules* **25**, 4065 (1992)

6. M. Morton, S. Kaizerman, M.W. Altier, *J. Colloid. Sci.* **9**, 300 (1954)

7. B.G. Manders, A.M. van Herk, A.L. German, J. Sarnecki, R. Schomäcker, J. Schweer, *Makromol. Chem., Rapid Commun.*, in press

8. J. Schweer, B.G. Manders, A.M. van Herk, to be published

9. G. Lichti, R.G. Gilbert, D.H. Napper in: *Emulsion polymerization*, I. Piirma, Ed., Academic Press, New York, 1982, p. 93

10. I. Schnöll-Bitai, O.F. Olaj, *Makromol. Chem.* **191**, 2491 (1990)

Contribution to the IPCG Newsletter from
the Sydney University Polymer Centre
Reporter: Bob Gilbert
Chemistry School, Sydney University, NSW 2006, Australia.

The following abstracts from various members of the SUPC summarize current research directions.

*Measurement of propagation rate coefficients using pulsed-laser polymerization and matrix-assisted laser desorption/ionization mass spectrometry*. P.O. Danis, D.E. Karr, D.G. Westmoreland, M.C. Piton, D.I. Christie, P.A. Clay, S.H. Kable and R.G. Gilbert. Macromolecules, in press.
Abstract: Matrix-assisted laser desorption/ionization (MALDI) mass spectrometry is applied as a tool in the measurement of propagation rate coefficients by pulsed-laser polymerization (PLP), which requires a knowledge of the number molecular weight distribution for relatively low molecular weight species. It is found that MALDI has the sensitivity to give a sufficiently precise point of inflection in the molecular weight distribution (at about 8000 amu) and can therefore provide a means of obtaining propagation rate coefficients in a way that obviates some of the disadvantages of the GPC analysis hitherto used for this purpose.

*Entry and exit rate coefficients in butyl methacrylate emulsion polymerizations*. S Patrick and R G Gilbert. A series of seeded emulsion polymerizations on butyl methacrylate have been carried out with chemical initiator to measure the rate coefficients for entry (initiator efficiency) and exit (desorption). The results for this new monomer are in excellent accord with models previously proposed and tested on styrene and MMA [I.A. Maxwell, B.R. Morrison, D.H. Napper, R.G. Gilbert, *Macromolecules*, **24**, 1629 (1991); B.S. Casey, B.R. Morrison, R.G. Gilbert, *Prog. Polym. Sci.*, **18**, 1041 (1993)].

*Measurement and meaning of rate coefficients controlling molecular weights in free-radical polymerizations*. Johan P A Heuts, David I Christie, Paul A Clay, Mark C Piton, Jelica Hutovic, Scott H Kable and Robert G Gilbert (plenary lecture at Third Pacific Polymer Conference).
Abstract: The molecular weight distribution in a free-radical polymerization is controlled by the rate coefficients for radical creation from initiator, propagation, and chain-stoppage events: termination by combination and disproportionation, and transfer (to monomer, chain transfer agent or polymer). Prediction of the MWD can be carried out from knowledge of these rate coefficients (including dependences on chain length, etc.), but literature compilations are uncritical and show a wide range of values under what are ostensibly the same conditions. An IUPAC Working Party has begun to establish reliable values and measurement techniques for some of these quantities. We give new data for some of these polymerization reactions. *Propagation*. Pulsed-laser polymerization (PLP) is a particularly reliable method for determining $k_p$. Attempts to use PLP on acrylates have hitherto failed. We have found that consistent data can be obtained for butyl acrylate (BA) using PLP at very low temperatures (–40 to –10 °C). *Transfer*. Although the traditional means of obtaining $k_{tr}$ has been from the *average* molecular weight in a polymerizing system, we show that considerably more information can be obtained from the complete molecular weight distribution. Accurate values of $k_{tr}$ are found from the high molecular weight limit of the MWD; moreover, the PLP technique provides a good means of carrying out such measurements.

* The following publications have appeared since the previous Newsletter from various members of the SUPC (with their publication details):

Solvent effects on the propagation rate coefficient for free-radical polymerization. B.R. Morrison, M.C. Piton, M.A. Winnik, R.G. Gilbert and D.H. Napper. *Macromolecules*, **26**, 4368-72 (1993).

Pulsed laser study of the propagation kinetics of acrylamide and its derivatives in water. P. Pascal, M.A. Winnik, D.H. Napper and R.G. Gilbert. *Macromolecules*, **26**, 4572-6 (1993).

Diffusion of oligomeric species in polymer solutions. M.C. Piton, R.G. Gilbert, B. Chapman and P.W. Kuchel. *Macromolecules*, **26**, 4472-7 (1993).

Chain-length dependent termination rate processes in free-radical polymerizations: II - Modeling methodology and application to methyl methacrylate emulsion polymerizations. G.T. Russell, R.G. Gilbert and D.H. Napper. *Macromolecules*, **26**, 3538-52 (1993).

The role of aqueous-phase kinetics in emulsion polymerizations. B S Casey, B R Morrison and R G Gilbert. *Progress in Polymer Science*, **18**, 1041-96 (1993).

Small angle neutron scattering studies of inhomogeneities in latex particles from emulsion homopolymerizations. M.F. Mills, R.G. Gilbert, D.H. Napper, A. R. Rennie and R.H. Ottewill. *Macromolecules*, **26**, 3553-62 (1993).

Spatial inhomogeneities in emulsion polymerizations: Repulsive wall calculations. C.A. Croxton, M.F. Mills, R.G. Gilbert and D.H. Napper. *Macromolecules*, **26**, 3563-71 (1993).

INTERNATIONAL POLYMER COLLOIDS GROUP NEWSLETTER

Contribution from
Hideki Matsuoka, Department of Polymer Chemistry,
Kyoto University, Kyoto 606-01,
Kensaku Ito, Department of Chemical and Biochemical Engineering,
Toyama University, Toyama 930,
and
Toshiki Konishi and Norio Ise,
Fukui Research Laboratory, Rengo Co. Ltd.,
10-8-1 Jiyūgaoka, Kanazu-cho,
Sakai-gun, Fukui 919-06, Japan

Reporter: Norio Ise

## Bonse-Hart Type Ultra-small-angle X-ray Scattering of Colloidal Dispersions with Synchrotron Radiation Source

Polymethylmethacrylate-based latex aqueous dispersions were studied with synchrotron radiation in a very low angle region. The particle dispersion in ordered state showed several distinct Bragg peaks in addition to particle scattering. From the relative positions of the peaks, the lattice system was concluded to be of a face-centered cubic lattice at 3.3 %. (H. Mastuoka et al. Photon Factory Activity Report, No. 9, 331 (1991))

The synchrotron radiation source was used in combination with a sagital focusing device for a study of polystyrene-based latex particles in aqueous dispersions. It was possible to obtain a clear peak and a maximum of these dispersions with a short accumulation time (10 sec), which could not be studied without the focusing device. The method was further applied to polymethylmethacrylate-based latex particles and silica particles. (H. Matsuoka et al. Photon Factory Activity Report, in press.)

## Small-angle and Ultra-small-angle X-ray Scattering Study of the Ordered Structure in Polyelectrolyte Solutions and Colloidal Dispersions

The small-angle and ultra-small-angle X-ray scattering studies of ionic polymer solutions and colloidal dispersions were reviewed. The single, broad peak was observed in the small-angle region, which was attributed to ordering of the ionic polymers. From the Bragg spacing being smaller than the average spacing, the two-state structure was suggested (N. Ise et al. J. Am. Chem. Soc., 102, 7901 (1980)). A paracrystal theory was developed for three-dimensional lattice systems, by which the observed single, broad peak was rationalized to be due to highly distorted ordered structures (H. Matsuoka et al., Phys. Rev. B36, 1754 (1987); Phys. Rev., B41, 3854 (1990)). The Bonse-Hart type ultra-small-angle X-ray scattering apparatus (H. Matsuoka et al.

Proc. Natl. Acad. Sci. USA, 88 6618 (1991)), by which a micron-size density fluctuation can be investigated, was applied to structural studies of latex dispersions, polymer alloy and metal alloys. A distinct upturn was observed at low angles by small-angle neutron scattering method for salt-free polystyrenesulfonate solutions. This justifies the two-state structure, and the size of the localized structure was approximately determined from the Guinier plots. Attention was drawn to direct microscopic study of polymer latex dispersions, which provided compelling evidence of the two-state structure. Various counterinterpretations of the single, broad scattering peak were critically discussed. (H. Matsuoka, N. Ise, Advances in Polymer Science, in press.)

## Neutron Scattering Study of Polystyrenesulfonate Solutions at Very Low Angles

Small-angle neutron scattering studies were performed for sodium polystyrenesulfonate-$D_2O$ solutions. A steep upturn was observed at very small angles below 0.01 $Å^{-1}$, in addition to an intermacroion interference peak at 0.04 - 0.10 $Å^{-1}$. The peak position was consistent to that found in our previous SAXS study (N. Ise, et al. J. Chem. Phys., 81, 3294 (1984). The upturn was attributed to the presence of localized ordered structures in solutions. Its radius of gyration was estimated to be in the range of 400 and 1000 Å by Guinier, Debye-Bueche, and Porod analyses. Model calculations were performed to estimate the number density of the localized ordered structures by using absolute scattering intensity. (H. Matsuoka, D. Schwahn, N. Ise, Macro-Ion Characterization: From Dilute Solutions to Complex Fluids, K. S. Schmitz, Ed. ACS Monograph, 1994, in press)

## Further Study of Void Structures in Latex Dispersion

By using a confocal laser scanning microscope, an exploratory study was performed of the time evolution of void structures in highly purified polymer latex dispersions. Very huge ($\simeq$ 50 x 150 x 50 $\mu$m), stable voids were found to exist in the dispersion. In such dispersions, which were initially homogeneous, the voids were seen to grow with time when the dispersions were kept standing and were formed more quickly internally than close to the glass-dispersion interface. Void formation is thus confirmed not to be an artifact due to the interface effect. It is reminded that the long time scale of the motion of latex particles and their size enabled us to make real time microscopic observation of the structural inhomogeneity. In light of very long time scale of the life-span of void structures in colloidal dispersions, the presence of void cannot be ignored, if the

thermodynamic properties of the dispersions are to be correctly understood. A similar kind of structural inhomogeneity, in apparently homogeneous systems, is discussed for simple ionic solutions, ionic polymer solutions, and Langmuir-Blodgett films. (K. Ito, H. Yoshida, N. Ise, Science in press)

## Dynamic Light Scattering and SAXS Study of Salt-free Polystyrenesulfonate Solution: Effect of Filtration

The two-state structure (coexistence of ordered and disordered regions) was concluded by us for polystyrenesulfonate solutions on the basis of small-angle X-ray scattering data (N. Ise, H. Matsuoka et al., J. Chem. Phys., 81, 3294 (1984)). Such a structural inhomogeneity was directly confirmed for polymer latex dispersions by microscopy. The microscopy shows the coexistence of almost freely moving particles and very slowly moving ordered structures. For such solutions, two diffusion coefficients may be observed. This has been substantiated by dynamic light scattering (DLS) for polystyrenesulfonate. Recently Reed et al. reported that the slow mode could not be observed if the sample solutions were filtrated by using a 0.05 $\mu$m filter, and claimed that the slow mode is due to aggregates filterable by membrane (W. F. Reed et al., Macromolecules, 25, 806 (1992); Biopolymers, 32, 1105 (1992)). This interpretation is in contradiction with microscopic observation on latex dispersions, which shows rather dynamic nature of the localized ordered structures. Thus we carried out DLS and SAXS studies with and without filtration.

According to UV measurements, the polymer concentration of a salt-free (0.001 g/ml) solution of sodium polystyrenesulfonate (Pressure Chemicals, $M_w$ = 177,000) has not changed by filtration with a 0.05 $\mu$m filter (MF-Millipore). This is in contrast to Reed et al.'s observation. The time correlation function could be reproduced by assuming two exponential functions, indicating that there exist two diffusion modes. The slow diffusion coefficient ($D_1$) was about $3 \times 10^{-8}$ cm$^2$/sec whereas the fast one ($D_2$) was $3 \times 10^{-6}$ cm$^2$/sec. The $D_1$ value was practically constant even when filtration was performed with 0.025 and 0.1 $\mu$m filters, whereas the order of magnitude of $D_2$ stayed unchanged by the filtration. The sizes of diffusing entities (free macroions and localized ordered structure, according to our interpretation) were estimated, though very approximately, to be about 0.1 ~ 0.2 $\mu$m for $D_2$ and 15 ~ 20 Å for $D_1$, respectively. The size of the localized ordered structure is much larger than the pore size. Thus the slow mode is not due to filterable aggregates or impurities. Our interpretation is that the localized ordered structures were broken by filtration and regenerated after filtration. Such a situation is judged to be very likely on the basis of dynamic characters of the localized structure of latex particles observed by microscopy.

The SAXS study at 0.04 g/ml indicated no change in the peak position and height on filtration (with 0.2 and 0.1 $\mu$m filters). This implies that the intermacroion spacing was not changed and probably the size of the localized structure was not affected, either.

It was thus concluded that the two-state structure, or the simultaneous existence of the two diffusion modes, is not an artifact that is caused, for example, by aggregates or impurities as Reed et al. claimed, but a genuine property of ionic solutions or dispersions. There remains a question why the slow mode disappeared in the experimental treatment by Reed et al. (H. Matsuoka, H. Tomita, N. Ise, to be published; H. Matsuoka, Y. Nakatani, N. Ise, to be published.)

## Determination of Particle Size and Size Distribution by Ultra-Small X-ray Scattering

By using the infinitely thin and long beam approximation, the scattering data obtained by our ultra-small-angle X-ray (USAXS) apparatus were desmeared. Colloidal silica spheres (KE-P10, Nihon Shokubai Co. Ltd., Osaka, Japan) were investigated in the powder state and their scattering data were desmeared. The results were compared with theoretical form factors. With the radius R = 570 Å and the standard deviation = 9.5 %, an excellent agreement was reached by a curve fitting procedure, while the diameter given by the producer was 0.1 $\mu$m. This technique to measure the size and its distribution excels the conventional ones using electron microscopy in that the former method furnishes more reliable results from an incomparably larger number of populations than the latter. In comparison with the electron micrography, which deals with solid samples only, it is to be noted, the scattering technique can be applied to the determination of the particle size and its distribution in solutions or in dispersions as well as in dried samples. (T. Konishi, H. Matsuoka, N. Ise, to be published.)

**Progress in Colloid & Polymer Science** Progr Colloid Polym Sci 91:149–152 (1993)

# Dynamic light scattering by non-ergodic media

J. G. H. Joosten

Department for Physical and Analytical Chemistry, DSM Research, Geleen, The Netherlands

*Abstract*: The basic notions of dynamic light scattering (DLS) on non-ergodic media are presented and discussed. We present the results, obtained by DLS, for the intermediate scattering function of polystyrene latex particles that are dispersed in aqueous polyacrylamide gels. It is shown that these systems display non-ergodic features, implying that the time-averaged intensity correlation function (ICF) is not equal to the ensemble-averaged ICF.

*Key words:* Light scattering – non-ergodic media – gels – tracer diffusion

# Inversion of Static Light Scattering Measurements for Particle Size Distributions

ROBERT FINSY,*,[1] LUC DERIEMAEKER,* ERIC GELADÉ,† AND JACQUES JOOSTEN†

**Theoretical Physical Chemistry, Vrije Universiteit Brussel, Pleinlaan 2-B-1050 Brussels, Belgium and †Department for Physical and Analytical Chemistry, DSM—Research, P.O. Box 18—N-6160 MD Geleen, The Netherlands*

Received June 25, 1991; accepted March 12, 1992

The inversion of static light scattering measurements (SLS) for the evaluation of particle size distributions is reported. The performances of two inversion methods, i.e., the maximum entropy method and a constrained regularization method (Contin), are illustrated with simulated data and experiments on samples with unimodal, bimodal, and trimodal distributions of spherical particles and on a sample with a broad size distribution. Some experimental results are compared to assessments by photon correlation spectroscopy (PCS) and electron microscopy (EM). It appears that a significantly better resolution in particle size is obtained by SLS than by PCS. However, for a sample with a broad distribution in particle sizes, not all details of the distribution observed by EM were resolved. 

# Behavior of Low Molecular Weight Model Heur Associative Polymers in Concentrated Surfactant Systems

A. P. Mast,*,† R. K. Prud'homme,‡ and J. E. Glass§

*DSM Research, Department FA-GF, P.O. Box 18, 6160 MD Geleen, The Netherlands, Department of Chemical Engineering, Princeton University, Princeton, New Jersey 08544; and Polymers and Coatings Department, North Dakota State University, Fargo, North Dakota 58105*

*Received January 31, 1992. In Final Form: December 7, 1992*

The interaction between hydrophobically modified water-soluble polymers and surfactants has gained a growing interest in recent years. In this paper we present our results on the behavior of hydrophobically modified ethoxylate urethanes (HEUR) in concentrated surfactant systems, using an ethoxylated sulfate surfactant. The HEUR's differ in hydrophobic group, molecular weight, extent of modification, and polydispersity. As will be clear from our results the purification and characterization of these polymers are very difficult but also essential for the understanding of the characteristic behavior of these materials. Our experimental results from rheological experiments, phase-behavior, and flow birefringence are presented. Furthermore a mechanism describing the interaction between the surfactants and polymers will be discussed.

# Fiber Optic Dynamic Light Scattering (FODLS); neither Homodyne nor Heterodyne

Leon G.B. Bremer[1,2], Luc Deriemacker[1], Robert Finsy[1], Erik Geladé[2], Jacques G.H. Joosten[2]

1 Theoretical Physical Chemistry, Vrije Universiteit Brussel, Pleinlaan 2, B-1050 Brussel, Belgium

2 Department for Physical, Analytical and Computational Chemistry, DSM Research, P.O. Box 18, 6160 MD Geleen, The Netherlands

## Abstract

Homodyne and heterodyne fiber-optic dynamic light scattering (FODLS) techniques are studied using concentrated dispersions of mono-disperse latices. It is shown that pure homodyne or heterodyne detection cannot be achieved in many situations. Analysis of the data with a singular value decomposition method shows that the results may constitute of a homodyne and a heterodyne contribution. The proportion of both contributions can be calculated from the intercept of the autocorrelation function (ACF). If the ratio between both contributions is known the field ACF can be calculated from the data. This method is used to analyze measurements of mono-disperse latices and of binary mixtures of mono-disperse latices.

# PARTICLE SIZING BY PHOTON CORRELATION SPECTROSCOPY

## Part IV : Resolution of bi-modals and comparison with other particle sizing methods.

Robert FINSY [1], Luc DERIEMAEKER [1], Nicolas DE JAEGER [2], Rik SNEYERS [2], Jan VANDERDEELEN [3], Paul VAN DER MEEREN [3], Hugo DEMEYERE [4], Jeanine STONE-MASUI [5], Anne HAESTIER [5], Julius CLAUWAERT [6], Walter DE WISPELAERE [7], Pascal GILLIOEN [8], Sabine STEYFKENS [9], Erik GELADÉ [9]

1 Prof. Dr. R. Finsy, Ing. Luc Deriemaeker, Vrije Universiteit Brussel, Theoretische Fysische Scheikunde, Pleinlaan 2 - 1050 Brussel, Belgium.
2 Ing. N. De Jaeger, Ing. R. Sneyers, Agfa-Gevaert N.V., Colloid Department 3179, Septestraat 27 - 2640 Mortsel, Belgium.
3 Dr. J. Vanderdeelen, Dr. P. Van der Meeren, Senior Research Assistant NFWO, Universiteit Gent, Faculteit Landbouw, Laboratorium Fysische en Radiobiologische Chemie, Coupure 653 - 9000 Gent, Belgium
4 Ing. H. Demeyere, Procter and Gamble, European Technical Center, Temselaan 100 - 1820 Strombeek-Bever, Belgium
5 Dr. J. Stone-Masui, Research Associate FNRS, Dr. A. Haestier, Université Catholique de Louvain, Faculté des Sciences Agronomiques, Unité de Chimie des Interfaces, Place Croix du Sud 2 - 1348 Louvain-La-Neuve, Belgium
6 Prof. Dr. J. Clauwaert, Universitaire Instelling Antwerpen, Departement Biochemie, Universiteitsplein 1 - 2610 Wilrijk
7 Ing. W. De Wispelaere, Analis, Leeuwerikstraat 28 - 9000 Gent, Belgium
8 Ing. P. Gillioen, Thermo Instrument B.V., Spinnerslaan 2A - 9160 Lokeren, Belgium
9 Ing. S. Steyfkens, Dr. E. Geladé, DSM-Research, P.O. Box 18 - 6160 MD Geleen, The Netherlands.

## ABSTRACT

The practical performances of single and multi-angle Photon Correlation Spectroscopy for resolving bi-modal distributions of industrial PMMA samples was investigated in a comparative study by several users from the academic and industrial world and by two suppliers of commercial equipment. The results for the harmonic intensity averaged diameters obtained by cumulants analysis reported by the different laboratories are in agreement as well as the results for the normalized second cumulants. The uncertainty on the latter quantities is however large. For the bi-modal samples with two populations with average diameters in a ratio of about 2.5 to 1, not all users were able to resolve the distribution in its components by single angle PCS. Some slight improvement was obtained by multi-angle PCS. Other indirect techniques (Polarisation Intensity Differential Scattering, Static Light Scattering data and Disk Photosedimentometer) appeared to be superior for resolving the bi-modal distributions.

# Contribution to IPCG Newsletter

by

**Dr. Peter A. Lovell**

Polymer Science & Technology Group, Manchester Materials Science Centre
University of Manchester & UMIST, Grosvenor Street
Manchester, M1 7HS, United Kingdom

## *Mechanical Properties of Rubber-Toughened Acrylic Polymers : An Overview*

*Sponsors:* Science & Engineering Research Council, ICI Acrylics

*Collaborator:* Professor Robert J. Young

*Research worker:* Matthew N. Sherratt

Rubber-toughened poly(methyl methacrylate) (RTPMMA) materials have been produced by blending PMMA with separately-prepared toughening particles, thereby allowing independent control of the properties of the matrix PMMA, the composition, morphology and size of the dispersed rubbery phase, and the level of inclusion of the toughening particles [1,2]. A range of nine different types of toughening particle have been prepared by sequential emulsion polymerisation (see *Figure 1*) and blended at four levels with Diakon LG156 (poly[(methyl methacrylate)-*co*-(n-butyl acrylate)] with 8 mol% n-butyl acrylate repeat units). An overview of the results from mechanical testing of these RTPMMA materials is presented here.

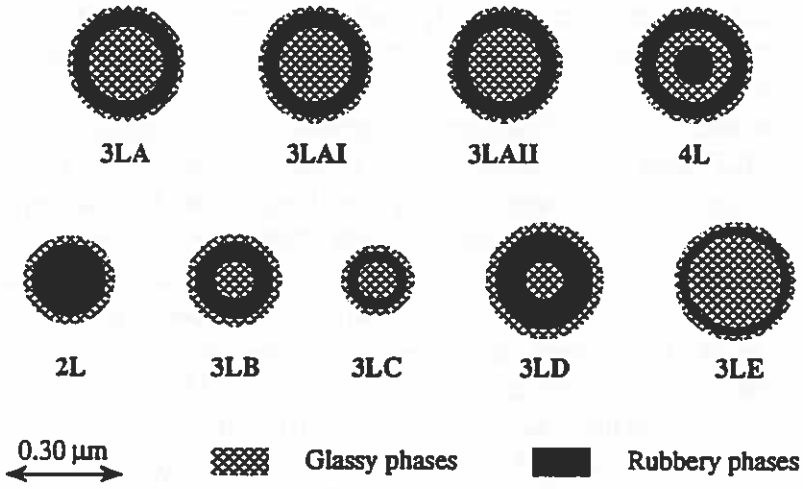


**Figure 1.** Schematic diagrams of sections through the equators of the two-, three- and four-layer (i.e. 2L, 3L and 4L) toughening particles showing their sizes and internal structures. In order to retain a high percentage transmission of visible light in the RTPMMA materials, the compositions of the rubbery and glassy phases of the particles were chosen such that their refractive indices match that of the matrix PMMA. The rubbery layers consist of crosslinked poly[(n-butyl acrylate)-*co*-styrene] and the glassy layers consist of poly[(methyl methacrylate)-*co*-(ethyl acrylate)], the inner glassy layers being crosslinked. Each layer is graftlinked to the other layers with which it is in contact. With the exception of the 3LAI and 3LAII particles, allyl methacrylate (ALMA) was used at constant levels for both crosslinking and graftlinking. In the preparation of the 3LAI particles, ALMA was used at higher-than-normal levels in the interfacial regions in order to increase the interfacial strength, whereas the 3LAII particles were prepared with ALMA at normal levels in the interfacial regions but replacing ALMA for crosslinking the bulk of the glassy and rubbery phases by identical molar quantities of ethan-1,2-diol dimethacrylate and hexan-1,6-diol diacrylate respectively.

Tensile testing reveals that, with the exception of 3LAII particles, each type of toughening particle is capable of inducing large-scale yielding in the matrix PMMA leading to much greater fracture strains (up to 30-50%, compared to 3% for the unmodified matrix PMMA) and greatly increased energies to fracture. The poor performance of the 3LAII materials (ca. 8% ultimate elongation for particle weight fractions > 0.20) results from the change in the chemistry of crosslinking in 3LAII particles which leads to a much higher crosslink density [3]. Although the other types of particle give ductile RTPMMA materials, there are significant differences in deformation behaviour.

The values of Young's modulus ($E$) and yield stress ($\sigma_y$) obtained from tensile testing are shown in *Figure* 2 together with the impact values of critical strain energy release rate ($G_{Ic}$). In each case, the data are plotted against the volume fraction of rubber ($V_r$), which excludes both the outer and internal glassy phases. Inspection of *Figures* 2*a* and 2*b* shows that $E$ and $\sigma_y$ are largely controlled by $V_r$ with small affects arising from particle size/morphology. In contrast, examination of *Figure* 2*c* reveals that $G_{Ic}$ depends strongly upon particle size/morphology.

Comparison of the results for the 2L and 3LB materials reveals that the effect of introducing a glassy core into a homogeneous rubbery particle is to increase $E$, $\sigma_y$ and $G_{Ic}$ for a given level of particles. The effects of particle size are apparent from comparison of the properties of the RTPMMA materials prepared from the 3LB, 3LC, and 3LD particles, which have 100 nm diameter glassy cores with rubbery-layer diameters of 202, 152 and 255 nm respectively. The values of $E$ and $\sigma_y$ show no dependence upon particle size. There is, however, a strong dependence of $G_{Ic}$ upon particle size, with the smallest particles (3LC) giving rise only to small increases in $G_{Ic}$ compared to the matrix PMMA. The increase in size from 3LC to 3LB particles leads to a major increase in $G_{Ic}$. The further increase in size from 3LB to 3LD particles leads to a much smaller increase in $G_{Ic}$, the increase arising mainly from the increased volume fraction of rubber. By considering the mechanical properties of the 3LA, 3LD and 3LE materials it is possible to examine the effects of glassy core diameter (200, 100 and 244 nm respectively) in three-layer toughening particles with approximately constant rubbery-layer diameter (284, 255 and 290 nm respectively). The increase in glassy core size leads to major increases in $E$, $\sigma_y$ and $G_{Ic}$ for a given level of particles, though the increases in $E$ and $\sigma_y$ arise mainly from decreases in $V_r$. The increase in $G_{Ic}$, however, is more evident when considered in terms of $V_r$, showing that increasing the glassy core size leads to more efficient use of the rubber. Hence, for the 3LE materials, the increase in $G_{Ic}$ is achieved with relatively small reductions in $E$. The introduction of a rubbery core into the inner glassy phase of 3LA particles has no major effect upon mechanical properties, and would appear to have advantage only in terms of circumventing the earlier patents covering these types of RTPMMA materials (compare *Ref.* 1*c* with *Refs.* 1*a* and 1*b*).

In addition to the effects of particle size/morphology, the effects of changing the crosslinking and graftlinking in the 3LA particles have been examined. The higher level of graftlinking at interfaces in the 3LAI particles leads to modest increases in $E$, $\sigma_y$ and $G_{Ic}$. The change of crosslinking agent from ALMA to hexan-1,6-diol diacrylate for the rubbery phases in the 3LAII particles, however, causes a dramatic loss of ductility with major decreases in $G_{Ic}$ to values not much greater than that of the matrix PMMA, though there is no major effect upon $E$. The reduction in toughness is most probably a consequence of the higher degree of crosslinking in the rubbery phase of the 3LAII particles [3].

In summary, the results from mechanical testing show that the toughness of RTPMMA under impact is strongly dependent upon the size, morphology and chemistry of the toughening particles, but that Young's modulus and yield stress are largely controlled by the volume fraction of rubber.

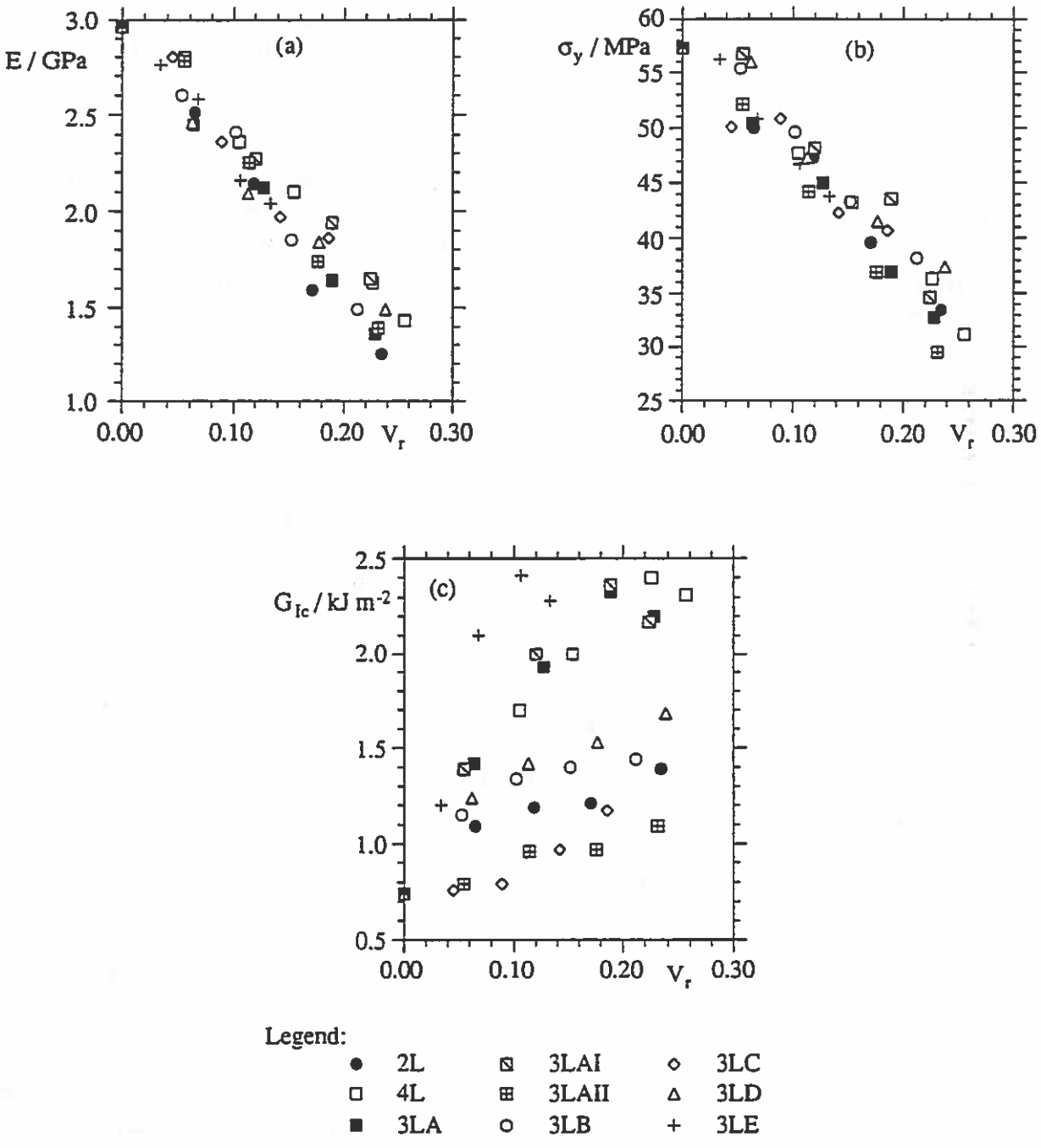


Figure 2. Plots of (a) Young's modulus ($E$), (b) yield stress ($\sigma_y$) and (c) 0.85 m s$^{-1}$ impact values of the critical strain energy release rate ($G_{Ic}$) against volume fraction of rubber ($V_r$) for each of the RTPMMA materials. [The matrix PMMA, the 3LAII materials, 2L11 and 3L10 did not yield and so fracture stresses have been plotted in (b) for these materials.]

Contribution to IPCG Newsletter
Peter A. Lovell, Manchester Materials Science Centre, University of Manchester & UMIST, UK

## *Phase Behaviour of Aqueous Poly(vinyl alcohol) Solutions*

*Sponsors:* Science & Engineering Research Council, Unilever plc

*Collaborator:* Professor Robert F.T. Stepto

*Research worker:* Kevin Frobisher

In order to establish conditions for controlled coating of oil-in-water microemulsion droplets by poly(vinyl alcohol), PVAl, the phase separation behaviour of aqueous PVAl solutions has been characterised in relation to percentage hydrolysis, molar mass, sodium chloride concentration and temperature.

Cloud point curves for poly(vinyl alcohol) samples of 12% residual acetate content are shown in *Figures 3a-3c*. For each set of conditions, the minimum of the curve defines the lower critical solution temperature, $T_c$ , and the critical volume fraction of PVAl, $\phi_{2c}$ . As expected, the cloud-point curves are skewed towards low volume fractions of PVAl and show trends for both $T_c$ and $\phi_{2c}$ to move to lower values as the molar mass of PVAl increases. Increasing the sodium chloride concentration for a given sample of PVAl moves $T_c$ to lower values but has no significant effect upon $\phi_{2c}$ .

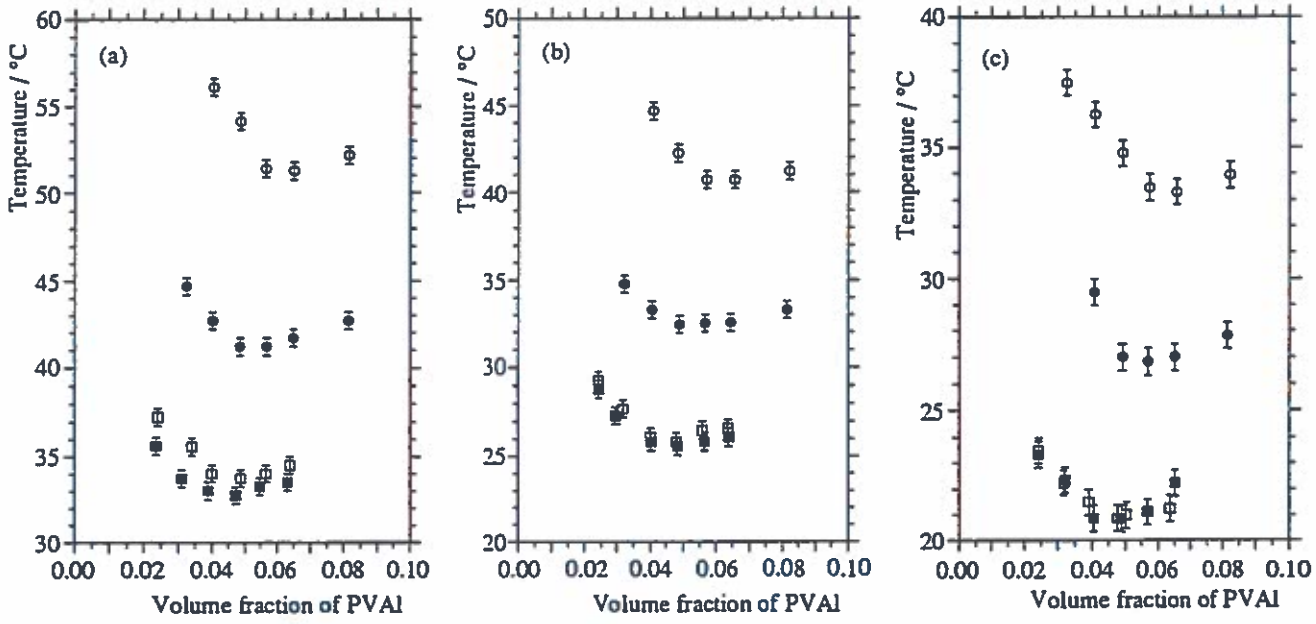


Figure 3. Effect of PVAl molar mass (o 10, • 25, □ 78 and ■ 125 kg $mol^{-1}$) upon the cloud-points for aqueous sodium chloride solutions of PVAl samples with 12% residual acetate content: (a) 1.026 mol $dm^{-3}$, (b) 1.368 mol $dm^{-3}$ and (c) 1.709 mol $dm^{-3}$ sodium chloride.

The critical conditions for phase separation of non-polar polymer solutions can be defined from Flory-Huggins theory [4]. However, for polar polymers in polar solvents, the contribution arising from dipole and/or ionic interactions must be taken into account. These interactions cause chain expansion, which is reduced in the presence of dissolved salt. Flory [4,5] developed a theory for chain expansion of polyelectrolytes which includes a contribution from ionic interactions and allows for the reduction in chain expansion due to screening of ionic interactions by mobile ions (i.e. added electrolyte) in solution. By

combining classical Flory-Huggins theory with the Flory theory for polyelectrolytes, the following equation has been derived for the dependence of critical temperature, $T_c$, upon chain length and salt concentration,

$$\frac{1}{T_c} = \frac{1}{\theta_{app}} + \frac{1}{\psi\theta}\left[\frac{1}{r^{1/2}} + \frac{1}{2r}\right] \qquad \textbf{Equation 1}$$

where

$$\frac{1}{\theta_{app}} = \frac{1}{\theta}\left[1 + \frac{1}{\psi}\left(\frac{C_I}{C_M}\right)\frac{1}{I_S}\right] \qquad \textbf{Equation 2}$$

in which $\theta$ is the theta (or Flory) temperature of the fully-screened polymer chain, $\psi$ is the Flory entropy parameter for polymer-solvent interaction, $r$ is the number of segments in a polymer chain, $C_M$ is the (non-polar) Flory-Fox constant which depends upon polymer segment density distribution, $C_I$ is a molecular constant that is proportional to the square of the number of polar sites in a polymer segment and $I_S$ is the ionic strength of with respect to mobile ions.

The second term in *Equation 2* vanishes when ionic/polar interactions are absent ($C_I = 0$) and/or when the ionic strength is sufficiently high to render negligible the effect of such interactions (i.e. $I_S \rightarrow \infty$). Under either of these conditions $\theta_{app} = \theta$ and *Equation 1* takes the form derived from classical Flory-Huggins theory. Hence, the temperature $\theta$ defines the unperturbed state of the fully-screened polymer chain. The ratio $C_I/C_M$ may be considered as a constant that depends upon chain structure and, in particular, the balance between ionic/polar and non-polar contributions to chain expansion.

*Figure 4a* shows that using *Equation 1* the $T_c$ data from *Figures 1a-1c* can be correlated with $r$ at specific salt concentrations to give values of $\theta_{app}$ that depend upon $I_S$. Since PVAl bears no permanent ionic charges, this observation may be ascribed to contributions from interactions between dipoles that are screened, in a similar manner to ionic interactions, by mobile ions. The values of $\theta_{app}$ have been correlated with $I_S$ according to *Equation 2*, as shown by the plot presented in *Figure 4b*. The intercept corresponding to $I_S = \infty$ gives $\theta = 275$ K for poly(vinyl alcohol) with 12% residual acetate content.

In summary, the effect of molar mass upon the lower critical solution temperatures of aqueous sodium chloride solutions of poly(vinyl alcohol) samples with 12% residual acetate content can be characterised in terms of a single theta temperature corresponding to the fully-screened chain, together with an entropy parameter and a constant that depends upon chain structure, both in terms of characteristic ratio and concentration of polar groups.

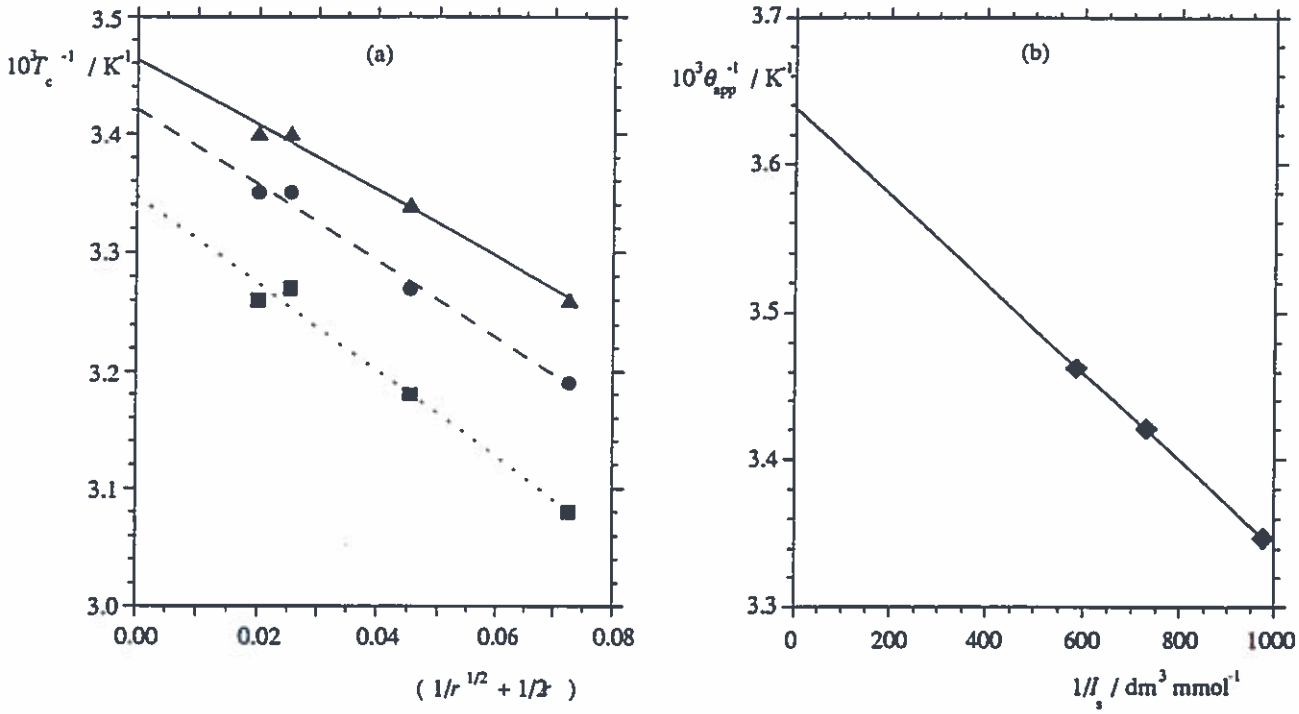


**Figure 4.** Analysis of critical-temperature data for aqueous sodium chloride solutions of PVAl samples with 12% residual acetate content using Equations 1 and 2. (a) Plot of $1/T_c$ against $1/r^{1/2} + 1/2r$ for: ■, 1.026 mol dm$^{-3}$; ●, 1.368 mol dm$^{-3}$; and ▲, 1.709 mol dm$^{-3}$ sodium chloride. (b) Plot of $1/\theta_{app}$ against $1/I_S$.

*References*

1. (a) Rohm and Haas Company, Brit. Patent No. 1 340 025 (1973);
   (b) Rohm and Haas Company, Brit. Patent No. 1 414 187 (1975);
   (c) E.I. Du Pont de Nemours and Company, Gt. Brit. Patent Appl. No.2 039 496A (1979)
2. P.A. Lovell, J. McDonald, D.E.J. Saunders and R.J. Young, *Polymer*, 34, 61 (1993)
3. F. Heatley, P.A. Lovell and J. McDonald, *Eur. Polym. J.*, 29, 255 (1993)
4. P.J. Flory, *Principles of Polymer Chemistry*, Cornell University Press, Ithaca, 1953
5. P.J. Flory, *J. Chem. Phys.*, 21, 162 (1953)

***Publications related to Polymer Colloids (April 1993 - September 1993)***

"Effects of Multiple-Phase Toughening-Particle Morphology upon the Properties of Rubber-Toughened Poly(methyl methacrylate)"

P.A. Lovell, J. McDonald, D.E.J. Saunders, M.N. Sherratt and R.J. Young
*Toughened Plastics I: Science & Engineering* (Ed. C.K. Riew and A.J. Kinloch), American Chemical Society, Advances in Chemistry Series, 233, 61-77 (1993)

# Synthesis and characterization of a short-haired poly(ethylene oxide)-grafted polystyrene latex

Marc C.L. Maste, Ans P.C.M. van Velthoven, Willem Norde, Johannes Lyklema
Department of Physical and Colloid chemistry, Wageningen Agricultural University, P.O. Box 8038, 6700 EK Wageningen, The Netherlands.

## Abstract

A preparation method is discussed to prepare charge-stabilized polystyrene latex particles, carrying terminally grafted short PEO-chains. The latices have relatively large particles (480 nm), a surface charge and possess on the surface a PEO-350/methacrylate molecule. The surface properties of this latex are compared to those of a similar latex but without the PEO-surface group.

The presence of the PEO-moiety on the particle surface could be established by the colloidal stability against salt, complexation with molybdatophosphoric acid, protein adsorption and proton NMR. From the molybdatophosphoric acid- and $^1$H NMR-results it follows that the average surface coverage of PEO-350 is roughly one molecule per nm$^2$.

Keywords: Poly(ethylene oxide); steric stabilization; stability ratio; molybdatophosphoric acid

Correspondence to: Marc C.L. Maste, Department of Physical and Colloid Chemistry, Wageningen Agricultural University, P.O. Box 8038, 6700 EK Wageningen, The Netherlands

Subm. Colloids & Surfaces A

# Characterization of Surface Groups of Latices using Potentiometry, Conductometry and Voltammetric Titrations in the Presence of Cadmium(II).

Jeannette H.A.M. Wonders, José M. Diaz-Cruz, Herman P. van Leeuwen and Johannes Lyklema.
Physical and Colloid Chemistry
Wageningen Agricultural University
Dreijenplein 6
6703 HB Wageningen
The Netherlands

Phone: +318370-82178
Fax: +318370-84141
Email: Fysko@FenK.wau.nl

## Introduction

The aim of this study is the characterization of surface groups of latices by conductometry, potentiometry and voltammetry. Different types of latex have been used: a polystyrene latex with high density of carboxylic groups on the surface (coded AKB20) and core-shell latices, which consist of a polystyrene core and a covalently bound hydrophilic polymer coating with a low density of carboxylic groups and some sulphonic groups (coded AOY 5,8,20 and 22). For binding of metal ions, the reaction scheme is written in terms of an electroactive metal ion (M) which may form electroinactive complexes $MS_i$ with the surface groups $S_i$. The index i distinguishes between sites with different affinities for M, resulting from differences in the intrinsic chemical nature of these sites and/or from electrostatic binding. Thus:

$$\begin{array}{ccccc} M & + & S_i^- & \underset{k_{d,i}}{\overset{k_{a,i}}{\rightleftharpoons}} & MS_i \\ + & & + & & \\ n\,e & & H^+ & & \\ \downarrow\uparrow & & \uparrow\downarrow\ K_{a,i} & & \\ M^\circ & & HS_i & & \end{array} \qquad (1)$$

Charges of the metal ion and metal complexes are omitted for the sake of clarity. The association and dissociation rate constants $k_{a,i}$ and $k_{d,i}$ are related to the equilibrium constant $K_i$ of the particular class of sites i:

$$K_i = k_{a,i}/k_{d,i} = [MS_i]/[M][S_i^-] \qquad (2)$$

If the association and dissociation rate constants are large compared to the time scale of the voltammetric experiment, the metal complex formed is called labile.

In the case of labile binding of the metal ions, the model of de Jong and van Leeuwen[1] can be used to calculate (series of) stability constants. The nature of the binding is relevant for the way of treatment of data from voltammetric titration, in which metal ions are used to determine the amount of adsorbing groups.

From conductometry and potentiometry, information about the amount and the types of surface groups can be obtained and compared to the data of the voltammetric titration. Conductometry is used to determine the amounts of strong and weak surface groups. These groups not necessarily correspond to sulphonic and carboxylic groups, respectively. $K_a$ (acidity constant) values were determined according to a Henderson-Hasselbalch analysis of the potentiometric data. Further, from potentiometry information can be extracted about the dependency of $K_a$ on the degree of dissociation of all surface groups ($\alpha_d$) and about the fractions of strong and weak acid groups.

The protolytic equilibrium of the acidic group $HS_i$ of a (poly)acid can be expressed by:

$$S_i^- + H^+ \underset{\leftarrow}{\overset{K_{a,i}}{\rightarrow}} HS_i \qquad (3)$$

where $K_{a,i}$ is the dissociation constant of the acidic group $HS_i$:

$$K_{a,i} = \frac{[H^+][S_i^-]}{[HS_i]} \qquad (4)$$

**Results and Discussion.**

In Table 1, the fractions of strong acid groups ($f_1$) are shown. Within experimental error, fractions obtained by potentiometry are similar to the ones obtained from conductometry. From further analysis we conclude that the fraction of strong acid groups corresponds to the sulphonic fraction, and the fraction of weak acid groups to the carboxylic fraction. The latices show polyelectrolytic behaviour, indicated by a slope m higher than 1. The m value of AKB 20 is 1.78, which is not very high compared to the m values of the AOY-types. This difference can be explained as follows: the AOY types have two types of surface groups with two pK values each, influencing each other, whereas AKB 20 has only carboxylic groups. In Table 1 the average distance between two surface groups is included. The value of m should increase with decreasing average distance between two surface groups, if randomly distributed. Comparing m to the average distance between to surface groups does not yield this trend. This might be due to a heterogeneous site density.

---

[1] H.G. de Jong, H.P. van Leeuwen and K. Holub, J. Electroanal. Chem 234 (1987) 1
H.G. de Jong, H.P. van Leeuwen, J. Electroanal. Chem 234 (1987) 17
H.G. de Jong, H.P. van Leeuwen, J. Electroanal. Chem 235 (1987) 1

Table 1. Data obtained from conductometry and potentiometry of different types of latices.

| | Core-shell latices | | | | core only latex |
|---|---|---|---|---|---|
| Latex | AOY 5 | AOY 8 | AOY 20 | AOY 22 | AKB-20 |
| | conductometric titrations | | | | |
| $f_1$ | 0.29 | 0.35 | 0.51 | 0.36 | 0.00 |
| ctot (mol m-2) | $9.0*10^{-7}$ | $5.7*10^{-7}$ | $7.7*10^{-7}$ | $5.6*10^{-7}$ | $10.3*10^{-6}$ |
| distance(nm)@ | 2.1 | 2.2 | 1.6 | 2.7 | 0.4 |
| | potentiometric titrations | | | | |
| pKa intrinsic | 3.63 | 4.18 | 3.01 | 3.15 | 7.88 |
| pKa average | 6.13 | 5.93 | 5.44 | 5.49 | 8.55 |
| $f_1$ from $\alpha_n$ v. $\alpha_d$ plot | 0.34 | 0.38 | 0.50 | 0.40 | 0.00 |
| slope & | 3.49 | 2.39 | 2.93 | 3.03 | 1.78 |

$f_1$ : fraction strong acid groups
@ average distance in nm between two surface groups if randomly distributed
$\alpha_n$: degree of neutralization of all surface groups
$\alpha_d$: degree of dissociation of all surface groups
& slope m of Henderson Hasselbalch plot

Table 2. Data of voltammetric titrations of different types of latices with cadmium(II).

| Latex | AOY 5 | AOY 8 | AOY 20 | AOY 22 | AKB 20 |
|---|---|---|---|---|---|
| Cd (eq/m2)* | $5.42*10^{-7}$ | $3.95*10^{-7}$ | $3.76*10^{-7}$ | $2.23*10^{-7}$ | $6.60*10^{-6}$ |
| $\alpha_d$ | 0.84 | 0.98 | 0.94 | 0.94 | 0.49 |
| pH begin | 8.53 | 8.79 | 8.35 | 8.38 | 8.45 |
| pH final | 7.67 | 7.81 | 7.33 | 7.33 | 6.33 |
| strong acid# (eq/m2) | $2.9*10^{-7}$ | $2.1*10^{-7}$ | $3.9*10^{-7}$ | $2.1*10^{-7}$ | --- |
| diss weak acid# (eq/m2) | $4.7*10^{-7}$ | $3.5*10^{-7}$ | $3.3*10^{-7}$ | $3.1*10^{-7}$ | $5.05*10^{-6}$ |
| Cd/Cs$ | 0.72 | 0.71 | 0.52 | 0.42 | 1.31 |

* expressed as surface groups. To adsorb 1 molecule of cadmium, two surface groups are needed.
#average values derived from Table 1
$ ratio of cadmium adsorbing groups over total amount of deprotonated surface groups determined by conductometry

If we compare the amount of surface groups determined by Cd(II) to the amount of dissociated weak acid groups, we see that in general the amount of weak acid groups is smaller for all latices. This evidences that Cd(II) is adsorbed by both types of surface groups. Sulphonic groups probably adsorb cadmium by electrostatic interaction only. The fraction of complexing groups of the latices increases with the fraction dissociated weak acid. For unknown reason, AOY 22 deviates from this trend. For the core-shell latices, the amount of surface groups which bind cadmium(II) was lower than the total amount of dissociated surface groups (Table 2). This is not the case for latex AKB20. Probably cadmium(II) binds to 1 surface group according to the model:

$$Cd^{2+} + S_i^- \rightarrow CdS_i^+$$

FUKUI UNIVERSITY
9-1, BUNKYO 3-CHOME
FUKUI-SHI 910, JAPAN

# Contribution to Polymer Colloids Group Newsletter

by
M. Nomura and H. Tobita
Department of Materials Science and Engineering,
Fukui University, Fukui, Japan.

Polymer International **30**, No.3 and 4 can be purchased directly from the publisher in a reduced price, which contained 39 papers out of 64 presented at "International Symposium on Polymeric Microspheres" held in Fukui in Oct. 23-26, 1991. Our papers on emulsion polymerization which have recently submitted or published are as follows:

## In Press:

**Mass Transfer Effects in Emulsion Polymerization Systems. I. Diffusional Behavior of Chain Transfer Agents in the Emulsion Polymerization of Styrene.**
M. Nomura, H. Suzuki, H. Tokunaga and K. Fujita, Department of Materials Science and Engineering, Fukui University, Fukui, Japan.

**SYNOPSIS** On the basis of the so-called two-films theory for mass transfer, a mathematical model for transfer of chain transfer agents from monomer droplets to polymer particles where chain transfer agent molecules are consumed by the chain transfer reaction is developed for an emulsion polymerization system. It is shown by the model that the concentration of chain transfer agent in the polymer particles during the polymerization is decreased to a value much less than that which would be attained if thermodynamic equilibrium for chain transfer agent were reached between the polymer particles and the monomer droplets, due mainly to the resistance to transfer of chain transfer agent molecules across the diffusion films at the interface between the monomer droplets and the water phase. The validity and utility of the model developed for predicting the diffusion and consumption rates for chain transfer agent are demonstrated experimentally using five normal aliphatic mercaptans from n-$C_7$ to n-$C_{12}$ as chain transfer agents in the seeded emulsion polymerization of styrene.

## Published:

**1) Kinetics and mechanism of Emulsion Polymerization Initiated by Oil-Soluble Initiators. IV. Kinetics Modeling of Unseeded Emulsion Polymerization of Styrene Initiated by 2,2'-Azobisisobutyronitle.**
M. Nomura, J. Ikoma, and K. Fujita, Department of Materials Science and Engineering, Fukui University, Fukui, Japan. *J. Polym. Sci., Part A Polym. Chem. Ed.* **31**, 2103 (1993)

**2) Crosslinking Kinetics in Emulsion Copolymerization of Methyl methacrylate and Ethylene glycol dimethacrylate.**
H. Tobita, K. Kimura, K. Fujita and M. Nomura. Department of Materials Science and Engineering, Fukui University, Fukui, Japan. *POLYMER* **34**, 2569 (1993)

# Contribution to the IPCG Newsletter

**Tsuneo Okubo**
Department of Polymer Chemistry, Kyoto University, Kyoto 606-01, Japan
Phone 81-75-753-5611, Fax 81-75-753-5609

This is my first contribution to the IPCG Newsletter. Research interests and recent publications are reported herewith. Our research group is now very small and contains two graduate students only. But, we believe the group grows up hereafter. Activity of all the groups(four or five groups) of polymer colloids in our Faculty of Engineering, i.e., Departments of Polymer Chemistry, Material Science, Chemical Engineering and Synthetic & Biological Chemistry will be reported in the next newsletter.

## Research Interests:

(1)***Colloidal Single Crystals***

Crystal growing processes, lattice structure, phase diagram, elastic and viscosimetric properties and others are studied by close-up photographs and video tapes, transmission- and reflection-spectroscopy, dynamic light scattering, etc. Development of photonics devices, experiments in a space schuttle, colloidal alloy and anisotropic crystals are also interested.

(2)***Properties of Deionized Systems***

Extraordinary properties of colloids and polyelectrolytes are studied in the deionized suspension or solution. Rotational and translational diffusion, viscosity, and refractive index are examples of the properties.

(3)***Thermodynamic Properties of Colloids and Polyelectrolytes***

Mean activity coefficient, partial molal volume, heat of dilution, surface tension, and other important parameters are measured for the giant melecular weight substances.

(4)***Fast Reaction Kinetics***

Stopped-flow(conductance, spectrophotometric absorbance, birefringence, etc.), temperature-jump, photo-chemical quenching methods are used for the kinetic analysis of the counterion association of macroions, metal ion complexation, polyelectrolyte complexation, inclusion, and other fast reactions.

**Publications** (1990- )

(1)"Centrifugal Compression of Crystal-like Structures of Deionized Colloidal Spheres", T.Okubo, *J.Amer.Chem.Soc.*,112,5420-5424 (1990).
(2)"Alloy Structures in Binary Mixtures of Highly Deionized Colloids at Sedimentation Equilibrium", T.Okubo, *J.Chem.Phys.*,93,8276-8283 (1990).
(3)"Amorphous Solid-like Distribution of Polydisperse Particles of Colloidal Clay and Microcrystalline Cellulose in Deionized Suspension", T.Okubo, *Colloid Polymer Sci.*, 268, 1159-1166(1990).
(4)"Phase Transition between Liquid-like and Crystal-like Structures of Deionized Colloidal Suspensions", T.Okubo, *J.Chem.Soc.,Faraday Trans.*86,2871-2876 (1990).
(5)"Extraordinary Properties of Synthetic and Biological Polyelectrolytes in Deionized Solution. 2.Expansion of Carboxylic Acid Type Gels", T.Okubo, *J.Phys.Chem.*,94,3210-3214(1990).
(6)"Adsorption of Synthetic Polyelectrolytes on Colloidal Spheres", T.Okubo,*Polymer Bull.*,23,211-218(1990).
(7)"Extraordinary Viscosity Behavior of Binary Mixtures of Highly Deionized Colloids", T.Okubo, *J.Phys.Chem.*, 94,1962-1966(1990).
(8)"Rotational Brownian Movement of Poly(tetrafluoroethylene) Colloids as Studied by the Conductance Stopped-Flow Technique", T.Okubo and T.Shimizu,*J.Colloid Interface Sci.*,135,300-303(1990).
(9)"Refractometric Studies of "Liquid-like" and "Crystal-like" Colloids in Deionized Solution", T.Okubo, *J.Colloid Interface Sci.*, 135,294-296(1990).
(10)"Highly Elastic "Crystals" of Deionized Colloidal Spheres", T.Okubo,*J.Colloid Interface Sci.*,135,259-262(1990).
(11)"Elastic Modulus of Crystal-like Structures of Deionized Colloidal Spheres in Aqueous Organic Solvent Mixtures", T.Okubo, *J.Chem.Soc.,Faraday Trans.* 86,151-156(1990).
(12)"Counter-ion Specificity in Colloidal "Crystals" and "Liquids" as Studied by Transmitted-light Spectroscopy", T.Okubo, *J.Chem.Soc.,Faraday Trans.*,87, 1361-1363(1991).
(13)"Viscoelastic Investigation of Crystal-liquid Transition in Concentrated Monodisperse Latices", T.Matsumoto and T.Okubo, *J.Rheol.*,35,135-148(1991).
(14)"Melting Temperature of Colloidal Crystals of Polystyrene Spheres", T,Okubo, *J.Chem.Phys.*,95,3690-3697(1991).

(15)"Cholesteric Pitch of Aqueous Hydroxypropylcellulose in the Presence of Synthetic Polyelectrolytes", T.Okubo, *J.Chem.Soc.,Faraday Trans.*,87, 1361-1363(1991).
(16)"Suspension Structures of Deionized Colloidal Silica Spheres As Studied by the Reflection and Transmission Spectroscopy", T.Okubo, *Ber.Bunsenges.Phys.Chem.*,96,61-68(1992).
(17)"Melting Temperature of Colloidal Crystals of Monodisperse Silica Spheres", T.Okubo, *J.Chem.Phys.*,96,2261-2268(1992).
(18)"Giant Single Crystals of Colloidal Spheres in Deionized and Diluted Suspension", T.Okubo, *Naturwissenschaften*,79,317-320 (1992).
(19)"Blinking of Colloidal Single Crystals in Aqueous Suspensions of Monodisperse Colloidal Silica Spheres", T.Okubo, *J.Colloid Interface Sci.*, 153, 587-591(1992).
(20)"Melting Temperature of Colloidal Crystals of Monodisperse Silica Spheres in Ethanol-Water and Ethylene Glycol-Water Mixtures", T.Okubo,*Colloid Plymer Sci.*,270,1018-1026(1992).
(21)"Growing Process of Giant Colloidal Single Crystals(Japanese)", T.Okubo, *Nippon Kessho Seicho Gakkaishi*,19,263-275(1992).
(22)"Extraordinary Properties of Synthetic and Biological Polymers in Deionized Solution. 3.Expansion of Water-soluble Neutral Polymers and Polymers Having a Small Amount of Ionizable Groups", T.Okubo, *Ber.Bunsenges.Phys.Chem.*,96,816-820(1992).
(23)"Large Simgle Crystals of Colloidal Silica Spheres Appearing in Deionized and Diluted Suspension", T.Okubo, *Colloid Polymer Sci.*, 271,190-196(1993).
(24)"Polymer Colloidal Crystals", T.Okubo, *Prog.Polymer Sci.*,16,481-516(1993).
(25)'Elasticity of the Crystal-like, Amorphous Solid-like, and Liquid-like Structure in Deionized Suspensions of Colloidal Silica Spheres", T.Okubo, *Colloid Polymer Sci.*,271, in press(1993).
(26)"Revisit to the Melting Temperature of Colloidal Crystals in the Completely Deionized Suspension", T.Okubo, *Colloid Polymer Sci.*, in press.
(27)"Phase Diagram Ionic Colloidal Crystals", T.Okubo, *Am.Chem.Soc.Book*, in press.
(28)"Giant Colloidal Single Crystals of Polystyrene and Silica Spheres in Deionized Suspension", T.Okubo, submitted.
(29)"Sedimentation Velocity of Colloidal Spheres in Deionized Suspension", T.Okubo, submitted.

# Superlattice Formation in Binary Mixtures of Hard-Sphere Colloids

P. Bartlett,[1] R. H. Ottewill,[1] and P. N. Pusey[2]

[1]*School of Chemistry, Bristol University, Cantock's Close, Bristol, BS8 1TS, United Kingdom*

[2]*Department of Physics, Edinburgh University, Mayfield Road, Edinburgh, EH9 3JZ, United Kingdom*

(Received 11 February 1992)

Binary mixtures of suspended hard-sphere colloidal particles, radius ratio $R_B/R_A=0.58$, were observed to undergo entropically driven freezing transitions into both the $AB_2$ and the $AB_{13}$ superlattice structures at different relative proportions of the two species. The structures were identified by powder light crystallography and by electron microscopy of the dried solid phases. An approximate (constant volume) phase diagram containing three eutectics was determined. The results are compared with earlier work at size ratio 0.62.

PACS numbers: 82.70.Dd, 61.55.Hg, 64.70.Dv, 81.30.Dz

Remarkably, the first examples of superlattice structures in colloidal crystals were found by Sanders [1] in native gem opals, which consist of dried arrays of colloidal silica spheres. By electron microscopy of a particular sample of Brazilian opal, Sanders observed mixtures of large, $A$, spheres and small, $B$, spheres (radii $R_A=181$ nm, $R_B=105$ nm, radius ratio $R_B/R_A\sim0.58$) arranged in both the $AB_2$ (atomic analogs: borides such as $AlB_2$) and $AB_{13}$ (atomic analogs: $NaZn_{13}$, $UBe_{13}$, etc.) structures. Subsequently Yoshimura and Hachisu [2], by direct optical microscopy near the wall of the sample cell, observed at least five different superlattices, including $AB_2$ and $AB_{13}$, in a binary suspension of charge-stabilized spheres. However, in neither of these pioneering studies were the conditions required for superlattice formation well characterized. Here we describe the main findings of an experimental investigation of the phase behavior and structure of suspensions of binary mixtures of "hard-sphere" colloidal particles; a more detailed account will be given later. As with the opals the size ratio was about 0.58 and, in regions of the phase diagram whose boundaries were determined reasonably accurately, both the $AB_2$ and $AB_{13}$ structures were observed. Probably the most interesting implication of these findings is that a system as simple, conceptually, as a mixture of hard spheres can "self-assemble" into quite complex structures, driven purely by entropic (or "packing") contributions to its free energy.

The particles used consisted of polymethylmethacrylate (PMMA) cores, stabilized sterically by thin, $\sim10$ nm, layers of poly-12-hydroxystearic acid [3]. They were suspended in mixtures of decalin and carbon disulphide in proportion chosen to achieve a near match with the refractive index, $\sim1.5$, of the particles, thus providing nearly transparent suspensions suitable for quantitative light scattering studies. One-component suspensions of this type have been studied extensively with emphasis on particle dynamics [4], phase behavior [5], crystallization [6], and glass formation [7]. These studies have established that the interparticle interaction is steep and repulsive and is well approximated by that of hard spheres. We have also reported work [8] on a binary mixture at a slightly larger size ratio, 0.62, which will be compared below with the present research.

The particle radii were determined to be $R_A=321$ nm and $R_B=186$ nm [9]. As in previous work, cited above, particle volume fractions, $\phi_A$ and $\phi_B$, in the suspensions were calculated by scaling the accurately measured weight fractions by factors chosen to ensure that freezing of the individual one-component systems occurred at the hard-sphere value $\phi_A=\phi_B=0.494$. The points in Fig. 1

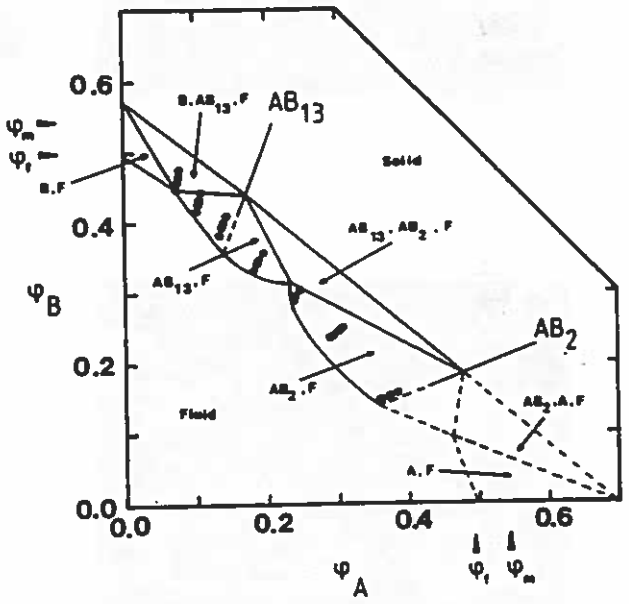


FIG. 1. Constant-volume phase diagram of binary hard-sphere mixtures at size ratio $R_B/R_A=0.58$. The axes are the partial volume fractions $\phi_A$ and $\phi_B$ of each species; $\phi_f$ and $\phi_m$ indicate the pure-component freezing and melting concentrations. The points show the samples studied. The low-concentration state is fluid. At higher concentrations four regions of coexistence of crystal ($B$, $AB_{13}$, $AB_2$, or $A$) and fluid ($F$) are found; the $A$,$F$ and $B$,$F$ regions were studied in earlier work [8] at $R_B/R_A=0.62$. The triangles at still higher concentrations are three-phase (two crystals+fluid) eutectic regions and at the highest concentrations, not studied in this work, crystal/crystal coexistence is expected. The two lines radiating from the origin indicate the $AB_2$ and $AB_{13}$ stoichiometries.

show the samples studied. This representation of the phase diagram, in which the axes are $\phi_A$ and $\phi_B$, is a natural one for colloidal mixtures [10] which (as for colloidal systems in general) are studied at essentially constant volume; lines radiating from the origin correspond to changing the total volume fraction, $\phi_A+\phi_B$, at a fixed ratio, $n_B/n_A$, of the numbers of the two species. As described elsewhere [11], sedimentation of the particles was minimized by subjecting the samples to "time-averaged zero gravity."

The crystalline structures formed were characterized mainly by "powder light crystallography" [6,8]; an expanded laser beam illuminated many small, randomly oriented crystallites of typical dimension 25 $\mu$m. In a few cases the solid phase was also imaged by scanning electron microscopy. The suspension medium was allowed to evaporate over several months. The dried "compact" of colloidal spheres was then fractured and sputter coated with gold in vacuo.

We consider first the $AB_2$ structure which was observed in suspensions with number ratios $n_B/n_A$ of the species of 4 and 6 and total volume fractions $\phi_A+\phi_B$ between 0.525 and 0.557 (see Fig. 1). About five weeks after preparation the initially homogeneous samples had each separated into a lower solid phase, containing small homogeneously nucleated crystallites, and an upper (colloidal) fluid phase, in differing proportions by volume. Figure 2(a) shows an electron microscope image of the dried solid phase. Long-ranged binary order is clearly visible. The models shown in Fig. 2(b) demonstrate that this and other similar micrographs are consistent with the $AB_2$ structure which consists of alternating hexagonal

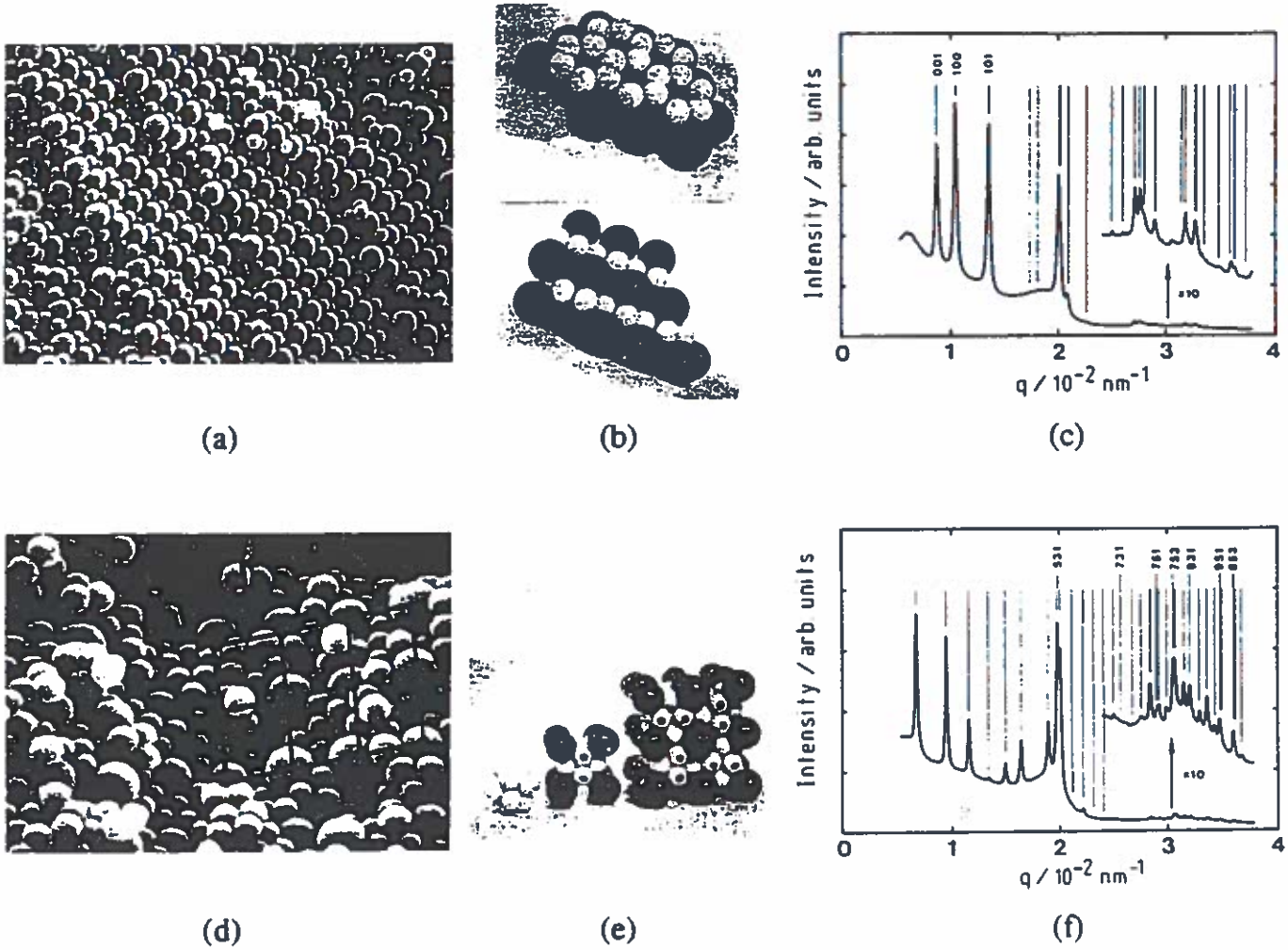


FIG. 2. (a) Electron micrograph of $AB_2$ superlattice; original composition (OC) of sample $n_B/n_A=6$, $\phi_A+\phi_B=0.536$; (b) model of $AB_2$; (c) light powder diffraction pattern of $AB_2$ sample with OC $n_B/n_A=4$, $\phi_A+\phi_B=0.533$; the vertical lines indicate the expected Bragg reflections; (d) micrograph of $AB_{13}$ from sample of OC $n_B/n_A=14$, $\phi_A+\phi_B=0.553$; twelve ordered large spheres are indicated, comprising the 011 face; pentagons of small spheres can be seen below the arrows; (e) model indicating construction of $AB_{13}$: an icosahedral arrangement of thirteen small spheres, the cubic subcell and the unit cell; two small spheres in each icosahedron are marked to indicate the rotation by $\pi/2$ between subcells; (f) powder pattern of $AB_{13}$ sample with OC $n_A/n_B=9$, $\phi_A+\phi_B=0.552$; the vertical lines indicate the expected reflections; the labeled reflections with odd indices arise from the large unit cell; the unlabeled reflections are those expected for a simple cubic structure but multiplied by 2, i.e., 200, 220, 222, 400, etc.

layers of large and small spheres. The larger $A$ spheres are stacked above one another along the $c$ axis; the smaller $B$ spheres occupy the trigonal prismatic cavities between the $A$ layers. Figure 2(a) can be recognized as showing an approximate 011 section in which the hexagonal layers lie at roughly 45° to the plane of the micrograph; the model in Fig. 2(b) is constructed to also reveal the 011 face.

Figure 2(c) shows a typical powder pattern of one of these samples; the scattered intensity $I(q)$ is plotted against the usual scattering vector $q$. Quantitative analysis of patterns such as these is complicated by the fact that it is very difficult to measure the form factors of the individual species of particle under conditions of near refractive-index match [8]; thus scattered intensities cannot be calculated easily. However, as is indicated in Fig. 2(c), the experimental and theoretical positions of the Bragg reflections can be compared. Although a few lines are missing (due presumably to destructive interference or minima in the particle form factors), the experimental powder pattern is clearly consistent with the $AB_2$ structure (space group $P6/mmm$). The rather high background intensity observed at low $q$ probably comprises both scattering from amorphous regions of the solid phase (which were also observed in the electron micrographs) and incoherent scattering associated with a small degree of particle polydispersity [7]. The dimensions of the hexagonal unit cell used to calculate the line positions shown in Fig. 2(c) were $a=693$ nm and $c=724$ nm. The density, $\phi_A+\phi_B=0.64$, of the $AB_2$ crystal, calculated from these lattice parameters and the particle radii, is considerably larger than that of the suspension from which it crystallizes. Finally we mention that, surprisingly, suspensions prepared with $n_B/n_A=2$ (the $AB_2$ stoichiometry) did not crystallize over several months, but remained amorphous.

The second superlattice structure, $AB_{13}$, was found in suspensions rich in small spheres, $n_B/n_A=9$, 14, 20, and 30, with $\phi_A+\phi_B=0.512$–$0.553$. Crystallization was rapid compared to $AB_2$; crystallites of $AB_{13}$ were observed within a few days of sample preparation (cf. five weeks for $AB_2$). The structure of $AB_{13}$ is modeled in Fig. 2(e). It is visualized most easily in terms of a cubic subcell. This contains an icosahedral arrangement of twelve small spheres surrounding an additional small sphere which is itself positioned at the center of a primitive cubic cell of large spheres. The full unit cell consists of eight such subcells stacked so that neighboring icosahedra alternate in orientation by $\pi/2$. Convincing evidence for this remarkably complex structure comes from powder crystallography. A typical powder pattern $I(q)$ is shown in Fig. 2(f). The reflections index on a cubic lattice $[4\le(h^2+k^2+l^2)\le 120]$ with the space symmetry $Fm\bar{3}c$. The cubic lattice constant is $a=1877$ nm and the calculated density of the $AB_{13}$ crystal is $\phi_A+\phi_B=0.59$ (cf. $\sim 0.64$ for $AB_2$). As indicated in Fig. 2(f), the observed reflections separate into two sets with the Miller indices $(hkl)$ either all even or all odd. Two lines in the latter set, 531 (the strongest line observed) and 931, are clearly evident. Symmetry arguments show that *only* scattering from the *alternating* orientational order of the icosahedra within each unit cell contributes to the intensity of these odd labeled reflections. If, for example, the icosahedra were orientationally disordered then the space symmetry would reduce to the simple cubic group $Pm3$ (with a consequent halving of the unit cell dimension) and this set of reflections would be absent. Hence the data of Fig. 2(f) provide strong evidence for the full $AB_{13}$ structure described above.

Electron microscopy of $AB_{13}$ was less successful than that of $AB_2$. For reasons which are uncertain, the structure appeared to be disrupted on drying and amorphous arrangements of the two species were observed most often. Figure 2(d) shows one of the better micrographs. A reasonably well-ordered arrangement of twelve (marked) large spheres, comprising the 011 face of the structure, is evident. Order among the smaller spheres is still less obvious although pentagons of small spheres, which result from cleavage of the icosahedra, can be seen near the center of the micrograph.

We now consider the consequences of our observations for the form of the equilibrium fluid-solid phase diagram. Our experiments show examples of four stable crystalline phases, $A$, $AB_2$, $AB_{13}$, and $B$, and in the work reported here we have studied in detail the two-phase regions of fluid/$AB_2$ and fluid/$AB_{13}$ equilibria. In earlier work [8] on a mixture of spheres of size ratio 0.62 (see below) we investigated the fluid/$A$ and fluid/$B$ equilibria, and established that the small spheres are largely insoluble in a crystal of large spheres and vice versa. This fact, combined with the different symmetries of the superlattices, suggests that the equilibrium phase diagram will contain four regions of fluid/crystal coexistence and three eutectic regions corresponding to the equilibria $A/AB_2$, $AB_2/AB_{13}$, and $AB_{13}/B$. In a constant volume, $(\phi_A,\phi_B)$ representation, each eutectic region is described by a triangular three-phase domain with the vertices of the triangle corresponding to the densities of the eutectic fluid and the two coexisting solid phases [10]. Although the exact topology of the phase diagram is still under investigation, we can estimate the positions of two of the three eutectic fluids. In particular, the observation of $AB_2$ formation in suspensions of compositions $n_B/n_A=6$ but $AB_{13}$ formation at compositions $n_B/n_A=9$ and above indicates that the $AB_2/AB_{13}$ eutectic fluid lies at a stoichiometry with $n_B/n_A$ between 6 and 9. Furthermore the position of the $AB_{13}/B$ eutectic is indicated by the experimental observation of three phase equilibria in samples of composition $n_B/n_A=30$ and concentration $\phi_A+\phi_B=0.54-0.56$. Such samples contain two crystalline phases, $AB_{13}$ and $B$ (identified by powder diffraction), together with a single isotropic fluid. Approximate phase boundaries implied by

these observations are sketched in Fig. 1; the right-hand side of the diagram is uncertain because, as mentioned above, suspensions with $n_B/n_A = 2$ showed no observable crystallization in our experiments.

Our previous work [8] involved a binary mixture at size ratio $R_B/R_A = 0.62$, in which the $A$ spheres were the same, $R_A = 321$ nm, but the $B$ spheres had $R_B = 199$ nm, cf. 186 nm in the present study. In this mixture we never observed crystalline $AB_2$; samples with $2 < n_B/n_A < 10$ remained amorphous over the many months duration of the experiments. Around $n_B/n_A = 13$ $AB_{13}$ was observed, but appeared to be metastable: It formed much more slowly than at size ratio 0.58, seemed to "redissolve" after many months, and was always found to be mixed with crystals of pure $B$. (It seems remarkable that changing the size of one species by just 7% should have such profound effects.)

Discussing these findings, we note first that, following initial vigorous debate, the existence of an entropically driven freezing transition in a *one-component* assembly of hard spheres (which, of course, have no attractive part in their pair potential) is nowadays accepted [5,6,12]. Freezing occurs at a concentration at which the loss of the system's entropy associated with the formation of long-ranged order is more than offset by the gain in entropy associated with the extra free volume available to the spheres in an ordered spatial arrangement [12]. One can expect similar principles to apply to the freezing of binary hard-sphere mixtures. Eldridge and Madden [13] have recently calculated by computer simulation the free energy of $AB_{13}$. In reasonable agreement with our observations, they find stability of $AB_{13}$ (compared to colloidal fluid and phase-separated crystalline $A$ and $B$) over a significant range of concentration for $R_B/R_A = 0.58$ and instability for $R_B/R_A > 0.62$. Simulations of $AB_2$ are in progress [13]. Approximate calculations based on estimating free volume give similar results for $AB_{13}$ and also suggest that $AB_2$ should be stable at $R_B/R_A = 0.58$ [14].

Intriguing, as yet unexplained, observations include the facts that the complex $AB_{13}$ structure grew significantly faster than $AB_2$ and that $AB_2$ itself grew fastest from a metastable fluid at the $n_B/n_A = 6$ stoichiometry (close to the $AB_2/AB_{13}$ eutectic, see above) and not at all at $n_B/n_A = 2$. The latter is surprising since glass formation is usually expected near to a eutectic rather than at the stoichiometry of a crystalline compound [15].

It is clear that purely entropic contributions to the free energies of simple systems can lead to the formation of complex structures. Obvious future directions include more detailed studies of the kinetics and mechanisms of superlattice formation and of the binary glass transitions, and the possibility of fabricating new materials by mixing, for example, plastic and metallic or semiconductor particles of different sizes.

We thank M. D. Eldridge and P. A. Madden for communicating their results prior to publication. This research was supported by a joint grant from the Science and Engineering Research Council and the Ministry of Defense, and was performed in part while P.N.P. was at the Royal Signals and Radar Establishment, Malvern, United Kingdom.

[1] J. V. Sanders, Philos. Mag. A **42**, 705 (1980).
[2] S. Yoshimura and S. Hachisu, Prog. Colloid Polym. Sci. **68**, 59 (1983).
[3] L. Antl, J. W. Goodwin, R. D. Hill, R. H. Ottewill, S. M. Owens, S. Papworth, and J. A. Waters, Colloid Surf. **17**, 67 (1986).
[4] P. N. Pusey and W. van Megen, J. Phys. (Paris) **44**, 285 (1983); W. van Megen and S. M. Underwood, Langmuir **6**, 35 (1990).
[5] P. N. Pusey and W. van Megen, Nature (London) **320**, 340 (1986); S. E. Paulin and B. J. Ackerson, Phys. Rev. Lett. **64**, 2663 (1990).
[6] P. N. Pusey, W. van Megen, P. Bartlett, B. J. Ackerson, J. G. Rarity, and S. M. Underwood, Phys. Rev. Lett. **63**, 2753 (1989).
[7] W. van Megen and P. N. Pusey, Phys. Rev. A **43**, 5429 (1991); W. van Megen, S. M. Underwood, and P. N. Pusey, Phys. Rev. Lett. **67**, 1586 (1991).
[8] P. Bartlett, R. H. Ottewill, and P. N. Pusey, J. Chem. Phys. **93**, 1299 (1990).
[9] These radii were calculated from the expression $\phi = \frac{4}{3}\pi R^3 \rho$, the number density $\rho$ being obtained from the measured lattice parameters of the one-component crystals at melting (volume fraction $\phi = \phi_M = 0.545$ for hard spheres). This approach leads to a size ratio of 0.62 for the system described in Ref. [8], rather than the value 0.61 quoted there.
[10] P. Bartlett, J. Phys. Condens. Matter **2**, 4979 (1990).
[11] P. Bartlett, P. N. Pusey, and R. H. Ottewill, Langmuir **7**, 213 (1991).
[12] For a recent discussion, see H. N. W. Lekkerkerker, in *Phase Transitions in Soft Condensed Matter*, edited by T. Riste and D. Sherrington (Plenum, New York, 1989), p. 165.
[13] M. D. Eldridge and P. A. Madden (to be published); (private communication).
[14] P. Bartlett (unpublished).
[15] F. Spaepen and D. Turnbull, Annu. Rev. Phys. Chem. **35**, 241 (1984).

# The interaction of surfactants with poly(N-isopropylacrylamide) microgel latexes.

K.C. Tam, S. Ragaram and R.H. Pelton

The effects of surfactant type and concentration on the particle size and electrophoretic mobility of crosslinked poly(N-isopropylacrylamide) [polyNIPAM] microgel latexes were studied. Without surfactant the particle diameter of the polyNIPAM decreased by a factor of two when the temperature was increased above 31 °C, the cloud point temperature [CPT] for polyNIPAM homopolymer in water. Anionic sodium dodecyl sulfate [SDS] in the concentration range 0.001 M to 0.008 M caused the particle diameter to increase and the CPT to shift to higher temperatures. Higher SDS concentrations caused further swelling of the latex and the diameters became nearly independent of temperature in the range 10 to 60 °C. Nonionic Triton X-100 had no effect on the particle diameter/temperature behavior indicating no surfactant binding. Below the CPT cationic dodecyltrimethyl ammonium bromide had no effect on swelling whereas the cationic surfactant induced latex coagulation at the CPT.

Surfactant binding was also reflected in the electrophoretic mobilities. Low levels of SDS binding gave higher negative mobilities which were temperature sensitive. High SDS concentrations removed the temperature swelling transition so mobility was temperature insensitive. Cationic surfactant binding increased the mobility of positively charged polyNIPAM latex, however, in contrast to SDS, the mobility was temperature sensitive at high surfactant concentrations.

## Polymer Colloid Newsletter Contribution

**R. Pelton, A. Hamielec and Y. Deng**
McMaster University

### Temperature Sensitive Flocculants

High molecular weight cationic copolymers of polyacrylamide are known to be effective flocculants. Typically, optimum flocculation corresponds to between 5 and mole % cationic monomer and bridging is considered to be the mechanism.

Copolymers of diallyldimethyl ammonium chloride, DADMAC, and N-isopropylacrylamide were prepared and their ability to flocculated polystyrene latex was accessed as a function of polymer concentration and temperature. Copolymer with 20 mole percent cationic groups had a cloud point temperature of about 38 °C. Above this temperature the copolymer exists as colloidal particles about 100 nm in diameter and as soluble polymer at lower temperatures.

Shown below are the flocculation results expressed as turbidity of residual latex (i.e. the lower the relative turbidity, the better the flocculation). At 25 °C good flocculation was observed over a narrow range of polymer concentrations whereas at 45 °C the polymer concentration range giving effective flocculation was much broader. We believe that bridging is the flocculation mechanism at room temperature whereas heteroflocculation of cationic polyNIPAM particles with anionic polystyrene latex occurred at 45 °C. The is system offers the unique possibility of studying flocculation as a function of hydrodynamic volume of the flocculating polymer while keeping the molecular weight constant. These studies are in progress.

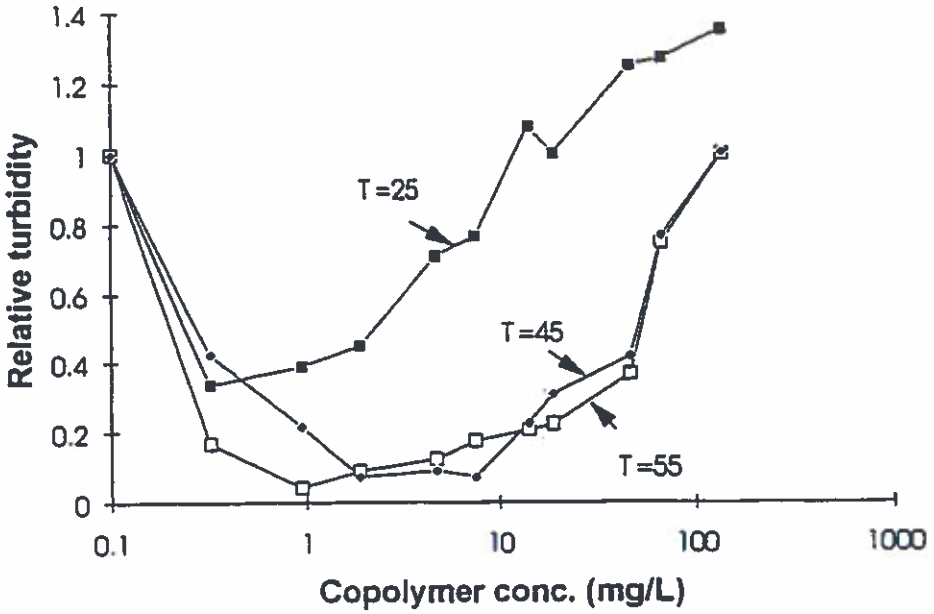

# Emulsion polymerization kinetics of methyl methacrylate and ethylene glycol dimethacrylate

Hua Guo, A. E. Hamielec*

Institute for Polymer Production Technology
Department of Chemical Engineering
McMaster University
Hamilton, ONT, L8S 4L7

Emulsion polymerization of the methyl methacrylate(MMA) and ethylene glycol dimethacrylate (EGDMA) system leads to crosslinking and the peculiar characteristics of kinetics. Herein,is provided the first part of experimental research done to date. The polymerization conditions were: temperature, 50°C; weight ratio of monomer to water, 1:6.5; potassium persulfate (KPS) as initiator,$2.2X10^{-3}$ mol/L; sodium dodecyl sulphate(SDS) as emulsifier, $3.5x10^{-3}$mol (below CMC) and $10X10^{-3}$mol (above CMC); level of the EGDMA in the monomer feed 5% wt, 10% wt and 100% wt. Total monomer conversion was determined by gravimetry. Particle size was measured versus time by dynamic light scattering. The relative residue content of pendant double bonds was determined by FTIR and DSC. Tetrahydrofuran was used as solvent for equilibrium swelling of latex.

It has been found that EGDMA level in monomer feed has a pronounced effects. The latex from pure EGDMA was not stable, and total monomer conversion was below 10% wt. Comparing the results of pure MMA and those of 5%wt; 10%wt, it has been found that there was not much difference in the polymerization rate, while the particle diameter and swelling ratio of final polymer latex decreases and the particle number of the final polymer latex increases with increase in EGDMA level in the monomer feed. Results for monomer conversion profiles and particle diameter are very different when polymerizations are done below and above the critical micelle concentration.

---

* to whom the correspondence should be addressed.

# Contribution to IPCG Newsletter

**From Laboratoire de Chimie des Procédés de polymérisation (LCPP-CNRS)**
**and Unité Mixte CNRS-bioMérieux**
**Lyon- France**
**(submitted by C. Pichot)**

---

## Preparation of polymer latex particles with immobilized sugar residues

J. Revilla, A. Elaissari, C. Pichot, B. Gallot (UMR 103 - CNRS-bioMérieux and LMOPS)

A liposaccharidic monomer, based on maltosamide, with a styrene polymerizable group has been prepared, characterized, and copolymerized with styrene in various proportions via radical polymerization. All the homopolymers and copolymers were found to exhibit lamellar liquid-crystalline structures (smectic) resulting from the superposition of hydrophilic and hydrophobic layers.

This monomer was utilized to prepare a serie of polymer colloids with immobilized sugar residues. X-ray photoelectron spectroscopy (XPS) has been performed for the surface chemical analysis. The quantitative elemental and chemical state XPS information suggests the presence of the steric stabilizing water-soluble polymer layer at the particle surface. The changes within the C1s core level spectra from the XPS analysis reflected the increase in the surface level of the saccharidic monomer with increasing bulk levels of the maltosamide derivative. These changes correlate well with the observed substantial decrease in the electrophoretic mobility of the various polymer colloids as a fonction of the surface-active monomer, reflecting the presence of a steric stabilizing water-soluble polymer layer at the particle interface.

In order to verify these conclusions and to compare the behavior of a hydrophobic interaction controlled adsorption process to that of an electrostatic interaction controlled process, the adsorption isotherms of monomeric Bovine Serum Albumine (BSA) onto the polymer colloids were established. The amount of adsorbed protein reached a plateau of 2.8 $mg/m^2$, at pH 4.5 and ionic strength $10^{-2}$, for the seed latex ($-SO4^-$ charged polystyrene model colloids), whereas in the case of functionalized latex a plateau is reached at 0.4 $mg/m^2$. The amount of adsorbed protein versus the pH showed a maximum around the isoelectric point of the protein.

## Preparation and characterization of cationic poly (N-isopropylacrylamide) copolymer latexes

F. Meunier, C. Pichot, A. Elaissari
(UMR 103 - CNRS-bioMérieux)

Poly (N-isopropylacrylamide) hydrogel copolymer latexes bearing bioactive groups have been prepared in aqueous phase using a cationic initiator and vinyl benzyl isothiouronium chloride (VBIC), a monomer having a thiol protected group. In order to get a better understanding of the polymerization mechanism, a kinetic study was investigated by following the monomer(s) consumption, the polymerization rate and particle size upon varying some pertinent parameters of

the polymerization recipe. The effect of the VBIC was quite significant even at very low concentration and kinetic results suggest that this monomer also acts as a strong transfer agent. Replacement by other monomers bearing bioactive protected groups is currently carried out and preliminary results show the same tendancies with respect to polymerization kinetics and particle size upon varying the fonctional monomer concentration.

## Adsorption and desorption studies of oligonucleotides onto positively charged latex particles

A. Elaïssari, G. Mouterde, R. Kürfurst, T. Delair, Ph. Cros, C. Pichot
(UMR 103 - CNRS-bioMérieux)

The adsorption of oligonucleotides onto polymer latex particles is of great interest in the development of biomaterials, which can be used as adsorbents for DNA fragments, in medical diagnostics (immunoassay kits ...) as well for immobilization of various biomolecules. The effect of the latex surface characteristics on the adsorption of a well-defined oligonucleotide with a sequence arrangement such as $d(A)_{15}d(T)d(A)_{14}$, showed that many factors, such as the hydrophilic-hydrophobic ratio of the oligonucleotide and the surface charge density of the latex surface, control the adsorption and desorption process.
Following our preliminary study, this phenomenon is currently investigated onto a monodisperse aminated polystyrene latex. Stable cationic latexes were prepared by soap free-emulsion polymerization of styrene with vinylbenzylamine hydrochloride (VBAH) as a comonomer using 2-2' Azobis (2-amidinopropane) as initiator. Various processes were carried out in order to control the surface end group density without altering the size monodispersity. A colorimetric titration method and zeta potential measurements showed that positively charged particles were obtained with a fairly high surface incorporation yield of the functional monomer.

Our main objective is to understand the effect of the surface amino end group density, the pH and the ionic strength of the incubation medium on the adsorption and desorption of oligonucleotide. Adsorption isotherms were established in 0.01M phosphate buffer using fluorescence spectroscopy as analytical technique. Experiments have been performed in the pH domain between 4 and 9 dealing with electrostatic interactions. Adsorption isotherms develop a well-defined plateau, the level of which varying with pH showing a maximum under acidic conditions. Such a study allows one to discriminate between electrostatic and hydrophobic contributions to the binding affinity and also to get a better understanding of the adsorption-desorption phenomenon as well as to the conformation of the oligonucleotide under adsorbed state.

## Recent Publications

" Adsorption of bovine serum albumin onto amphiphilic acrylic acid copolymer-stabilized polystyrene latexes ", F. Betton, A. Theretz, A. Elaissari, C. Pichot, Colloids and Surfaces B: Interfaces, 1 (1993) 97

" Synthesis of a hexyl methacrylate-terminated disaccharide monomer and study of its radically initiated homo- and copolymerizationwith styrene, M.T. Charreyre, P. Boullanger, C. Pichot, T. Delair, B. Mandrand, M.F. LLauro, Die Makromoleculare Chemie, 194, (1993) 117

"Preparation and characterization of polystyrene latexes bearing disaccharide surface groups", M. T Charreyre, P. Boullanger, T. Delair, B. Mandrand, C. Pichot, Colloid and Polymer Sci, 271 (1993) 668

# SUSPENDED EMULSION, A NEW PROCESS FOR VINYL CHLORIDE POLYMERIZATION : MORPHOLOGY CONTROL THROUGH SURFACE ACTIVE ADDITIVES

Ph. VINDEVOGHEL [1], P. NOGUES [2] and A. GUYOT [1]
(1) CNRS - Laboratory de Chimie et Procedes de Polymerization
Department de Genie des Procedes de E.S. CPE LYON
BP 24 - 69390 VERNAISON France

(2) ELF - ATOCHEM CERDATO 27470 SERQUIGNY (France)

## ABSTRACT

Suspended emulsion is a new polymerization process in which a water phase containing the initiator is suspended in an organic phase containing the monomer ; the polymer formed is insoluble in both organic and water phase. The final morphology of the polymer is a powder of grains (around 100-300 microns) formed with agglomerates of primary particles (around 1 micron). The paper describes the effects of small amounts of either suspending agents (water soluble polymers) or surfactants. These effects concern mainly the morphology (grain and particle size), but also the polymerization kinetics. Rather homogeneous distribution of grains and particles inside the grain may be obtained by using a cellulosic polymer as suspending agent and an anionic surfactant such as Sodium Dodecyl Sulfate.

# Study of the thermal decomposition of potassium persulfate by potentiometry and capillary electrophoresis.

A. M. SANTOS, Ph. VINDEVOGHEL, C. GRAILLAT, A. GUYOT and J. GUILLOT
CNRS - Laboratoire de Chimie et Procédés de Polymerisation
BP 24 - 69390 Lyon-Vernaison, France

Two methods of analysis, potentiometry and capillary electrophoresis, were used for first time to study the decomposition of potassium persulfate (KPS) in aqueous solutions. The experiments were carried out in a glass reactor equipped with a control system developed in our laboratory. The temperature and the pH during the reactions were continuously controlled by this system. The effect of the pH on the decomposition of KPS was investigated. The rates of decomposition in the presence of a variety of additives (monomers, surfactants and inhibitor) which are used in emulsion polymerization recipes were studied. It has been found that the rate of disappearance of the persulfate ion is strongly increased in the presence of hydroquinone but changes very little in the presence of surfactants and monomers such as acrylonitrile.

POLYMER COLLOIDS NEWSLETTER CONTRIBUTION FROM
THE UNIVERSITY OF AKRON
Submitted by Irja Piirma

EMULSION COPOLYMERIZTION OF CHLOROTRIFLUOROETHYLENE WITH VINYL ACETATE AND VINYL PROPIONATE - experimental work carried out by David L. Murray

INTRODUCTION. Studies as early as in the 1950's have shown that monomer pairs in bulk (solution) and emulsion copolymerizations result in differences in monomer-polymer composition curves, and variances in $r_1$ and $r_2$ values between the two systems. Nomura et al.[1] investigated the early stages of styrene emulsion copolymerizations with methyl methacrylate and methyl acrylate, and concluded that differences in the mole fractions of styrene and the acrylates in the copolymers could be correlated with differences in water solubilities of these two acrylates. Clearly the heterogeneous nature of the emulsion polymerization system creates a variety of polymerization phases and thus contributes to the observed results in copolymerization. Some studies have been described in the literature on solvent effects in solution copolymerizations[5]. These studies have involved especially systems where the polarity of the comonomers differs greatly such as styrene-methacrylic acid[2,3], styrene-acrylic acid[4,5], styrene-acrylamide[6], and vinylidene chloride-methacrylonitrile[7,8]. Copolymerizations of these monomer pairs yield monomer-polymer composition curves that vary as the solvent employed is changed. These investigators have also found that with the same composition of comonomers there is a consistency in the triad distributions for the copolymers produced. This demonstrates that the same conditional probabilities, i.e. reactivity ratios, govern the distributions in all solvents. Obviously, the local concentration of the monomers in the polymerization site varies with the solvent employed for polymerization. Thus, the so-called "bootstrap"[9] effect in solution polymerization demonstrates the importance of local monomer concentration variances during polymerization.

The purpose of this investigation was to explore emulsion copolymerizations of monomers with differing water solubilities, and by determining sequence distributions along with copolymer composition data to obtain information on both the reactivity ratios and the concentration of monomer at the polymerization site. The comonomers chlorotrifluoroethylene, CTFE were vinyl acetate, VAc and vinyl propionate, VPp

EXPERIMENTAL. The polymerizations were carried out in 40 $cm^3$ stainless steel bombs rotated in a 25°C water bath at 45 rpm (detailed experimental procedures can be found in Macromolecules 26, 5577, 1993). The polymerization recipe contained a 20g/100g total monomer to water ratio, 1.5g ammonium perfluoroctanoate, and a redox initiator combination of ammonium persulfate-ammonium bisulfate-$Fe^{++}$. The thermal characteristics of the copolymers were measured using a

DuPont 910 Differential Scanning Calorimeter. The $^1H$ NMR spectra of the copolymers were obtained using a Varian 200 MHz NMR.

RESULTS. All the copolymers produced by these experiments were soluble in common solvents such as acetone, methanol, chloroform etc. The DSC thermal traces of the copolymers showed no sign of crystallinity, and only one glass transition temperature. The $T_g$'s of the copolymers were a linear function of the monomer weight fraction in the polymer, indicating a non-blocky structure for the copolymers[10].

The reactivity ratios were calculated using the method of Mortimer and Tidwell[11], which were for CTFE with VAc 0.68_0.11 and 0.04_0.02 and VPp 0.63_0.08 and 0.08_0.01

1. Vinyl Acetate and CTFE. From the $^1H$ NMR spectra of a poly(VAc-co-CTFE) the influence of the neighboring CTFE unit can be realized in both the methine (4.5-6.5 ppm) and the methylene (2.0-3.0 ppm) region. In all cases, the integration of the methine region to all other protons yielded the expected 1:5 ratio. The splitting of the methine region showed an interesting pattern when all the copolymer compositions were compared. Here the three groups of peaks appear to be coupled to the copolymer composition giving an indication that the peaks maybe due to the vinyl acetate triads. The fractional peak areas of the methine region were examined to see if they corresponded to a 1st-order Markoffian satistical distribution. To do this, the single peak at 4.9 ppm was assumed to be due to the AAA fraction (A = VAc) since PVAc shows only one peak in this region. The group of three peaks in the 5.1-5.8 ppm range were larger at high VA concs and were thought to be due to the AAB triads. The last set of peaks were large at low VAc concentrations and assumed to be due to the BAB triad fractions. The larger peak area between the AAA and BAB fractions was chosen as the standard and the expected peak fractions were calculated in accordance to the following equations: (1) $f_{AAA} = P(A/A)^2$; (2) $f_{BAB} = P(B/A)^2$; (3) $f_{BAA} = 2P(A/A)P(B/A)$; (4) $P(A/A) + P(B/A) = 1$. From these relationships the calculated fractional areas were compared to the experimental fraction peak areas, and found to obey closely the assigned distributions. On this basis, the single peak at 4.9 ppm was labeled for the AAA triad, the 5.1-5.8 ppm range were labeled for the BAA triad and the two peaks in the 6.0-6.4 region were labeled for the BAB triad.

2. Calculated and Experimental Sequence Distributions. For a comparison of the triad fractions obtained from the NMR studies to those calculated using the experimentally determined r values a computer program described by Harwood[17] was used. In all cases the fractional conversion was taken into account. The results showed that, although the overall composition was modeled correctly, the from NMR spectra

obtained vinyl acetate centered triad fractions varied significantly from the ones calculated using the r values (Table 1). After eliminating other possibilities, it was concluded that the probable reason for the discrepancy could be the difference in concentration of the monomers as charged to the reactor and that actually present in the site of polymerization, as is the case in the bootstrap model. A concentration variance would not be surprising in the emulsion system given the large difference in water solubilities of the two monomers. The water solubility of VAc is $2.32 \times 10^{-1}$ mol/L at 25°C while CTFE is sparingly water-soluble with a solubility of $4.69 \times 10^{-5}$ mol/L at 20°C and 760 mm Hg. To explore the significance of the concentration variances, the apparent concentration in the polymerization site was calculated from the experimental sequence distributions. The probability of a CTFE (B) unit adding to VAc (A) unit (P(B/A)) depends on the reactivity ratio and the monomer concentration as follows: $P(B/A) = 1/(1 + r_A[A]_f/[B]_f$ (Eq.5). The r values determined from the Mortimer-Tidwell method and the probability of a B given an A as determined from the fractional peak areas of the AAA and BAB triads using equations 1 to 5 were used to calculate the VAc concentration that would give rise to such a triad distribution. The results of the calculation, shown in Table 2, demonstrate the difference between the from NMR triads calculated VAc concentration at the site of polymerization and the one originally charged to the reaction. The A-centered triad distributions were then recalculated based on the monomer concentrations determined from the triad distributions and the experimental r values. The improvement in fitting the experimental sequence distribution is shown in Table 1. There still remain discrepancies in the data and, therefore, the effect of the water solubility of the comonomer was explored using vinyl propionate.

3. Vinyl propionate and CTFE. The water solubility of vinyl propionate is $8.0 \times 10^{-2}$ mol/L, i.e. about 3 times less than that of VAc. A different profile in the concentration at the polymerization site versus the charged composition could, therefore, be expected for vinyl propionate copolymerizations with CTFE. A comparison of the experimental and calculated VPp-centered triad distributions did show significant differences. The calculated apparent concentration of VPp at the site of the polymerization is listed in Table 3.

Surprisingly, a comparison of the VAc and VPp data on the apparent and actually charged monomer concentrations show great similarities. A plot of the difference of the apparent vinyl ester concentration at the polymerization site and the actual concentration added to the reactor as a function of the mol% vinyl ester charged (Figure 1) shows a maximum in the low mol% vinyl ester range followed by a decrease until the difference in the calculated and actual concentration is negative.

DISCUSSION. In this emulsion polymerization system, very large differences exist in the water solubility of the

monomers. This creates a problem since the most likely site of the early stage polymerization is in the aqueous phase. Initiator decomposition into radicals occurs in the aqueous phase and the radicals continue to grow until they become too water insoluble and precipitate. Once precipitated, these procursor particles can grow either by coagulation with other precursor particles or by absorbing monomer and polymerizing. Thus, polymerization in the latter stages can be distributed between the aqueous and the particle phase, creating a truly heterogeneous system.

The difference in the amount of monomer at the polymerization site and the amount added to the reactor is a reflection of the differences in water solubilities of the vinyl esters and CTFE. The maximum difference in the calculated and actual vinyl ester concentration occurs at low vinyl ester feed compositions. This would be the predicted result if most of the polymerization occured in the aqueous phase. At low vinyl ester concentrations all the monomers are dissolved in the aqueous phase. As the vinyl ester concentration increases beyond the solubility limit, a separate vinyl ester phase is present but the amount in the aqueous phase remains constant thus decreasing the apparent amount at the polymerization site. The solubility of the vinyl ester in water is not the only variable that causes the differences in monomer concentration. This becomes obvious when the maximum differences in the calculated and vinyl ester concentrations for vinyl acetate and vinyl propionate are compared. If solubilitu of the vinyl ester in the water phase was the only variable, then the maximum difference for vinyl propionate in Figure 2 should be a a lower vinyl ester concentration than for vinyl acetate. It may be that CTFE is soluble in the vinyl esters and the creation of a separate oil phase may enhance the solubility of the CTFE in the entire system. Therefore, as the concentration of the vinyl ester increases more CTFE is solubilized in the system and the apparent difference of the monomer concentration at the polymerization site and the actual amount added tends to decrease.

**CONCLUSIONS.** The use of sequence distributions to obtain apparent concentrations of monomers at the polymerization site is very useful, especially in emulsion polymerizations. It is also obvious that emulsion copolymerization data cannot be used for the determination of reactivity ratios. Attempts to apply a correction factor based on monomer solubility in water to the r values is an oversimplification of the problem since the concentration of monomers at the polymerization site is much more complex, depending on initial charge, conversion, increased solubility in water or organic phase of one monomer due to the presence of the other monomer.

**REFERENCES.**

1. M. Nomura, U.S. Satpathy, Y. Kouno, K. Fujita, J. Polym. Sci. Polym. Let. Ed. 26, 385 (1988)
2. F. Fowler in Vinyl Polymerization, Part II, Chp. 2, G.E.Ham ed., Marcel Dekker (1969)

3. K. Plochocka, H. J. Harwood., Polym. Prepr. 19, 240 (1978)
4. S. Toppet, M. Slinckx, G. Smets, J. Polym. Sci., 13, 1879 (1975)
5. R. E. Bockrath. Ph.D. Dissertation, The University of Akron, 1971
6. L. M. Minsk, C. Kotlarchik, R. S. Darlak, G. N. Meyer, J. Polym. Sci., 11, 353, 3037 (1973)
7. K. Y. Park, E. R. Santee, H. J. Harwood, Polym. Prepr., 27, S1 (1986)
8. J. R. Saggate, Makromol. Chem., 179, 1217 (1978)
9. H. J. Harwood, Macromol. Symp. 10/11, 331 (1978)
10. L. A. Wood, J. Polym. Sci., 28, 319 (1958)
11. P. W. Tidwell, G. A. Mortimer, J. Polym. Sci., 3, 369 (1965)

Table 1
Comparison of the Vinyl Acetate Centered Triads Found by NMR and Calculated Based of r Values, Initial Concentrations of Monomers Charged and Conversion.

| Mol% VAc charged | Conv.% | | Mol% VAc in polymer | VAc Centered Triads $f_{AAA}$ | $f_{BAA}$ | $f_{BAB}$ |
|---|---|---|---|---|---|---|
| 9.7 | 18.0 | (*) | 37.7 | 0.01 | 0.16 | 0.83 |
| | | (**) | 38.7 | 0.00 | 0.10 | 0.89 |
| | | (***) | | 0.01 | 0.12 | 0.87 |
| 13.7 | 23.0 | (*) | 41.9 | 0.03 | 0.27 | 0.70 |
| | | (**) | 42.9 | 0.01 | 0.15 | 0.70 |
| | | (***) | | 0.02 | 0.24 | 0.74 |
| 35.4 | 20.0 | (*) | 56.4 | 0.10 | 0.46 | 0.44 |
| | | (**) | 56.7 | 0.09 | 0.42 | 0.49 |
| | | (***) | | 0.09 | 0.43 | 0.47 |
| 39.1 | 23.0 | (*) | 61.1 | 0.12 | 0.47 | 0.41 |
| | | (**) | 58.2 | 0.11 | 0.44 | 0.45 |
| | | (***) | | 0.11 | 0.45 | 0.44 |
| 51.5 | 9.0 | (*) | 64.5 | 0.17 | 0.58 | 0.25 |
| | | (**) | 64.5 | 0.22 | 0.50 | 0.28 |
| | | (***) | | 0.20 | 0.50 | 0.30 |
| 72.9 | 10.0 | (*) | 72.1 | 0.32 | 0.56 | 0.12 |
| | | (**) | 76.4 | 0.48 | 0.43 | 0.09 |
| | | (***) | | 0.33 | 0.50 | 0.17 |
| 81.3 | 16.0 | (*) | 76.1 | 0.45 | 0.48 | 0.07 |
| | | (**) | 82.7 | 0.63 | 0.32 | 0.04 |
| | | (***) | | 0.46 | 0.44 | 0.10 |

(*) from NMR; (**) calc using r value; (***) recalculated

Table 2
Calculations of the Apparent Feed Compositions of Vinyl Acetate/CTFE from the Experimental Triad Fractions

| Actual mol% VAc in feed | P(S/A) calculated from $f_{AAA}$ | P(S/A) calculated from $f_{BAB}$ | $[A]_f/[B]_f$ | Apparent mol% VAc in feed |
|---|---|---|---|---|
| 9.7 | - | 0.910 | 0.145 | 12.7 |
| 13.7 | 0.826 | 0.837 | 0.299 | 23.0 |
| 35.4 | 0.684 | 0.633 | 0.713 | 41.6 |
| 39.1 | 0.654 | 0.640 | 0.802 | 44.5 |
| 51.5 | 0.587 | 0.509 | 1.213 | 54.8 |
| 72.9 | 0.434 | 0.346 | 2.030 | 67.0 |
| 81.8 | 0.329 | - | 3.098 | 75.6 |

Table 3
Calculations of the Apparent Feed Composition of Vinyl Propionate/CTFE from the Experimental riad Fractions

| Actual mol% VPp in feed | P(B/A) calculated from $f_{AAA}$ | P(B/A) calculated from $f_{BAB}$ | $[A]_f/[B]_f$ | Apparent mol% VPp in feed |
|---|---|---|---|---|
| 7.2 | - | 0.956 | 0.073 | 6.8 |
| 10.1 | - | 0.911 | 0.155 | 13.4 |
| 30.7 | 0.717 | 0.671 | 0.700 | 41.2 |
| 41.2 | 0.668 | 0.608 | 0.901 | 47.4 |
| 54.2 | 0.588 | 0.529 | 1.255 | 55.7 |
| 61.2 | 0.575 | 0.458 | 1.484 | 59.7 |

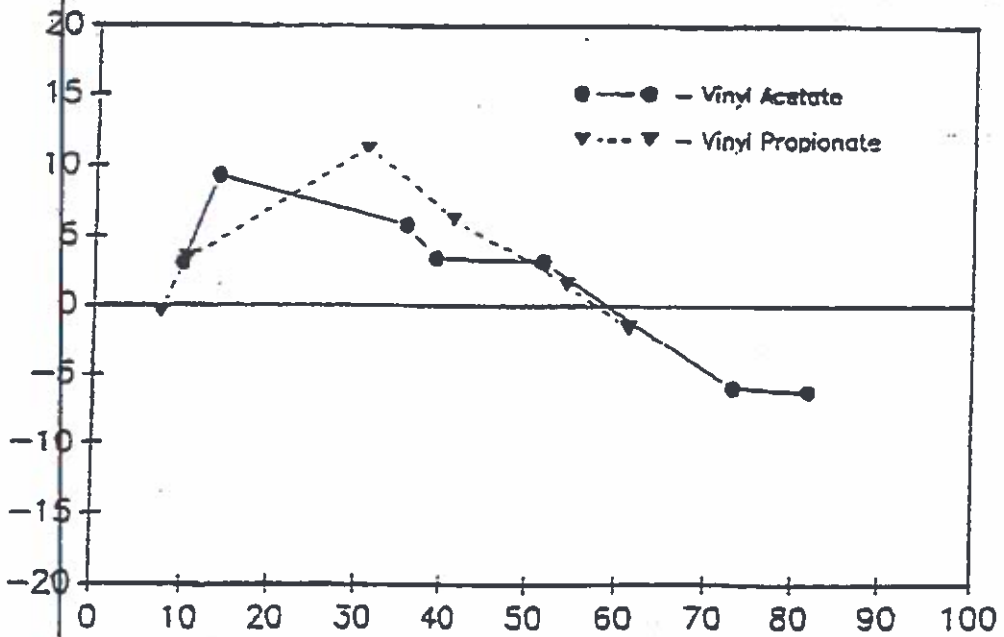


Fig.

# Polymerization of AN in a Continuous Stirred-Tank Reactor

Ryosuke Nishida*
F. Joseph Schork
Gary W. Poehlein

School of Chemical Engineering
Georgia Institute of Technology
Atlanta, GA 30332-0100

*Japan Exland Company

## INTRODUCTION

Polyacrylonitrile (PAN) for the manufacture of carbon-fiber precursor is sometimes produced via emulsifier-free water-slurry polymerization in an unseeded continuous stirred-tank reactor (CSTR). Conversion oscillations like those reported for conventional emulsion polymerization reactions in CSTR's are often observed. The purpose of this work was to determine the influence of a tubular prereactor on the performance of the CSTR and on the characteristics of the product.

## EXPERIMENTAL WORK

Two experimental runs were made in CSTR's, with and without a tubular prereactor. Table 1 gives the recipes, in terms of flow rates and the conditions for these experiments.

TABLE 1
AN POLYMERIZATION RUNS

| Ingredient | Concentration (mol/l ) | Run 1 | Run 2 |
|---|---|---|---|
| | | (ml/min) | |
| AN Monomer | Neat | 0.23 | 0.27 |
| Sodium Metabisulfite Solution | 0.0040 | 1.5 | 1.5 |
| Sodium Chlorate Solution | 0.0037 | 1.0 | 1.2 |
| Sulfuric Acid | 0.0044 | 1.2 | 1.2 |
| Reaction Temperatures: | PFR = 25°C (ambient)<br>CSTR = 55°C | | |
| Residence Time: | PFR = 160 seconds<br>CSTR = 54 minutes | | |

## RESULTS

Conversion-time profiles for the unseeded (i.e., no pretubular reactor) are shown in Figure 1. Steady-state conversion levels are not achieved even after more than 20 mean residence times.

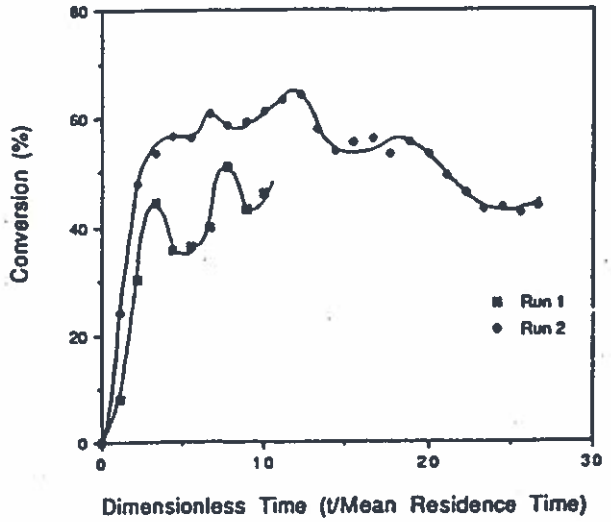


FIGURE 1. Conversion Transients in CSTR

Experiments were also carried out with a tubular prereactor comprised of a 1/8" diameter teflon tube. Nitrogen injection upstream of the tube was used to generate plug flow and the tube length could be varied.

Figure 2 shows the influence of reactor residence time (space time) on conversion at room temperature.

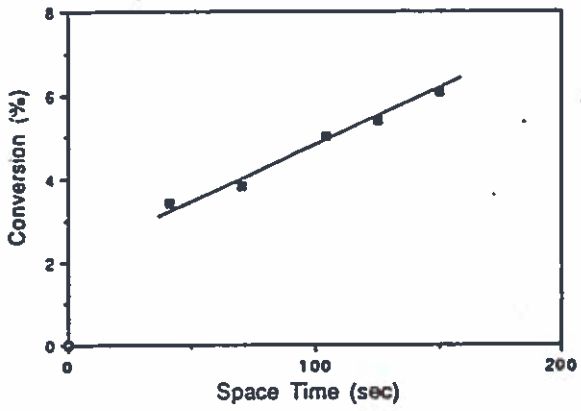


FIGURE 2: Tubular Reactor Conversion Profile

The tube length and nitrogen flow were adjusted to achieve a monomer conversion of about 5% when the tube was used upstream of the CSTR. Under these conditions the PRF produces a seed for the CSTR and particle nucleation in the stirred-tank should be eliminated or significantly

reduced. Figure 3 illustrates the conversion-transients for the PRF-CSTR system. Clearly steady-state operation can be achieved.

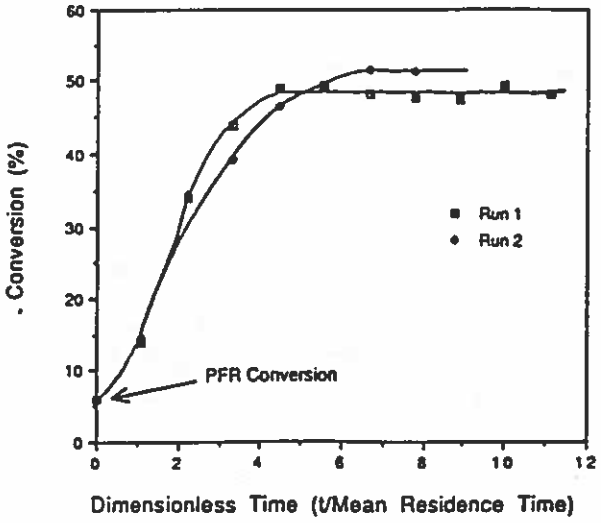


FIGURE 3: Conversion Transients in PRF-CSTR System

The influence of reactor type and operation on product characteristics is of interest to those that manufacture commercial products. Particle size and molecular weight properties were measured for some of the samples from the experiments described in this paper. Table 2 gives particle diameters for several samples. The data shown indicate that small particles, nucleated in the PFR, coagulate to form larger particles in the CSTR. A particle growth mechanism such as shown in Figure 4 is suggested.

TABLE 2
PARTICLE SIZES AND PARTICLE NUMBERS FOR SELECTED SAMPLES

| | Mean Diameter (μm) | Particle Number (#/dm$^3$) |
|---|---|---|
| Tube-CSTR | 136.0 | $1.8 \times 10^{10}$ |
| Unseeded-CSTR | 130.0 | $1.8 \times 10^{10}$ |
| At max Conversion in unseeded CSTR | 86.0 | 9.0x1010 |
| At min Conversion in unsteed CSTR | 99.3 | $4.0 \times 10^{10}$ |
| Seed Particle (PFR) | 0.14 | $2.5 \times 10^{18}$ |
| Particles on surface of Coagulated Polymer | 0.25 | $2.9 \times 10^{18}$ |

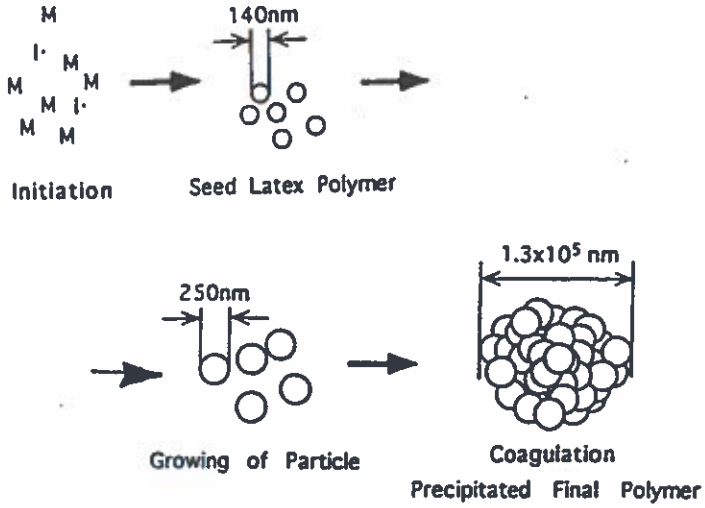


FIGURE 4. Particle Growth Mechanism

PSD data for the effluent from the unseeded CSTR are shown in Figure 5. A significantly higher fraction of small particles are present when the conversion cycle is at or near the maximum.

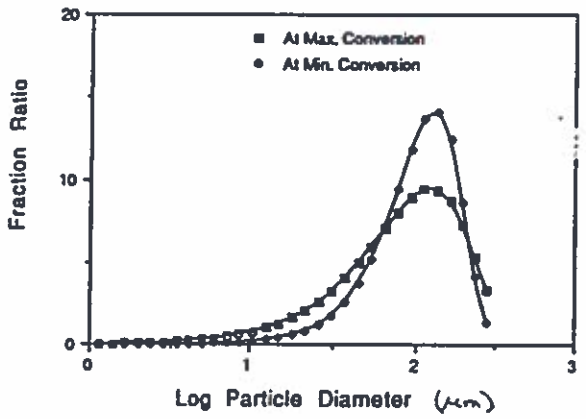


FIGURE 5. PSD During CSTR Cycle

Molecular weight data are shown in Table 3 and in Figure 6. The number average molecular weights are about the same for all samples. The molecular weight distributions, however, are broader for the effluent from the CSTR's. This would be expected because of the distributions of residence times, particle sizes and the corresponding differences in reaction environment.

TABLE 3
MOLECULAR WEIGHTS OF POLYACRYLONITRILE

| | Mn ($\times 10^4$) | Mw ($\times 10^5$) | Mz ($\times 10^5$) | Mw/Mn |
|---|---|---|---|---|
| Seed Polymer | 5.60 | 1.46 | 3.84 | 2.60 |
| Polymer from Tube-CSTR | 5.56 | 4.19 | 418 | 7.54 |
| Polymer from CSTR unscoded | 5.18 | 4.82 | 443 | 9.31 |

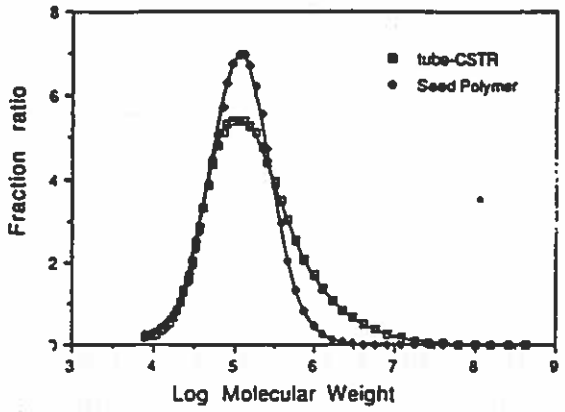


FIGURE 6. MWD Curves of Seed Polymer and Final Polymer

Langmuir

THE AMERICAN CHEMICAL SOCIETY'S
JOURNAL OF SURFACES AND COLLOIDS

Department of Chemistry, LGRC-T 102
University of Massachusetts Box 34510
Amherst, Massachusetts 01003
Phone: (413) 545-0247, 6091
Fax: (413) 545-1232

Robert L. Rowell, *Associate Editor*

October 7, 1993

IPCG Newsletter

I would be delighted to receive manuscripts for LANGMUIR even though it is taking an increasing amount of my time!

In my personal research, we remain focussed on the development of fingerprinting of colloidal particles as an approach that provides a) immediate and useful characterization of an "unknown" dispersion and b) a systematic means of representing the experimental data so that data inversion can lead to meaningful results. Thus we are working on the inversion problem as opposed to the direct problem where in one assumes a model, performs calculations and obtains meaning from the concordance or discordance with experimental data.

Our most recent work appeared in the August LANGMUIR:

*Langmuir* 1993, *9*, 2071–2076

# Characterization of Polystyrene Latexes by Hydrodynamic and Electrophoretic Fingerprinting

James H. Prescott,† Shaw-ji Shiau,† and Robert L. Rowell*

*Department of Chemistry, LGRT-102, University of Massachusetts, Amherst, Massachusetts 01003*

*Received August 10, 1992. In Final Form: June 11, 1993*

We report the first measurements of the new approach of hydrodynamic fingerprinting. The hydrodynamic fingerprint is the isothermal contour diagram of the hydrodynamic size as a function of pH and pλ (the logarithm of the conductivity (μS/cm)). The general applications of fingerprinting are discussed, and we compare hydrodynamic fingerprints with electrophoretic fingerprints on similar systems. The electrophoretic fingerprint is the isothermal isomobility contour diagram in the pH–pλ domain. Measurements are reported on five model polystyrene latexes with carboxyl or sulfate surface groups (ranging from 401 to 1050 nm) from the Interfacial Dynamics Corp. We find that the hydrodynamic size depends on pH, pλ, and time, and is generally larger than the electron microscopy size. The hydrodynamic fingerprint, like the electrophoretic fingerprint, is a characteristic pattern of a particular colloidal system. The advantages of the colloid system variable pλ over the classical ionic strength are illustrated. The fingerprinting approach is a correlation of variables that can be used to spot errors and assess the general significance of a function of two independent or characteristic variables.

**William B. Russel** **Department of Chemical Engineering**
**Princeton University**
**Princeton NJ 08544-5263**
**USA**

Abstracts of Papers Presented at the AIChE Annual Meeting
St. Louis MO
November 1993

## The Viscosity Anomaly and Pair Interactions in AOT Microemulsions

Udit Batra and William B. Russel

The single phase region of AOT (sodium di-2-ethylhexyl sulfosuccinate) based microemulsions consists of water droplets, ranging in size from 2 - 10 nm, suspended in oil with the surfactant stabilizing the interface. Studies of the structure and interactions of these systems reveal a relatively simple dependence of droplet size and volume fraction on composition (1-3). For instance, the droplet size increases linearly with X, the molar ratio of water to AOT, and is independent of temperature and droplet volume fraction. However, comparable delineation of the rheology is not available.

This paper focuses on the dependence of the low shear viscosity on composition. For fixed volume fraction and temperature the viscosity increases from a finite value at $X = 0$ to a maximum around $X = 8$ and then falls to a nearly flat minimum for $X \geq 20$ (4). This result is puzzling because several papers report interdroplet attractions that rise linearly with X (1,3). Hence, this behavior is termed anomalous. Since most of the studies in the literature focus on relatively high volume fractions (4,5), we decided to isolate unambiguously the effect of pair interactions by measuring the low shear viscosity for dilute solutions ($0.025 \leq \phi \leq 0.1$). The resulting Huggins coefficients indeed indicate that the anomaly arises from pair interactions. Furthermore, preliminary static light scattering measurements of the second virial coefficient confirm that the interparticle attraction also passes through a maximum around $X = 8$. Thus the anomaly lies in the variation of the attraction with X, not the viscosity itself. We are also investigating the effect of polydispersity on the reported second virial coefficients as well as the $\tau$ parameter in and adhesive sphere model. This model will also be used to make quantitative comparisons between static light scattering and viscosity measurements. Dynamic light scattering measurements are continuing to probe further the thermodynamic and hydrodynamic contributions to the dynamics.

### References

1. Huang, J. S., J. Surface Sci. Tech., 5 (2) 83 - 131 (1989).
2. Eastoe, J., B.H. Robinson, D.C. Steytler, and D. Thorn-Leeson, Adv. Coll. Int. Sci, **36** 1-31 (1989).
3. Kotlarchyk, M., J. S. Huang, and S. -H. Chen, J. Phys. Chem. **89** (20) 4382 (1985).
4. Peyrelasse, J., M. Moha-Ouchane, and C. Boned, Phys. Rev. A., **38** (8) 4155 (1988).
5. Berg, R. F., M. R. Moldover, and J. S. Huang, J. Chem. Phys., **87** (6) 3687 (1987).

## Quantitative Theory for the Steady Shear Viscosity and Linear Viscoelasticity of Concentrated Colloidal Dispersions

R.A. Lionberger and W.B. Russel

A quantitative theory developed herein for the rheology of concentrated colloidal dispersions accounts for the nature and effect of potential, as well as hydrodynamic, interactions. A configuration-space conservation equation for the pair density $P_2$ provides a fundamental basis for calculating the nonequilibrium microstructure under shear, including three-body couplings due to the pairwise additive interparticle potential. The resulting many-body forces depend on the three-particle distribution function, necessitating an additional equation to completely specify $P_2$. A nonequilibrium closure based on hypernetted chain (HNC) equilibrium closure relates these forces to the interparticle force and pair distribution function and completes the formulation.

A computational algorithm exploiting Fast Fourier Transforms solves the resulting integro-differential equations for weak flows, yielding the perturbed pair density as a function of the volume fraction f and the interparticle potential. Calculation of the stresses is then straightforward.

First, we calculate the low-shear limiting viscosity as a function of $\phi$ for hard, soft, and charged spheres without hydrodynamic interactions and demonstrate satisfactory agreement with the limited results available from computer simulations and experiment. Second, we incorporate rescaled hydrodynamic mobilities and the viscous stress, based on extant results for the short-time self-diffusion coefficient and the high frequency limiting viscosity, to account for hydrodynamic interactions. The corresponding predictions of the low shear viscosity and high frequency limiting shear modulus for hard spheres lie within 20% and 100%, respectively, of extensive experimental data for $0 < \phi < 0.60$. Third, calculations of the structure for small amplitude oscillations yields the frequency ($\omega$) dependent shear modulus and dynamic viscosity, elucidating the transition in the former from growth as $\omega^{1/2}$ to a constant asymptote in terms of the relative size of the lubrication and diffusional boundary layers.

## Sedimentation Velocity and High-Frequency Viscosity of Colloidal Dispersions

W.T. Gilleland, W.B. Russel and S. Torquato

The transport properties of a colloidal dispersion such as the high frequency limiting viscosity and the mean sedimentation velocity depend on the hydrodynamic interactions between the particles in the suspension. An exact treatment of hydrodynamic interactions has proven intractable due to non-convergent integrals of the slowly decaying particle disturbance field.

Our approach is to bound the transport properties based on knowledge of the equilibrium microstructure and trial flow fields. The exact energy dissipation is bounded by minimum principles derived in terms of ensemble averages of trial fields, which satisfy either macroscopic continuity or conservation constraints that assure absolutely convergent integrals. Such a technique identifies the sign of the error and assures that subsequent improvements in the microstructure representation and the trial flow fields will yield correspondingly tighter bounds.

We have bounded the mean sedimentation velocity through two-particle statistical correlations and the flow fields due to isolated particles. We have determined that the upper bound on the sedimentation velocity relative to hard spheres increases with the addition of a short range attraction and decreases for longer range, soft repulsions. The next steps involve the incorporation of higher order, and possibly non-equilibrium, statistical correlation functions and pair-wise hydrodynamic interactions. A further extension is to introduce unequal forces on the particles and bound the short-time self-diffusion coefficient and the effective pair resistance and mobility functions.

# CONTRIBUTION TO POLYMER COLLOIDS GROUP NEWSLETTER

Max-Planck-Institute for Colloid and Interface Research, Teltow-Seehof, Germany
Kantstraße 55, D 14513 Teltow-Seehof
Reporter: Klaus Tauer

*(Contribution 1)*
K. Tauer, I. Müller

## *MODELLING SUSTAINED OSCILLATIONS IN CONTINUOUS EMULSION POLYMERIZATION OF VINYL CHLORIDE*

### 1. INTRODUCTION

The phenomena of sustained oscillations of latex properties (surface tension, particle number, particle size, particle size distribution, solid content) in continuous emulsion polymerization reactors both on laboratory and technical scale are well known for a variety of monomers (styrene, methyl methacrylate, vinyl acetate, vinyl chloride).

### 2. EXPERIMENTAL DATA

Summarising the experimental data known so far regarding sustained oscillations in steady state of continuous emulsion polymerizations it is to conclude that these phenomena can be explained qualitatively by an on-off particle nucleation mechanism depending on the free surfactant concentration in water. This qualitative picture works very well regarding an explanation of the observed oscillation of surface tension and particle concentration (particle diameter if the latex solid remains unchanged). According to this picture high particle nucleation rates occur when free emulsifier concentration in water is large (minimum of latex surface tension). Subsequently a large particle surface area is generated to cause a reduction of free emulsifier concentration in water (latex surface tension starts to rise) as well as a reduction of particle nucleation rate. Due to the continuous process emulsifier is continuously added and particles are continuously washed out so that the free emulsifier concentration increases (latex surface tension decreases) and leading again to higher nucleation rates. As a consequence of this picture a maximum of the latex surface tension should correspond to a minimum of the mean particle size and vice versa. Experimental data are known which show that this relation between latex surface tension and mean particle size is in many cases fulfilled.
Furthermore, it is assumed that at high conversion when monomer droplets are disappeared the TROMMSDORFF- or gel effect has an influence on the reactor behaviour. The importance of auto accelaration in polymerization kinetics with regard to stable and unstable operating points of continuous polymerization reactors has long been known.

### 3. MODELLING OF SUSTAINED OSCILLATIONS

However it is to perceive a lack regarding modelling results which show time development of latex properties (as for instance solid content, particle concentration, particle size, particle size distribution, surface tension) from the polymerization start up into steady state also for high conversion steady states comparable with more technical continuous polymerization systems.
The aim of this work is to present a model which enables us to describe in a qualitative way the experimental behaviour of continuous emulsion polymerization of vinyl chloride from the start up into polymerization steady state at high conversion. Due to the experimental facts that at steady state a superposition of more than one oscillation occurs we consider that it is not a very useful strategy to adjust model parameters to fit a curve between more or less randomly found experimental points.

### 4. THE MODEL

The model we derived consists out basically three ordinary, non linear differential equations for the water born products capable of particle nucleation ($P_W$) (1), the particle concentration (N) (2), and the total polymer volume (VP) (3) furthermore, two ordinary

differential equations for the total initiator (I) (6) and emulsifier concentration ($S_t$) (7) as well as a set of algebraic equations (4-5), (8-10).

**Particle nucleation**

Polymer particles are considered to be generated by homogeneous nucleation in accordance with experimental results that the free surfactant concentration in steady state never exceeds the critical micelle concentration. However, the free emulsifier concentration in water ($S_W$) influences directly the rate of particle nucleation in a way that the higher its concentration the higher the nucleation rate (first term on right side of equation (2)). It is assumed that particle generation occurs by precipitation of water soluble oligomeric products in a first order reaction when its concentration in water exceeds the solubility. No difference is made in nucleation rate regarding the chain length of the water soluble oligomers. However, it is considered that water soluble oligomers can be captured by existing polymer particles (second term on right side of equation (1)). The first order reaction rate constant ($k_{op}$) has to be fitted by numerical experiments.

$$P_W = 2fk_z I - k_{mp} AP\ (1 - BG)\ P_W - \frac{P_W}{t_m} \qquad (1)$$

**Particle coalescence**

For vinyl chloride emulsion polymerization particle coalescence plays an important role and the consideration of this reaction in modelling is unconditional necessary. We have used a proved formula developed by us to calculate the particle coalescence (second term on right side of equation (2)). It is assumed that there is no influence of emulsifier concentration on particle coalescence as the degree of coverage of particle surface with emulsifier is higher than 90 % and changes only within a few per cent. Whereas the influence of monomer concentration can not be ignored due to transition from saturation conditions to monomer starved conditions at conversions higher than 72 %. This influence is considered by $F_1$ in equation (2) assuming that at monomer conversion higher than 72 % when monomer droplets have disappeared the coalescence decreases proportional to $\phi_M$ and stops at conversions higher than $P_3$, i.e. following relations are valid:
if $P < P_3$ then $F_1 = \phi_M/\phi_{MSAT}$ and if $P > P_3$ then $F_1 = 0$.

$$N = k_{OP} P_W \left(1 + \frac{S_W}{S_{CMC}}\right) - k_C F_1 \frac{N^2}{D^2} - \frac{N}{t_m} \qquad (2)$$

**Particle growth**

It is assumed that monomer swollen polymer particles are the main reaction locus regarding monomer consumption. The mean number of radicals per polymer particle is calculated with a modified UGELSTAD formula (4). After monomer droplets have disappeared an empirical formula of GARDON is used to calculate monomer volume fractions (5).
As the rate of vinyl chloride emulsion polymerization is auto accelerated polymer volume growth rate is considered to depend on monomer concentration (monomer volume fraction) in a simple way expressed by $F_2$ in equation (3). The volume growth rate increases at conversions in between 72 % and $P_1$ proportional to $1/\phi_M$. At conversions in between $P_1$ and $P_2$ particle volume growth rate decreases proportional to (1 - P) due to the influence of the glass effect before it stops at conversions higher than $P_3$, i.e. the following relations are valid: if $P < P_1$ then $F_2 = \phi_{MSAT}/\phi_M$, if $P_1 < P < P_2$ then $F_2 = (1 - P)$, and if $P > P_2$ then $F_2 = 0$.

$$VP = k_P F_2 \frac{\phi_M}{1-\phi_M} \frac{d_M}{d_P} \bar{n} N - \frac{VP}{t_m} \tag{3}$$

$$\bar{n} = \sqrt{\frac{B_2 2 f k_Z I D^4}{N N_A}} \tag{4}$$

$$P \geq 72\% \Rightarrow \phi_M = \frac{(1-P)}{(1-P)\left(1-\frac{d_m}{d_P}\right)} \tag{5}$$

**Initiator and emulsifier balances**

Due to the simplicity of our model the initiator and emulsifier balances (6), (7) can be solved analytically. According to these equations continuous feed streams ($I_0$, $S_{t0}$) as well as initial reactor charges ($I_{00}$, $S_{t00}$) can be considered.

$$\dot{I} = -2 f k_Z I + \frac{I_0 - I}{t_m} \quad , t = 0 \Rightarrow I = I_{00} \tag{6}$$

$$S_t = \frac{S_{t0} - S_t}{t_m} \quad , t = 0 \Rightarrow S_t = S_{t00} \tag{7}$$

**Latex surface tension**

To calculate the latex surface tension a LANGMUIR-type emulsifier adsorption isotherm is used (equation (8)) /30/. $\gamma$ can be estimated with a simple experimentally obtained relation between surface tension air water ($\gamma$) and free emulsifier concentration in water ($S_W$) (equation (10)). The combination the solution of equation (7) with equation (8) results in a quadratic equation for $S_W$ (9).

$$S_A = \frac{k_1 S_W}{1 + k_2 S_W} \tag{8}$$

$$S_W^2 + \frac{k_1 A P - k_2 S_t + 1}{k_2} S_W - \frac{S_t}{k_2} = 0 \tag{9}$$

$$\gamma = z_1 \lg S_W - z_2 \qquad (10)$$

**Additional assumptions**
It is assumed to be valid that the reactor behaves like an ideal continuous stirred tank reactor, and that feed streams of monomer, emulsifier, initiator, and water as well as the polymerization temperature are kept constant over the whole polymerization time. Furthermore, no external disturbances are assumed.

**Numerical values of rate constants and model parameters**
Table 1 summarises numerical values for rate constants and model parameters corresponding to our standard run. These values should be valid for a vinyl chloride emulsion polymerization with sodium dodecyl sulfate as emulsifier, potassium persulfate as initiator, and a polymerization temperature of 50 °C.

Table 1: Standard parameter set

| Symbol | Explanation | value |
|---|---|---|
| $B2$ | complex constant for calculating n | $1\ 10^{41}$ cm$^{-7}$ |
| $d_m$ | monomer density | 0,8534 g cm$^{-3}$ |
| $d_p$ | polymer density | 1,4 g cm$^{-3}$ |
| $k_c$ | coalescence rate constant | $1{,}5\ 10^{-3}$ cm$^5$ mol$^{-1}$s$^{-1}$ |
| $k_{mp}$ | mass transfer coefficient for water soluble oligomers to particles; $k_{mp} = 2d_{mw}/D$ | |
| $d_{mw}$ | effective diffusion rate constant for oligomer capture by particles | $1\ 10^{-11}$ cm$^2$s$^{-1}$ |
| $k_{op}$ | nucleation rate constant | $1{,}5\ 10^{-5}$ s$^{-1}$ |
| $k_p$ | propagation rate constant | $8\ 10^6$ cm$^3$mol$^{-1}$s$^{-1}$ |
| $k_1$ | adsorption isotherm constant | $2{,}5\ 10^{-3}$ cm |
| $k_2$ | adsorption isotherm constant | $8\ 10^6$ cm$^3$mol$^{-1}$ |
| $P_1$ | critical conversion for beginning of glass effect | 0,9 |
| $P_2$ | critical conversion for stopping of chain growth | 0,98 |
| $P_3$ | critical conversion for stopping of particle coalescence | 0,9 |
| $S_{CMC}$ | critical micelle concentration | $5{,}38\ 10^{-6}$ mol cm$^{-3}$ |
| $z_1$ | constant in equation (10) | 32,9 mN m$^{-1}$mol cm$^{-3}$ |
| $z_2$ | constant in equation (10) | 141,495 mN m$^{-1}$ |

| | | |
|---|---|---|
| $2fk_Z$ | rate coefficient for generation of growing radicals | $4\ 10^{-6}\ s^{-1}$ |
| $\phi_{MSAT}$ | saturation monomer volume fraction | 0,3895 |
| $I_0$ | initiator concentration in feed stream | $3{,}65\ 10^{-6}$ mol $cm^{-3}$ |
| $I_{00}$ | initial initiator concentration in the reactor | $9{,}59\ 10^{-6}$ mol $cm^{-3}$ |
| $S_{t0}$ | emulsifier concentration in feed stream | $4{,}94\ 10^{-5}$ mol $cm^{-3}$ |
| $S_{t00}$ | initial emulsifier concentration in the reactor | 0 |
| $t_m$ | mean residence time | $3{,}138\ 10^4$ s |

**Numerical solution**

For the numerical solution we used an explicit RUNGE-KUTTA method (RUNGE-KUTTA-FEHLBERG method) which involves an effective step-size control based on an estimation of the local discretization error. This method works quite effective and stable as long as the stiffness of the system is not to high. However, for numerical treatment of stiff systems an implicit method is necessary.

For each time step $P_W$, N, VP, $S_W$, $\gamma$, n, P, $\phi_M$, and D are calculated, whereby the particle diameter is estimated from N and VP according to equation (11).

$$D = \sqrt[3]{\frac{6\,VP}{\pi\,N\,N_A}} \qquad (11)$$

## 5. RESULTS OF MODEL CALCULATIONS

Figures 1-3 show the dynamic reactor behaviour regarding latex properties like concentration of water soluble oligomers, particle concentration, mean particle diameter, surface tension, solid content, and degree of coverage of particle surface with emulsifier calculated with the standard parameter set. These results agree qualitatively well with experimental findings regarding the observed difference in oscillation behaviour of latex surface tension and solid content as well as regarding the order of particle surface coverage with emulsifier. Regarding a comparison between experimentally observed and calculated mean particle diameters it is to note that both values $D_{546}$ and D have a different meaning. D is calculated by the model according to equation (11) as if all particles are uniform in size. This is of course a strong restriction in the model and does not correspond to the real situation described above. For this reason only a qualitative comparison is useful between $D_{546}$ and D. In this sense the fact is important that oscillations in D are calculated by the model. Furthermore, Fig. 4 shows a shift in the oscillation maxima of $\gamma$ and D as it is expected and also observed in the experiments. These results clearly show that this model enables us to investigate the dynamic reactor behaviour from the start-up of the polymerization into the steady state by numerical experiments.

## 6. CONCLUSION

Specifically, the numerical analysis showed that the occurrence of sustained oscillations depends on the consideration of particle coalescence as well as on the consideration of a conversion dependence of both particle volume growth rate and particle coalescence rate. As far as we know this is the first model published which makes it possible to calculate the dynamic behaviour of continuous emulsion polymerization reactors with regard to latex

properties like particle concentration, mean particle size, latex surface tension, solid content, and degree of coverage of latex surface with emulsifier from the start-up into a high conversion steady state. The numerical solution of the equations is comparably easy with computation programs qualified for such differential equations. However, analytical considerations with regard to a stability analysis render more difficult due to the high degree of non-linear couplings between these equations. Due to this situation, the results presented here are only a part of all existing dependencies and interactions. Further work is to be done in this direction.

The complete paper is accepted for publication in Acta Polymerica.

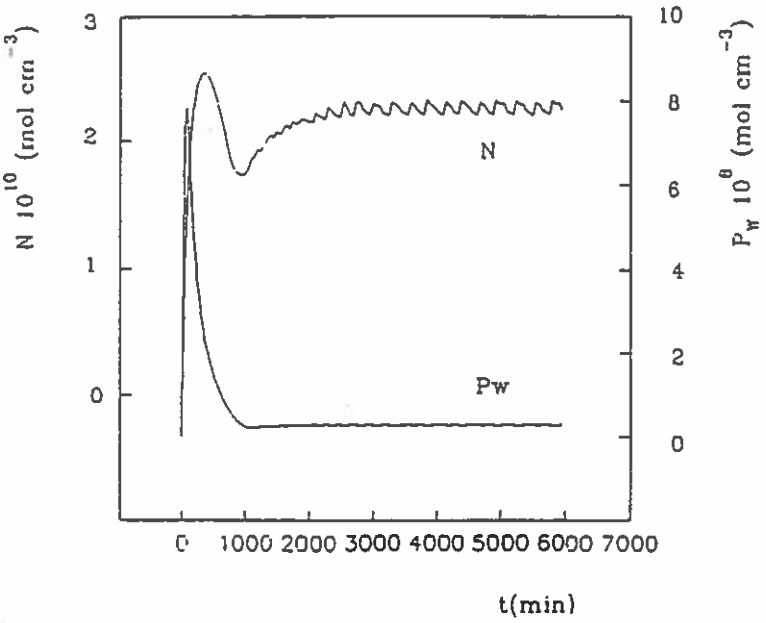


**Figure 1:** Calculated dynamic reactor behaviour with regard to particle concentration (N) and concentration of water soluble oligomers ($P_W$); standard parameter set

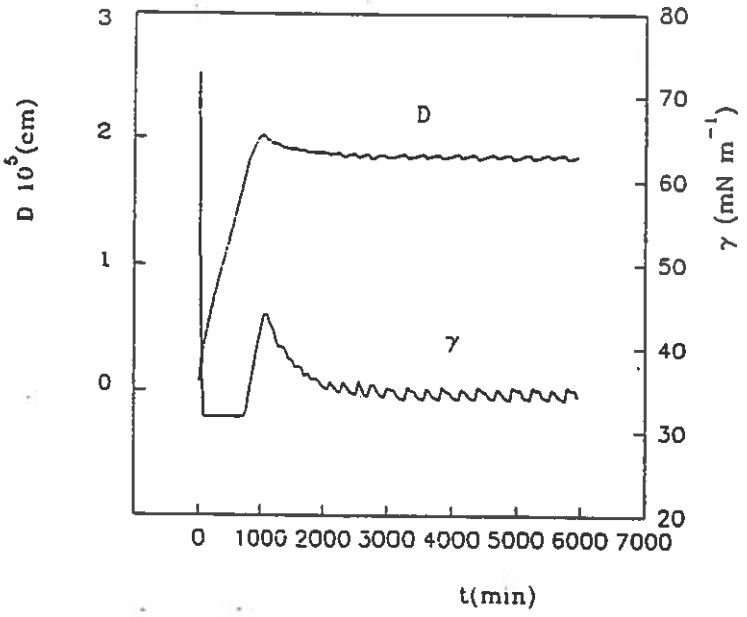


**Figure 2:** Calculated dynamic reactor behaviour with regard to mean particle diameter (D) and latex surface tension (γ); standard parameter set

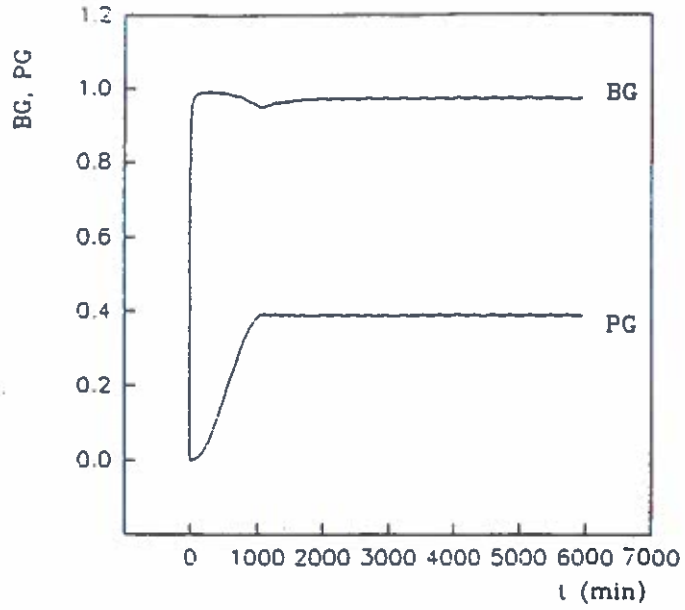


**Figure 3:** Calculated dynamic reactor behaviour with regard to degree of coverage of particle surface with emulsifier (BG) and latex polymer content (PG); standard parameter set

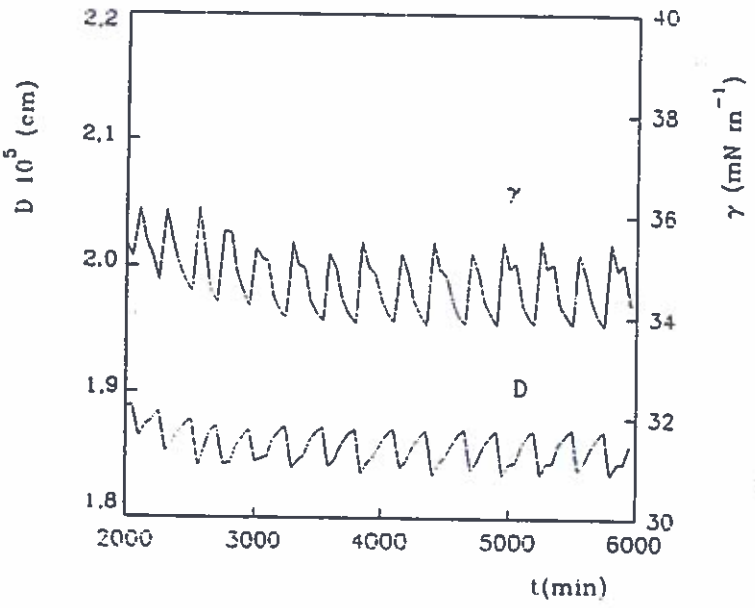


**Figure 4:** Calculated relation between latex surface tension (γ) and mean particle diameter (D) at steady state; standard parameter set

To Prof. D.H. Napper IPCG

fax 61-2-692-3329

From Utrecht-Group Van 't Hoff - Laboratory
(A.Vrij)

Colloids and Surfaces A: Physicochemical and Engineering Aspects, 73 (1993) 65–75
0927-7757/93/$06.00 

# Preparation of boehmite–silica colloids: rods, spheres, needles and gels

**Albert P. Philipse**
*Van't Hoff Laboratory for Physical and Colloid Chemistry, Utrecht University, Padualaan 8, 3584 CH Utrecht, The Netherlands*

(Received 14 January 1993; accepted 27 April 1993)

**Abstract**

A method is presented for the synthesis of amorphous silica rods with a boehmite core. The addition of boehmite needles to a mixture of tetraethoxysilane (TES), ethanol and aqueous tetramethylammonium hydroxide solution produces gels or aggregates. However, when boehmite needles are previously coated with silica in an aqueous sodium silicate solution, they serve in the TES solution as nuclei for the polymerization of part of the hydrolyzed TES into discrete, amorphous silica rods. The rods tend to stick together probably because of the increase in ionic strength caused by the TES hydrolysis. In the absence of boehmite nuclei, silica only forms discrete, non-aggregated spheres, which demonstrates that the Stöber silica sphere synthesis can be performed with a base other than ammonia.

*Key words:* Boehmite needles; Boehmite–silica gels; Silica rods; Silica spheres

Chemical Engineering Science, Vol. 48, No. 2, pp. 411–417, 1993.
Printed in Great Britain.

0009-2509/93 $5.00+0.00
Pergamon Press Ltd

# Preparation of (non-)aqueous dispersions of colloidal boehmite needles

Paul A. Buining, Chellappah Pathmamanoharan, Albert P. Philipse*, and Hendrik N.W. Lekkerkerker

Van 't Hoff Laboratory for Physical and Colloid Chemistry, University of Utrecht, Padualaan 8, P.O.Box 80.051, 3508 TB Utrecht, The Netherlands

(* Author for correspondence)

**Abstract**

A novel hydrothermal alkoxide method is presented for the preparation of stable, aqueous dispersions of fairly monodisperse, charged colloidal boehmite needles. A polymer coating

# SURFACE LENS CURVATURE IN COMPOSITE LATEX

J A Waters, ICI Paints, Slough, UK

*Extract based on a paper presented at the "Polymers at Interfaces" symposium, Bristol 1993, and accepted for publication in "Colloids and Surfaces".*

With composite particles comprising two polymers, fully phase-separated within each particle, one of the possible structures has the minor component by volume located at the surface of the other. The minor component may be considered as a lens. Usually the lens will be asymmetrical. This is analogous to an oil-lens floating on water (Fig. 1) except that the polymer lens is located on a curved surface.

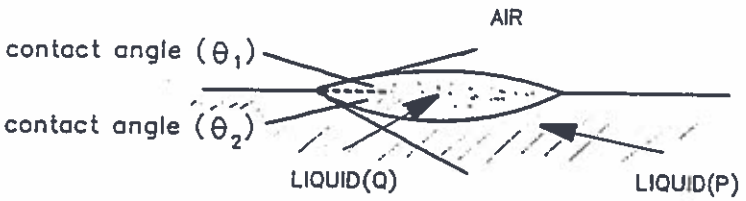


FIGURE 1

As a bi-convex lens, the surface domain may be considered partially engulfed by the other polymer and conversely as a concavo-convex lens, the domain may be considered to partially engulf the other polymer. 'Engulfed' polymers will be denoted as polymer(Q) and 'engulfing' as polymer(P).

The equilibrium shape for the lens is the one which gives the minimum interfacial energy (E) for the composite. For a given ratio of volumes and with known volumes for the three interfacial energies, the minimum may be identified by computing (E) with changes in the degree of engulfment and changes in the curvature of the P-Q interface. To do this, values are required for the three interfacial areas, which are the curved surface areas of truncated spheres. Expressions for these (and for the volumes, which will be required later) are shown (Fig. 2). The areas can be expressed in terms of f, the aperture radius (Fig 3), where

$$r = f/\sin\theta$$

$$A_{Q\text{-}W} = \frac{2\pi f^2}{\sin^2\phi_D}[1 + \cos\phi_D] \qquad (1)$$

$$A_{P\text{-}W} = \frac{2\pi f^2}{\sin^2\phi_E}[1 + \cos\phi_E] \qquad (2)$$

$$A_{P\text{-}Q} = \frac{2\pi f^2}{\sin^2\phi_I}[1 - \cos\phi_I] \qquad (3)$$

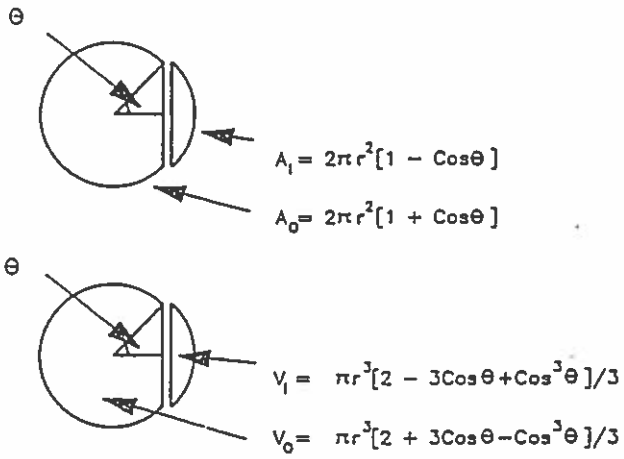


FIGURE 2

If the total composite particle volume is taken as unity, then fractional volumes ($\nu$) can be defined where

$$\nu_P + \nu_Q = 1$$

and if the volume engulfed is ($\nu_{eng}$) and the volume of the remaining truncated sphere is $\nu_{TQ}$, then

$$\nu_{eng} + \nu_{TQ} = \nu_Q \qquad (4)$$

To compute the angles $\phi_D$, $\phi_E$, $\phi_I$, it is useful to define a function

$$F(\theta) = \frac{2 + 3\cos\theta - \cos^3\theta}{\sin^3\theta} \qquad (5)$$

Now $\upsilon_{eng}$ is the volume of a truncated sphere

$$\therefore \upsilon_{eng} = \pi r_I^3(2 + 3\cos\psi_I - \cos^3\psi_I)/3 \qquad \text{(Fig. 2)}$$

$$= \pi f^3(2 + 3\cos\psi_I - \cos^3\psi_I)/3\sin^3\psi_I$$

$$= \pi f^3 F(\psi_I)/3 \qquad (6)$$

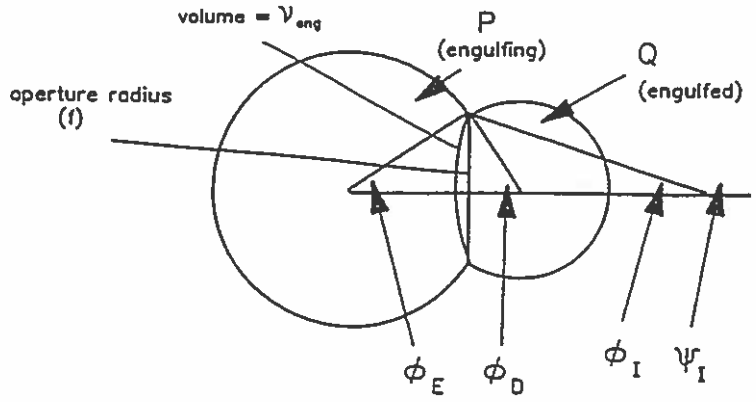


FIGURE 3

$$F(\psi_I) = \frac{3\upsilon_{eng}}{\pi f^3} \qquad (7)$$

From this $\psi_I$ can be determined by a process of iteration, and

$$\phi_I = \pi - \psi_I$$

Similarly, $\upsilon_{TQ} = (\pi f^3 F(\phi_D))/3$

$= \upsilon_Q - (\pi f^3 F(\psi_I))/3$ (from equations 4,6)

$$F(\phi_D) = \frac{3\upsilon_Q}{\pi f^3} - F(\psi_I) \qquad (8)$$

Hence $\phi_D$ by iteration.

Also $$\upsilon_{TP} = \upsilon_p + \upsilon_{eng} \qquad (9)$$

$$\frac{\pi f^3}{3} F(\phi_E) = \upsilon_P + \frac{\pi f^3}{3} F(\psi_I)$$

$$F(\phi_E) = \frac{3(1-\upsilon_Q)}{\pi f^3} + F(\psi_I) \qquad (10)$$

Hence $\phi_E$ by iteration.

Knowing the angles and hence the areas, E may be computed

$$E = \gamma_{Q\text{-}W} A_{Q\text{-}W} + \gamma_{P\text{-}W} A_{P\text{-}W} + \gamma_{P\text{-}Q} A_{P\text{-}Q} \qquad (11)$$

The interfacial energy for full engulfment is

$$Eo = 2(\pi/2)^{1/3}\, 3^{2/3} \left[\gamma_{P\text{-}W} + \upsilon_Q^{2/3}\, \gamma_{P\text{-}Q}\right] \qquad (12)$$

Using these equations it is possible to compute interfacial energy for all possible structures where the interfaces are part of a sphere surface or planar. Plots with dimensionless axes may be constructed using $\nu_{eng}/\nu_Q$; $f/r_L$ as the variables and calculating $E/E_o$, where $r_L$ is the radius of the core in the CORE SHELL case. If, for convenience, $\nu_{eng}/\nu_Q$ is denoted as positive when the engulfed polymer(Q) is relatively hydrophobic compared to polymer(P), giving CORE SHELL at full engulfment, and is denoted as negative when polymer(Q) is relatively hydrophilic, giving INVERTED CORE SHELL at full engulfment, then all possible structures including bi-convex and concavo-convex surface domains can be covered by a plot such as Figure 4. For example, if the volume fraction of the surface domain (D)

$\nu_D = 0.05$ and $\gamma_{M-W} = 0.19$; $\gamma_{D-W} = 0.05$; $\gamma_{M-D} = 0.16$

where M is the major component by volume, then the minimum interfacial energy ($E/E_o = 0.919$) is found to correspond to $\nu_{eng}/\nu_Q = 0$, $f = 0.5\ r_L$ (Fig. 4).

For this structure, the computational data showed that

$$\phi_I = 0 \ ; \quad \phi_D = 96.8° \ ; \quad \phi_E = 29.8°$$

indicating the preferred lens shape to be as depicted (Fig. 5), having a planar P-Q interface. The planar interface may be a general result within a range of compositions. This needs further consideration.

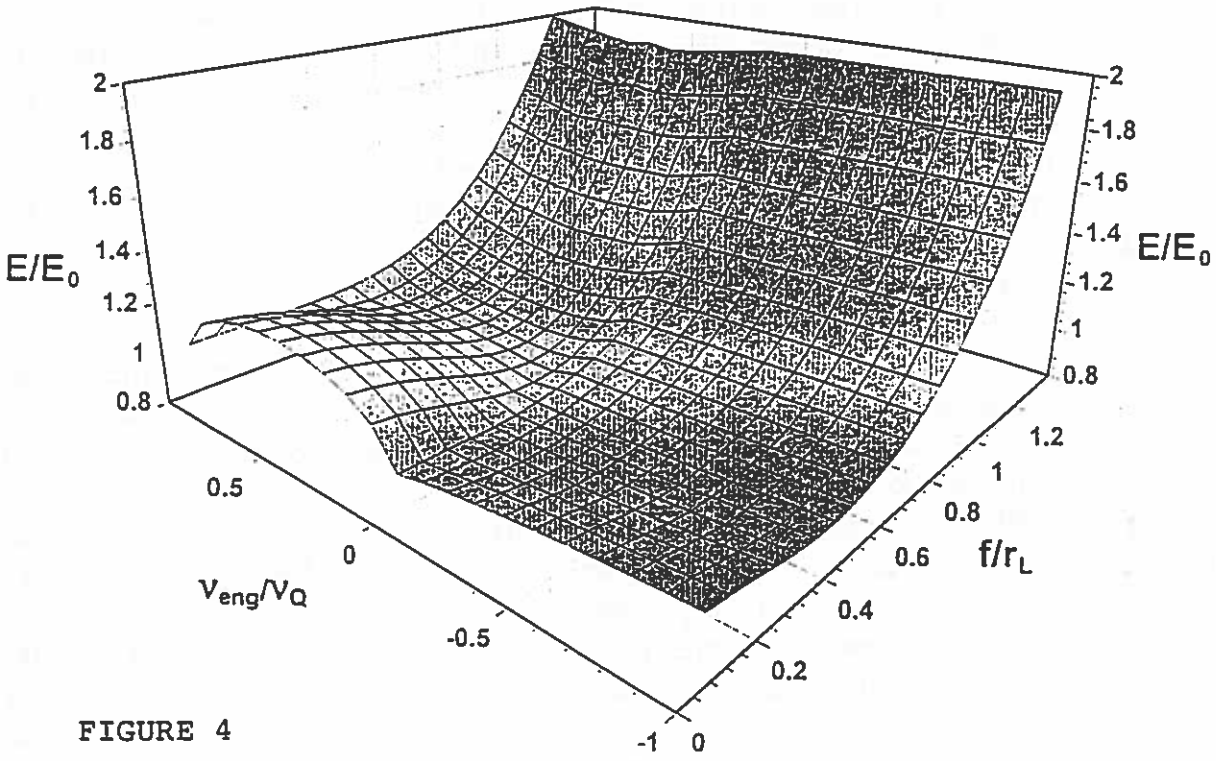


FIGURE 4

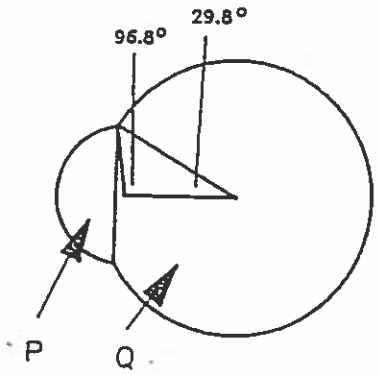


FIGURE 5

# NMR CHARACTERIZATION OF HEUR ASSOCIATIVE POLYMERS

Sabeshan Kanagalingam, Ahmad Yekta, Mitchell A. Winnik
Department of Chemistry, University of Toronto
Toronto, Ontario, Canada M5S 1A1

As we start to understand more about the association mechanism of hydrophobically modified water-soluble polymers in aqueous solution, we discover that one factor limiting our understanding is the extent to which these materials can be characterized. Our group has worked with samples of urethane-coupled poly(ethylene oxide) [PEO] polymers end-capped with linear alkyl substituents.[1] These materials are identical to those reported by Jenkins (now at Union Carbide),[2] and examined by light scattering by Ou-Yang[3] and neutron scattering by Ottewill.[4] Very similar materials were prepared at ICI and subjected to detailed rheological investigation by Annabel.[5] While one would like to have reliable values of molecular weights and their distributions, the most essential information is the hydrophobic group content of the material. This information should be available in a straight-forward way from high-field $^1$H NMR measurements in cases where the coupling agent linking the PEO components is toluene diisocyanate [TDI]. When the materials described above were prepared, isophorone diisocyanate [IPDI] was used in order to obtain a polymer with greater hydrolytic stability. This poses two problems for the polymer characterization: First, IPDU (the corresponding diurethane) resonances overlap those of the end group R. Second, the $^1$H NMR spectrum of IPDU is complicated and is rendered more complex by the presence of cis-trans isomers. There is a significant literature describing the NMR spectra of IPDI-derived polyurethanes,[6] since these spectra posed such a challenge to decipher.

Here we present 500 MHz $^1$H NMR spectra of two model compounds and two polymers, and show how one can use this information to determine the ratio of IPDU/R, and the moles of R per g of polymer. The two model compounds are the reaction products of IPDI (Aldrich) with excess methanol and with 1-hexadecanol. The sample with R = $C_{16}H_{33}$- was purified by column chromatography over silica gel, whereas the sample with R = Me was simply isolated as a crystalline solid directly from the reaction mixture. By gc-mass spectrometry it was found to be ca. 96%

pure, and we were concerned that purification might distort the cis-trans ratio of the sample. The $^1H$ NMR spectra of these species are shown in Figures 1 and 2. According to previous studies, it is the doublet at 2.85 ppm compared to more complex resonances at 3.1-3.3 ppm that are diagnostic for the cis-trans ratio.[6] In our model compounds, the ratio of cis/trans = 2.9; according to the literature various commercial IPDI samples have values of 2.3 to 3.0.

## MODEL COMPOUNDS

Quantitative analysis of the $Me_2$IPDU spectrum hinges on the recognition that the two doublets between 1.10-1.35 ppm together represent one proton. This must be half of an ABX pattern, with the corresponding partner buried under the methyl signals 0.7-1.0 ppm. We assign these peaks to the ring $CH_2$ labelled 3 in Table 1. To use the information in this spectrum to help analyze that of IPDU-modified PEO derivatives, it is not important that the assignment of ring protons be correct. The essential feature is that there is one H with a signal at 1.10-1.35 ppm and 12 IPDU protons in the region 0.7-1.1 ppm (cf Table 1).

In the $C_{16}H_{33}$- derivative, the two $CH_3$ groups from the alkyl chain appear as expected at ca. 0.8 ppm, and the next 13 $CH_2$ groups appear as a broad singlet at 1.24 ppm (cf Table 2). In this way we learn that the portion of the spectrum upfield of 1.10 ppm contains 12 protons per IPDU and 3 protons per alkyl chain. The region 1.1-1.4 ppm contains 1 H per IPDU and 26 H per $C_{16}H_{33}$- group. Based upon these observations, one can derive the following expressions, in terms of the integrated areas $I_{ppm}$ for analyzing molecules containing both IPDU and $C_{16}H_{33}$- groups:

$$I_{(0.70\text{-}1.10)} = 12\,(\text{IPDU}) + 3\,(\text{R}) \qquad [1]$$

$$I_{(1.10\text{-}1.90)} = 3\,(\text{IPDU}) + 28\,(\text{R}) \qquad [2]$$

$$I_{(1.10\text{-}1.40)} = 1(\text{IPDU}) + 26\,(\text{R}) \qquad [3]$$

In running these various spectra, the samples were dissolved in $CDCl_3$ containing a known amount (1.60 wt%) para-difluorobenzene. With this internal standard, the absolute intensity of the aliphatic proton signals could be determined and used to calculate the moles of end groups per gram of polymer. From the model compound spectra, the accuracy of this method was estimated to be ca 5-10%.

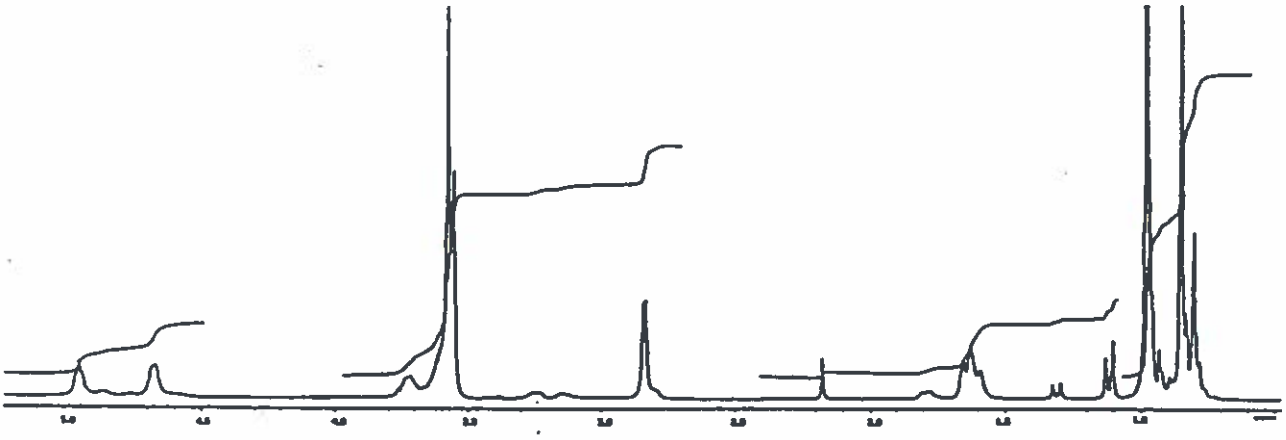

Figure 1. $^1H$ NMR spectrum of $CH_3O$-IPDU-$OCH_3$

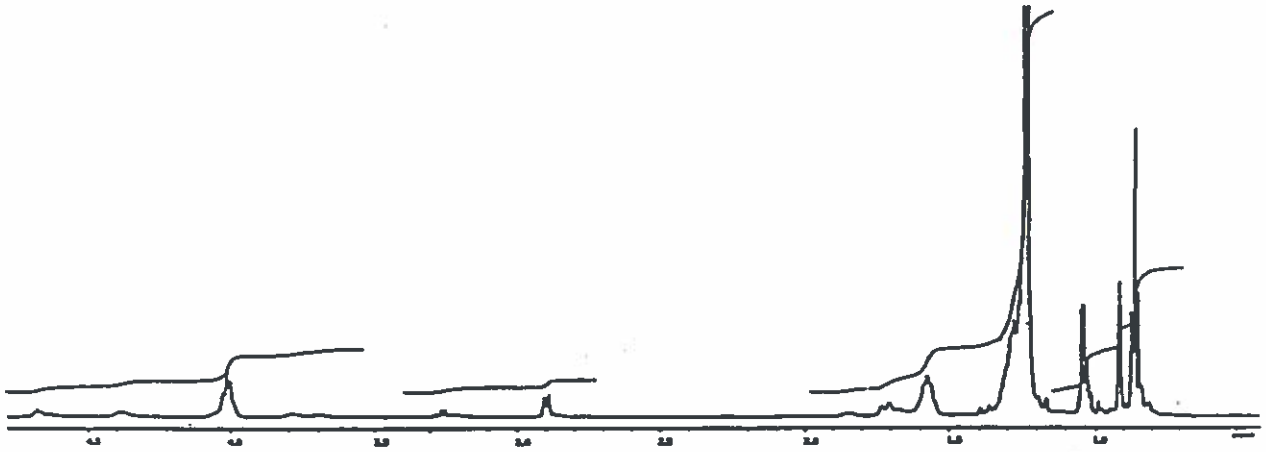

Figure 2. $^1H$ NMR spectrum of $C_{16}H_{33}O$-IPDU-$OC_{16}H_{33}$

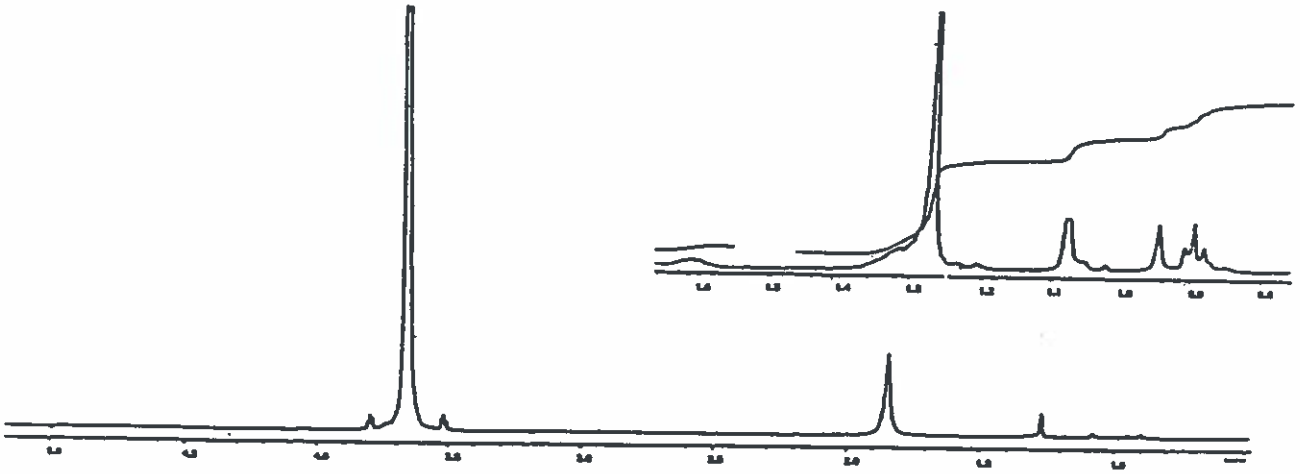

Figure 3. $^1H$ NMR spectrum of $C_{16}H_{33}O$-IPDU-end-capped PEO(35,000)

POLYMER SAMPLES

We show one example (and not the best example) of a model polymer prepared by Dr. S. Menchen of Applied Biosystems from a sample of PEO of M = 35,000 (Fluka) of narrow molecular weight distribution: n-Hexadecanol was reacted with a large excess of IPDI in the absence of a catalyst, and the excess IPDI was removed under vacuum. This was added in excess to a known amount of the PEO in the presence of a trace of dibultyltin laurate in $CH_2Cl_2$ solution. If the $C_{16}H_{33}$-IPDI adduct were pure, one would expect a ratio of IPDU/R = 1.0 in the final product, whereas if unreacted IPDI remained when the product was added to the PEO, then some condensation of the PEO chains would occur, leading to IPDU/R > 1. The $^1H$ NMR spectrum of this sample is shown in Figure 3. It provides a useful test of the ideas developed above. We find IPDU/R = 0.94, within experimental error of unity. On the other hand, by reference to the $C_6F_2H_4$ internal standard, we find only 2.65 x $10^{-5}$ mole R/g polymer. This corresponds to 0.96 $C_{16}H_{33}$- groups per polymer, indicating a problem in the second step of the reaction.

Finally we turn to an HEUR sample 46RCH22-2, prepared at Union Carbide by reaction in the melt of 4 moles of PEO (Carbowax 8000 with $M_n$=8200), 5 moles of IPDI, and 2 moles of hexadecanol. This sample should have $M_n$ = 34,200 The crude material was dried overnight in a vacuum oven. By NMR it showed 13.6 x $10^{-5}$ moles of IPDU and 5.60 x $10^{-5}$ moles of $C_{16}H_{33}$- groups/ g polymer. This translates into a ratio of IPDU/R/polymer of 4.64/1.91/1, which we take to mean that in the

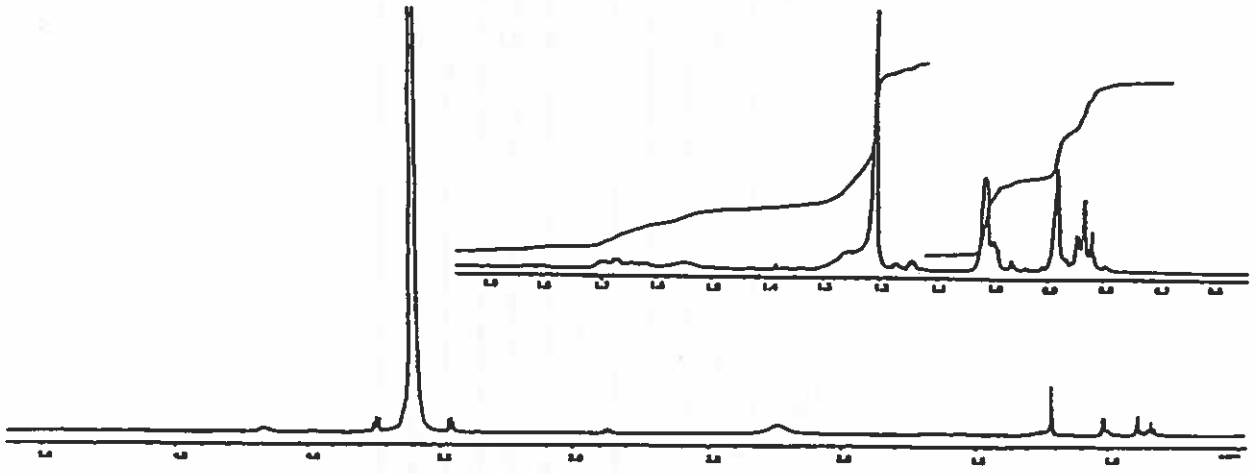

Figure 4. 1H NMR of 46RCHX22-2, recrystallized 3x from methanol

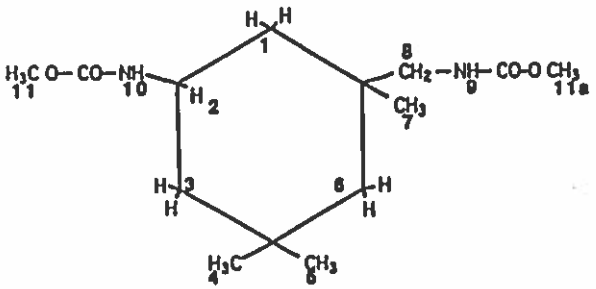

Figure 5. Expected reaction product of the reaction between IPDI and $CH_3OH$

| Label # | Chemical Shift | Multiplicity of peaks |
|---|---|---|
| | | |
| 1 | 1.55-1.85 | |
| 2 | 3.75 | |
| 3 | 1.10-1.35 & below 1.10 | |
| 4 | 0.70-1.10 | |
| 5 | 0.70-1.10 | |
| 6 | 0.70-1.10 | |
| 7 | 0.70-1.10 | |
| 8 | 2.85(cis), 3.1-3.3(trans) | doublet(cis) |
| 9 | 4.95 | triplet |
| 10 | 4.65 | doublet |
| 11, 11a | 3.6 | |

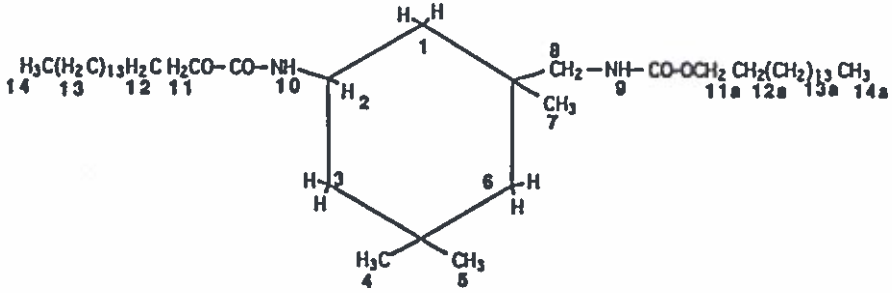

Figure 6. Expected reaction product of the reaction between IPDI and $C_{16}H_{33}OH$

| Label # | Chemical Shift | Multiplicity of peaks |
|---|---|---|
| | | |
| 1 | 1.60-1.90 | |
| 2 | 3.75 | |
| 3 | 1.25-1.35 & below 1.10 | |
| 4 | 0.70-1.10 | |
| 5 | 0.70-1.10 | |
| 6 | 0.70-1.10 | |
| 7 | 0.70-1.10 | |
| 8 | 2.90(cis), 3.1-3.3(trans) | doublet(cis) |
| 9 | 4.68 | triplet |
| 10 | 4.39 | doublet |
| 11, 11a | 4.03 | triplet |
| 12, 12a | 1.58 | |
| 13, 13a | 1.24 | |
| 14, 14a | 0.70-1.10 | |

unpurified solid, one recovers transformed what one put into the reaction mixture. In our experiments, we recrystallize the polymer several times from methanol. (Ethyl acetate is more convenient.) Here we obtain for one sample (Its spectrum is shown in Figure 4.) 13.9 x $10^{-5}$ moles of IPDU but only 1.46 x $10^{-5}$ moles of $C_{16}H_{33}$- groups per g polymer, a ratio of IPDU/R/polymer of 4.73/1.46/1. From this we infer that there must be a significant amount of $(C_{16}H_{33})_2$-IPDU present in the unpurified sample. This material, of course, is undesirable from an applications point of view.

## ACKNOWLEDGMENTS

We would like to thank David Bassett and Richard Jenkins of Union Carbide and Dr. Steve Menchen of Applied Biosystems for the polymer samples.

## REFERENCES

1. A. Yekta, J. Duhamel, H. Adiwidjaja, P. Brochard, M.A. Winnik, Langmuir, **1993**, 00, 0000.
2. R.D. Jenkins, Ph.D. thesis, Lehigh University, 1990.
3. H.D. Ou-Yang, Z. Gao, J. Phys. II (France), **1991**, 1, 1375.
4. R. Ottewill, personal communication.
5. T. Annabel, R. Buscall, R. Ettelaie, D. Whittlestone, J. Rheology, **1993**, 00, 000.
6. D. Wendisch, H. Reiff, D. Dieterich, Ang. Makromol. Chem., **1986**, 141, 173; K. Hatada, K. Ute, J. Pol. Sci. Pol. Lett. **1987**, 25, 477; for $^{13}C$ spectra, see L. Born, D. Wendisch, H. Reiff, D. Dieterich, Ang. Makromol. Chem., **1989**, 171, 213; K. Hatada, K. Ute, K-I Oka, J. Pol. Sci. Pol. Chem. **1990**, 28, 3019; N. Bialas, H. Höcker, Makromol. Chem., **1990**, 191, 1843.